



Ruhr-Universität Bochum  
Fakultät für Geowissenschaften  
Geographisches Institut  
Arbeitsgruppe: Geomatik

DLR Oberpfaffenhofen  
Deutsches Fernerkundungsdatenzentrum  
Abteilung: Georisiken und zivile Sicherheit  
Team: Geostatistische Verfahren & Modellierung

**Validation of the European Urban Atlas  
&  
Automatic Classification of Urban Structures utilizing  
Cartosat-1 nDSM Data**

**MASTERTHESIS**

Zur Erlangung des akademischen Grades  
Master of Science (M.Sc.)

**Studiengang:**

Geographie

Vertiefungsrichtung „Geomatik“

**Eingereicht von:**

Ines Antje Standfuß  
Matrikelnr.: 108012266342

**Gutachter:**

Prof. Dr. Carsten Jürgens  
Dr. Hannes Taubenböck

Bochum, Juni 2015



**DECLARATION OF AUTHORSHIP**

---

---

**DECLARATION OF AUTHORSHIP**

Hereby, I affirm that I composed the present elaboration independently and to the best of my knowledge. It does not contain any materials previously published or written by another person. Thoughts taken over, directly or indirectly, from external resources are referenced in the text.

SIGNATURE:.....

DATE:.....

**ABSTRACT**

Ongoing urbanization and population growth affect physical, ecological and socio-economic processes within and beyond urban areas. In this context, the physical spatial structure of cities serves as a basis for understanding urban areas in their entirety in order to achieve a sustainable urban growth. Remote sensing is a cost-effective data source to derive information on the physical spatial structure of urban areas in large areal and temporal coverage. The European Urban Atlas dataset is generated mainly on the basis of remotely sensed data and provides information on landuse/landcover of cities with more than 100,000 inhabitants in Europe. However, as proved within this study, the classification scheme does only partially hold distinct information on building structures and thus, as a matter of fact, does not contain holistic information on the morphology of urban areas. Within this study, a methodology towards the delineation of urban structures utilizing Cartosat-1 nDSM data and Urban Atlas building block information was developed. The nDSM data proved to be substantial in terms of building height classification but fails to add information on the building density. The methodology was applied in another city context achieving constant results and to an artificial reference unit of square objects achieving worse but still satisfactory results. The latter overcomes spatial limitations and allows for deriving information on urban structures independently from additional spatial data sources, on continental and even global scale. A cross-city structural analysis revealed differences and analogies of the urban morphology of Paris and London depending on the distance to the respective city center.

**KEYWORDS:** European Urban Atlas, Cartosat-1, Random Forest, urban remote sensing, urban structure types, urbanization

## ACKNOWLEDGEMENT

A variety of persons have supported me during the work on my thesis. I would like to express my gratitude to everyone who has contributed.

First, I would like to thank both of my supervisors, Professor Dr. Carsten Jürgens and Dr. Hannes Taubenböck for their advice, guidance and continuing encouragement during the elaboration of this study.

Many thanks go to the team “Modelling and Geostatistical Methods” who supported me during my time at the German Remote Sensing Data Center. Special thanks go to Dr. Michael Wurm and Martin Klotz for their technical advice as well as for many scientific and content-related discussions.

Furthermore, I would like to thank the participants of the “Praktikanten-Stadl” for support, discussions and distraction. Special thanks go to Anne for scientific talking, scientific laughing and scientific catastrophe prevention.

Now that I am going to leave the Ruhr Area after ten years of study, I would like to thank all my friends for their support, encouragement, advice, inspiration, patience, distraction and accommodation over that period of time. Special thanks go to Sophie, Chacha, Carlito, Anne, Sarah, Ariane, Marlene, Rasmus, Sebastian, Anna, Gerit and Thomas.

Finally, I would like to thank Katja, Akash and Valentina for accommodation, distraction and lots of good Indian Food during my residence in Munich.



**TABLE OF CONTENTS**

<b>DECLARATION OF AUTHORSHIP.....</b>	<b>I</b>
<b>ABSTRACT.....</b>	<b>II</b>
<b>ACKNOWLEDGEMENT.....</b>	<b>III</b>
<b>TABLE OF CONTENTS.....</b>	<b>V</b>
<b>LIST OF TABLES.....</b>	<b>VII</b>
<b>LIST OF FIGURES.....</b>	<b>VIII</b>
<b>ABBREVIATIONS.....</b>	<b>X</b>
<b>1. INTRODUCTION.....</b>	<b>1</b>
1.1 Urban Dynamics.....	1
1.2 Necessity of Information on Urban Structures.....	2
1.3 Urban Remote Sensing.....	4
1.4 Research Objectives.....	6
1.5 Research Framework.....	8
<b>2. STUDY SITES &amp; DATA.....</b>	<b>11</b>
2.1 Study Sites.....	11
2.1.1 London, England.....	11
2.1.2 Paris, France.....	12
2.2 Spatial Datasets.....	12
2.2.1 European Urban Atlas.....	13
2.2.2 UKMap - Building Inventory of London.....	15
2.2.3 OpenStreetMap – Building Footprint Data of Paris.....	16
2.3 Remote Sensing Datasets.....	16
2.3.1 Cartosat-1 – normalized Digital Surface Model (nDSM).....	16
2.3.2 TerraSAR-X & TanDEM-X – Global Urban Footprint (GUF).....	19
<b>3. METHODOLOGY.....</b>	<b>23</b>
3.1 Validation of the Urban Atlas Classification Scheme.....	26
3.1.1 Data Preprocessing.....	26
3.1.2 Aggregation of Physical Parameters.....	28
3.1.3 Validation Strategy.....	30
3.2 Urban Structure Classification utilizing Cartosat-1 nDSM-Data.....	31
3.2.1 Delineation of Urban Structure Types.....	32
3.2.2 Feature Calculation.....	35

## TABLE OF CONTENTS

---

---

3.2.3 Random Forest Classification .....	40
3.2.4 Accuracy Assessment .....	44
3.3 Transferability Evaluation of Urban Structure Type Classification.....	47
3.3.1 Different City Context .....	48
3.3.2 Square Objects.....	49
3.4 Cross-City Structural Analysis .....	51
<b>4. RESULTS &amp; ANALYSIS .....</b>	<b>55</b>
4.1 Validation of Urban Atlas Classification Scheme.....	55
4.1.1 Accuracy Assessment .....	55
4.1.2 Review of Urban Atlas Classification Scheme.....	57
4.2 Urban Structure Classification utilizing Cartosat-1 nDSM Data .....	60
4.2.1 Accuracy Assessment .....	60
4.2.2 Classification Results .....	64
4.2.3 Evaluation of Feature Importance .....	68
4.3 Transferability Evaluation of Urban Structure Classification.....	69
4.3.1 Different City Context .....	69
4.3.2 Square Objects.....	72
4.4 Cross-City Structural Analysis .....	75
4.5 Results in the Context of the Research Objectives .....	78
4.6 Discussion .....	82
<b>5. CONCLUSION &amp; OUTLOOK.....</b>	<b>87</b>
<b>BIBLIOGRAPHY .....</b>	<b>89</b>
<b>APPENDIX .....</b>	<b>i</b>

**LIST OF TABLES**

<b>Table 1:</b> Research objectives and research questions of the study.....	8
<b>Table 2:</b> Urban Atlas nomenclature .....	13
<b>Table 3:</b> Cartosat-1 stereo scenes of London and Paris .....	17
<b>Table 4:</b> Overview of the selected physical parameters with the respective equations .....	29
<b>Table 5:</b> Class-breaks of physical parameters for different numbers of classes .....	34
<b>Table 6:</b> Example of urban structure type classification key .....	34
<b>Table 7:</b> Pixel-based equations of selected spatial features.....	36
<b>Table 8:</b> Description of selected Haralick texture features.....	37
<b>Table 9:</b> Cartosat-1 nDSM reclassification key.....	38
<b>Table 10:</b> Interpretation key for Kappa Values .....	47
<b>Table 11:</b> Ring-based equations of physical parameters .....	54
<b>Table 12:</b> Results of the accuracy assessment of the different classification schemes.....	60
<b>Table 13:</b> Confusion matrices of a) D2H2 classification, b) H3 classification and c) H2 classification of London on Urban Atlas level .....	62
<b>Table 14:</b> Comparison between classification results of London on Urban Atlas level and classification results of Paris on Urban Atlas level (Paris trained/London trained).....	70
<b>Table 15:</b> Comparison between classification results of London on Urban Atlas level and classification results of London on square object level.....	72

**LIST OF FIGURES**

**Figure 1:** Scale-dependent analysis and evaluation of urban structures (Sukopp and Wittig 1998) .....4

**Figure 2:** Outline of the thesis contents ..... 10

**Figure 3:** Schematic representation of nDSM calculation (Brüsshaber et al. 2010: 4) .....19

**Figure 4:** Schematic representation of the process chain of the "Urban Footprint Processor" (Esch et al. 2013: 1618) .....21

**Figure 5:** Methodological workflow of the study.....25

**Figure 6:** Schematic illustration of a boxplot.....30

**Figure 7:** Top-down segmentation scheme – Urban Atlas level (modified after Klotz 2012).38

**Figure 8:** Random Forest (RF) work flow (modified after Guo et al. 2011) .....42

**Figure 9:** Schematic representation of a confusion matrix (modified after Foody 2002).....45

**Figure 10:** Top-down segmentation scheme – square object level (modified after Klotz 2012) .....51

**Figure 11:** Location and building density of London on Urban Atlas level (modified after Wurm et al. 2015b) .....53

**Figure 12:** Boxplots displaying building densities of the “Discontinuous” and “Continuous Urban Fabric” classes.....55

**Figure 13:** Boxplots displaying a) building densities, b) floor space densities, c) mean heights and d) mean volumes of the Urban Atlas classes .....58

**Figure 14:** D2H2 classification of London on Urban Atlas level: a) reference data and b) classification result.....65

**Figure 15:** H3 classification of London on Urban Atlas level: a) reference data and b) classification result.....66

**Figure 16:** H2 classification of London on Urban Atlas level: a) reference data and b) classification result.....67

**Figure 17:** Feature importance ranking of a) H3 classification, b) H2 classification and c) D2H2 classification of London .....68

**Figure 18:** H3 classification of Paris on Urban Atlas level: a) reference data and b) classification result.....71

**Figure 19:** H3 classification of London on square object level: a) reference data and b) classification result.....74

---

---

## LIST OF FIGURES

---

---

<b>Figure 20:</b> Boxplots displaying alteration of a/b) building density, c/d) floor space density and e/f) mean height in London and in Paris depending on the distance to the city center .....	76
<b>Figure 21:</b> Direct comparison between normalized average a) building density, b) floor space density and c) mean height of London and Paris depending on the distance to the city center .....	78

**ABBREVIATIONS**

<b>DEM</b>	Digital Elevation Model
<b>DFD</b>	German Remote Sensing Data Center
<b>DLR</b>	German Aerospace Center
<b>DSM</b>	Digital Surface Model
<b>DTM</b>	Digital Terrain Model
<b>EEA</b>	European Environment Agency
<b>GHSL</b>	Global Human Settlement Layer
<b>GLCM</b>	Grey-Level-Co-occurrence Matrix
<b>GMES</b>	Global Monitoring for Environment and Security
<b>GUF</b>	Global Urban Footprint
<b>LIDAR</b>	Light detection and ranging
<b>MODIS</b>	Moderate Resolution Imaging Spectroradiometer
<b>nDSM</b>	normalized Digital Surface Model
<b>OA</b>	Overall Accuracy
<b>OOB</b>	Out-Of-Bag
<b>OSM</b>	OpenStreetMap
<b>PA</b>	Producer's Accuracy
<b>RF</b>	Random Forest
<b>SAR</b>	Synthetic Radar Aperture
<b>SRTM</b>	Shuttle Radar Topography Mission
<b>UA</b>	User's Accuracy
<b>VGI</b>	Volunteered Geographic Information
<b>VHR</b>	Very High Resolution

### 1. INTRODUCTION

Within this chapter background information on urban dynamics (1.1), the necessity of information on urban structures (1.2) and on urban remote sensing (1.3) is presented in order to identify research gaps. Subsequently, the research objectives (1.4) are derived and the research questions are outlined. Finally, the research framework (1.5) of this study is introduced.

#### 1.1 Urban Dynamics

The 21<sup>st</sup> century can generally be considered as ‘urban century’ (Heinzel and Kemper 2015: 151). A turning point was reached in 2007, when for the first time in human history a larger share of the world population lived in urban environments instead of in rural areas (Griffiths et al. 2010: 426).

The world population constantly continues growing and is predicted to reach 9.6 billion in 2050, which equals an increase of 2.3 billion compared to mid-2013 (United Nations 2013: 1). Within this context, it is expected that urban areas will carry the major share of population growth over the next decades (Esch et al. 2012: 2) – with the largest urbanization rates estimated for Africa and Asia (United Nations 2014: 1). As a consequence of the ongoing urbanization and population growth, the United Nations (2014: 1) predict, that by the year 2050 already around 70% of the world’s population will live in urban areas.

The continuing urbanization causes a significant increase of the number of megacities from today’s 28 (United Nations 2014: 13) to more than 100 (Esch et al. 2012: 2). According to the United Nations (2012: 5) megacities can be defined as urban areas inhabiting more than 10 million people. However, urban development is not solely restricted to megacities since almost half of the urban population is still living in small urban centers with less than 500.000 inhabitants (United Nations 2014: 1).

Compared to the large population proportion, urban areas do only cover a small part of 2 to 3% of the Earth’s surface (Esch et al. 2012: 2). Nevertheless, cities are the center of human activities and affect physical, ecological and socio-economic processes within and beyond their boundaries (Luck and Wu 2002: 328; Esch et al. 2012: 2).

The ongoing population growth leads to continuous spatial expansion and re-densification of urban areas (Wurm et al. 2010: 1). This dynamic change of cities has caused significant effects on biodiversity, energy flows, biogeochemical cycles and climate conditions (Luck and Wu

2002: 327; Voltersen et al. 2014: 193; Hahs et al. 2009: 1165–1166). Besides, urban expansion in developing countries is often unplanned due to the governments being unable to keep track with growth related processes (Griffiths et al. 2010: 426). As a result of this, a large proportion of the urban inhabitants are prone to poverty, insufficient basic infrastructures, substandard housing, overcrowding and unhealthy living conditions (Niebergall et al. 2008: 193).

Furthermore, cities affect large areas beyond their borders due to the magnitude of energy, nutrition, water and raw material demands of the inhabitants (Pacifici et al. 2009: 1276). Within this context, urbanization has caused landscape transformations around the world which resulted in a variety of effects on structure, function and dynamics of ecological systems (Luck and Wu 2002: 327; Niebergall et al. 2008: 193; Seto et al. 2011: 1).

### 1.2 Necessity of Information on Urban Structures

Structure and size of urban areas are the outcome of driving forces of urban development over time (Wurm et al. 2009: 1). Within this context, the social, cultural, economic, and political behavior of the human population and their interaction with the environment have marked the surface appearance of cities (Patino and Duque 2013: 1; Anas et al. 1998: 1426).

Besides being the most visible outcome of driving forces, the physical structure determines the social and environmental quality of cities. Therefore, it is important to understand the linkages between urban structures and socioeconomic as well as environmental issues (Pauleit and Duhme 2000: 1–2). In the scope of ongoing urbanization and population growth, city planners, economists, ecologists, resource managers and decision makers are in need of advanced methods and comprehensive knowledge of the cities (Pham et al. 2011: 223). Only these support intelligent decisions and help to guide the development of rapidly changing urban environments in order that a sustainable urban growth can be achieved (Herold et al. 2002: 1443).

All urban areas have their individual history, and although they share some basic similarities, each city represents an unique, stone-made urban ecosystem (Wurm et al. 2010: 1–2). However, cities exhibit not only variances between each other but also within their own boundaries by means of spatial variations in building densities and structural characteristics (Hermosilla et al. 2014: 68).

Thus, it is useful to divide cities into entities with homogeneous urban structures in order to understand urban areas in their entirety and achieve a sustainable growth. These entities are

commonly named urban structure types (Wurm and Taubenböck 2010a: 94; Wurm et al. 2010: 2; Voltersen et al. 2014: 192).

Urban structure types can be delineated with regard to type, amount and/or arrangement of urban objects (e.g. building, streets, trees, lawns, etc.) (Bochow et al. 2010: 1796; Osmond 2011: 1–2). Further characteristics which can be used for differentiation are landuse and land-cover (Bochow et al. 2010: 1796). Nevertheless, the main indicator for discrimination are the structural properties of the built-up physiognomy (Wurm et al. 2010: 2).

The approach of portioning the city into homogeneous entities brings many benefits. Urban structure types are indicators that allow for differentiating the urban fabric in order that typical characteristics like physical, functional and energetic factors can be identified (Banzhaf and Höfer 2008: 130). Urban structure types are often delineated on the basis of building blocks and therefore present a comparable and transferable classification framework for the total area of cities (Wurm and Taubenböck 2010a: 97; Osmond 2011: 17). At this scale the entities represent administrative units which fit in the hierarchical structure of cities, with a direct relationship to both, the individual urban objects (lower level) and the urban morphology of local districts (higher level)(see Figure 1) (Wurm and Taubenböck 2010a: 96). Furthermore, the urban structure type approach serves as a common spatial working fundament which allows for integrating a variety of technical, methodological and spatial approaches to urban areas (Wurm et al. 2010: 2).

Owing to the advantages, the concept of urban structure types has already been used in a variety of application fields. In this regard, those units were used as input for comparing the morphology of slums (Taubenböck and Kraff 2015), energy models (Gill et al. 2007) as well as for the extrapolation of ecological (Gill et al. 2008) and socioeconomic (Avelar et al. 2009) variables.

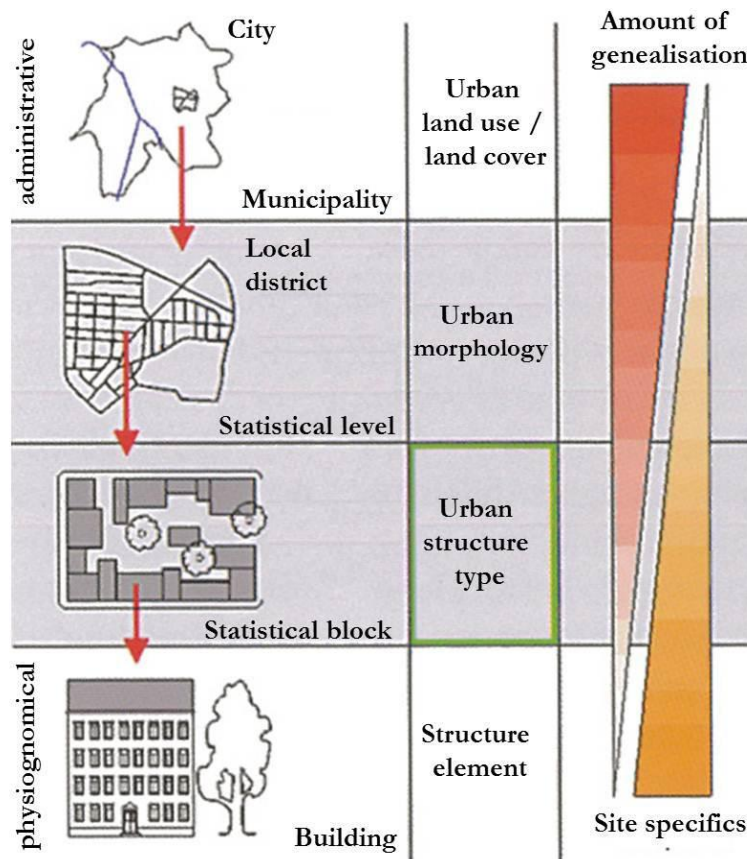


Figure 1: Scale-dependent analysis and evaluation of urban structures (Sukopp and Wittig 1998)

### 1.3 Urban Remote Sensing

Satellite based remote sensing is a consistent and comprehensive data source which enables to detect the global landcover and its changes over time (Griffiths et al. 2010: 426–427). The majority of remote sensing applications dealt with natural environments over the last decades (Weng and Quattrochi 2007: I). Nevertheless, due to the availability, temporal coverage and increasing cost effectiveness of satellite data, the added value of remote sensing to monitoring urban areas is widely accepted today (Donnay et al. 2001: 4). Within this context, a variety of approaches, using remote sensing to derive information on urban environments, were carried out on different spatial and thematic scales.

Attempts to map urban areas on large scale comprise among others Mod 500, the CORINE Landcover Programme as well as the European Urban Atlas. In the scope of Mod 500, a mask of the urbanized area was derived globally with a geometric resolution of 500m using satellite data of the Moderate Resolution Imaging Spectroradiometer (MODIS) from the year 2001

(Schneider et al. 2009). The CORINE landcover program focused on the detection of settlement areas in Europe. Within the framework of that program, landcover/landuse were mapped in the scale 1:100,000 mainly based on remote sensing data using a standardized mapping key (EEA 2010a). Another, more detailed dataset of the European urban environment is provided by the European Urban Atlas. In the scope of the European Urban Atlas initiative, landuse/landcover of cities with more than 100.000 inhabitants was mapped in the scale 1:10,000. Within this context, the derivation was mainly based on remote sensing data using 20 landuse/landcover classes (EEA 2010b). With regard to the Mod 500 outcome, thematic resolution and detail are criticized, which are too coarse in order to enable an effective support of analysis within the urban context (Esch et al. 2012: 4). The datasets on continental scale on the contrary, provide information on urban areas with increased thematic and geometric detail but exhibit limitations with regard to spatial coverage.

The progress of remote sensing technology over the last decades has led to a constant increase in spatial resolution of earth observation products. This in return facilitates more detailed classifications of landuse/landcover. New missions like the German TerraSAR-X and TanDEM-X sensors allow for deriving urbanized areas with high spatial detail. With the help of the automated ‘Urban Footprint Processor’ a global binary mask (Global Urban Footprint (GUF)) with a spatial resolution of 12m could be derived based on radar datasets of the two satellites from 2011 and 2012. This data discriminates ‘built-up’ and ‘none built-up’ areas and provides a suitable basis for the analysis of urban expansion (Esch et al. 2011; Esch et al. 2012; Esch et al. 2013). Comparable new datasets are e.g. the Global Human Settlement Layer (GHSL) of the joint Research Center (Pesaresi et al. 2013). Due to the GUF layer it was possible, to develop methods to monitor the growth of megacities (Taubenböck et al. 2012) as well as of megaregions (Taubenböck et al. 2014). Besides, the GUF data in combination with Landsat satellite data, enabled to trace the development of the investigated urban areas back to the 1970s. However, although the datasets brought urban analysis to a more detailed level, they still do not allow for identification of urban structures (Wurm et al. 2009: 1).

Nevertheless, the improved spatial detail of remote sensing data further enables to derive information of smaller spatial entities like individual buildings or urban structure types. Thus, detailed analysis of intra-urban structures and their composition utilizing remote sensing are increasingly in the focus of research. Within the scope of urban structure type classification, a variety of methodological approaches were applied comprising, e.g. spatial metrics and texture

(Herold et al. 2003), supervised classification (Bochow 2010) and object-based image analysis with decision trees (Wurm et al. 2009). Aiming at specific classes of urban structure types, mapping of slums and other informal settlements is a popular research field (e.g. Baud et al. 2010; Kuffer and Barros 2011; Taubenböck and Kraff 2014).

The usage of very high resolution (VHR) imagery and digital surface models (DSM) allow the delineation of building footprints and heights (e.g. Khoshelham et al. 2010; Wurm et al. 2014; Sirmacek et al. 2012). Those building information enable to generate 3-D city models which in turn provide the basis for the delineation of urban structure types of whole cities. Recent remote sensing studies of urban structure types comprise detailed classifications of European cities like Leipzig (Banzhaf and Höfer 2008), Munich (Wurm et al. 2010), Berlin (Voltersen et al. 2014) or Valencia (Hermosilla et al. 2014). These studies were based on VHR DSM and/or multispectral data and achieved good overall accuracies of around 80-95%. However, the VHR data used within these studies is cost-extensive and provides only limited spatial coverage. Hence, the applications mainly remain on the level of case studies and are not suited to derive area-wide information on the physical spatial structure of entire cities.

New approaches utilize Cartosat-1 DSM data, which are more favorable in terms of acquisition costs, availability and spatial coverage compared to e.g. LIDAR DSMs. Within this context, Wurm et al. (2014) developed a methodology which uses Digital Topographic Maps in the scale 1:25,000 to extract building footprints and combines those with height information from Cartosat-1 DSMs. This approach allows for localization of urban mass concentrations in urban and peri-urban regions in the magnitude of 100x100km. Besides, an extraordinary urban structuring application was investigated from Taubenböck et al. (2013) by delineating central business districts in Paris, London and Istanbul based on Cartosat-1 nDSM data.

### 1.4 Research Objectives

As indicated in the previous sections, ongoing population growth and urbanization have already caused rapid developments like expansion and re-densification of cities, and will continue to do so (Wurm et al. 2010: 1). With regard to this, the structure and size of urban areas is the most visible outcome of driving forces of urban development and further determines social and environmental quality (Pauleit and Duhme 2000: 1–2; Wurm et al. 2009: 1; ). Therefore, information on the physical structure of cities serves as a valuable information basis (Anas et al. 1998: 1426). These can help to gain comprehensive knowledge on urban areas in order

to support intelligent decisions for a sustainable urban growth (Herold et al. 2002: 1443). Thus, area-wide and up-to date information on urban structures is necessary (Wurm et al. 2009: 1).

Remote sensing is an independent and valuable source to provide area-wide information on cities and their suburban regions on various scales (Esch et al. 2010: 2–3). The European Urban Atlas is one of the large-scale approaches based on satellite data. It provides cost-free landuse/landcover information in polygon format of cities with more than 100,000 inhabitants in Europe (EEA 2010b). The Urban Atlas datasets allow for detailed urban analysis and have already been applied in a variety of research applications like urban heat island analysis (Fabrizio et al. 2011), analysis of urban development (Sapena and Ruiz 2015), land use modelling (Prastacos et al. 2011) and analysis of urban compactness (Stathakis and Tsilimigkas 2013). However, the datasets are spatially limited to large cities on the European continent and furthermore, are criticized for hiding information on the morphology of cities (Prastacos et al. 2011: 2). Nevertheless, the latter has never been proved quantitatively and therefore represents a gap in research. Due to the demonstrated importance of information about the physical spatial structure of cities, it is thus useful to evaluate if the Urban Atlas datasets are really not capable to represent the morphology of urban areas.

The progress of remote sensing technology has led to a constant increase of spatial resolution and thus, now facilitates to derive information on smaller entities like the urban structure types. New approaches toward the delineation of urban structure types are based on Cartosat-1 DSMs (Wurm et al. 2014; Taubenböck et al. 2013). However, the approach of Wurm et al. (2014) still relies on Digital Topographic Maps for building footprint extraction. The methodology of Taubenböck et al. (2013) on the contrary, relinquishes the extraction of building footprints and uses the pixels of Cartosat-1 nDSMs as building substitutes instead. Nevertheless, the approach aimed only at delineating a specific urban structure type, namely the central business district. Hence, a research gap still exists towards the capability of Cartosat-1 nDSMs to delineate further information on the physical spatial structure of cities.

With regard to the aforementioned research gaps, this study seeks *to validate the Urban Atlas classification scheme* on the one hand. On the other, a *classification methodology towards urban structure delineation* using the Urban Atlas entities in polygon format and Cartosat-1 nDSM data is developed. This methodology is further applied to another European city in order to gain confidence about the transferability to another city context. Furthermore, it is tested if the Urban

## 1. INTRODUCTION

Atlas entities can be substituted by an artificial reference unit of square objects. Thereby, it can be proved if the developed methodology works independently from the Urban Atlas datasets and thus, overcomes the spatial limitation to European cities with more than 100,000 inhabitants.

The following research objectives and questions are addressed in the scope of this study:

**Table 1:** Research objectives and research questions of the study

Research Objectives	Research Questions
1. Validation of the Urban Atlas Classification Scheme	1.1 Are the density ranges of the Urban Atlas ‘Discontinuous’ and ‘Continuous Urban Fabric’ classes accurate?
	1.2 Do the Urban Atlas classes feature information on urban structures?
2. Urban Structure Classification utilizing Cartosat-1 nDSM Data	2.1 Is it possible to automatically derive information on urban structures from Cartosat-1 nDSM datasets?
	2.2 Which features have the highest explanatory power for classification of urban structures?
3. Transferability Evaluation of Urban Structure Classification	3.1 Is the developed urban structure classification methodology transferable...?
	a) ...to another city context?
	b) ...to an independent spatial unit of square objects?
4. Cross-City Structural Analysis	4.1 Are there differences and/or analogies between the urban morphology – by means of the horizontal and vertical urban structure – of London, England and Paris, France?

### 1.5 Research Framework

In accordance with the research objectives and questions formulated in the previous section, the framework of this study comprises four working steps.

As mentioned above, the Urban Atlas datasets are criticized for hiding information of the morphology of urban areas. Inspired by this point of criticism, the central hypothesis of this study reads as follows: *The Urban Atlas classes do only partially contain information on the horizontal and vertical structure of cities.*

On the basis of this hypothesis, the *first working step* of the study comprises the validation of the Urban Atlas classification scheme. Within this context, an accuracy assessment is carried

out and the Urban Atlas classes are reviewed on whether they contain distinct information on urban structures or not. In order to do this, a spatial dataset of one of the test sites is used to aggregate physical parameters – suitable to describe the horizontal and vertical structure of cities quantitatively – on the level of the Urban Atlas polygons. The validation is conducted by comparing the calculated physical parameters with the Urban Atlas classes on the level of the Urban Atlas polygons.

In the scope of the *second working step*, a methodology for urban structure classification based on the Urban Atlas polygons and Cartosat-1 nDSM data is developed for one of the test sites. For that purpose, some of the physical parameters calculated within the first working step are used to delineate urban structures and create reference classifications. These are used to train the classifiers and to conduct an accuracy assessment of the classification results. Thereby, confidence is gained on the classification quality and performance.

In the *third working step*, the transferability of the previously developed urban structure classification methodology is tested. On the one hand, the methodology is applied on the Urban Atlas polygons and nDSM data of another test site in order to review the transferability of the methodology in another city context. On the other hand, the Urban Atlas polygons are substituted by an artificial spatial unit of square objects in order to test whether the developed methodology works independently from other than remote sensing datasets, too.

In the *fourth working step*, a cross-city structural analysis is conducted between the two test sites in order to prove that information on urban structures allows for detailed analysis of the morphological composition of cities. For that purpose, some of the physical parameters of the first working step are used again.

An outline of the contents of this thesis is presented within Figure 2. Within the *first chapter* background information on urban dynamics, the necessity of information on urban structures and on urban remote sensing is presented in order to identify research gaps. Subsequently, the research objectives are derived and the research questions are outlined. The *second chapter* introduces the selected study sites as well as the utilized spatial and remote sensing datasets. In the *third chapter* the methodological approaches of the Urban Atlas validation, of the urban structure classification, of the transferability evaluation of the urban structure classification as well as of the cross-city structural analysis are outlined. Finally, the results of this study are presented and analyzed within the *fourth chapter*.

# 1. INTRODUCTION

With the results gained during this study, the central hypothesis can be proved or falsified and the research questions can be answered. Subsequently, the outcomes are reviewed critically in terms of a discussion on the limitations of the applied methodology and the used data.

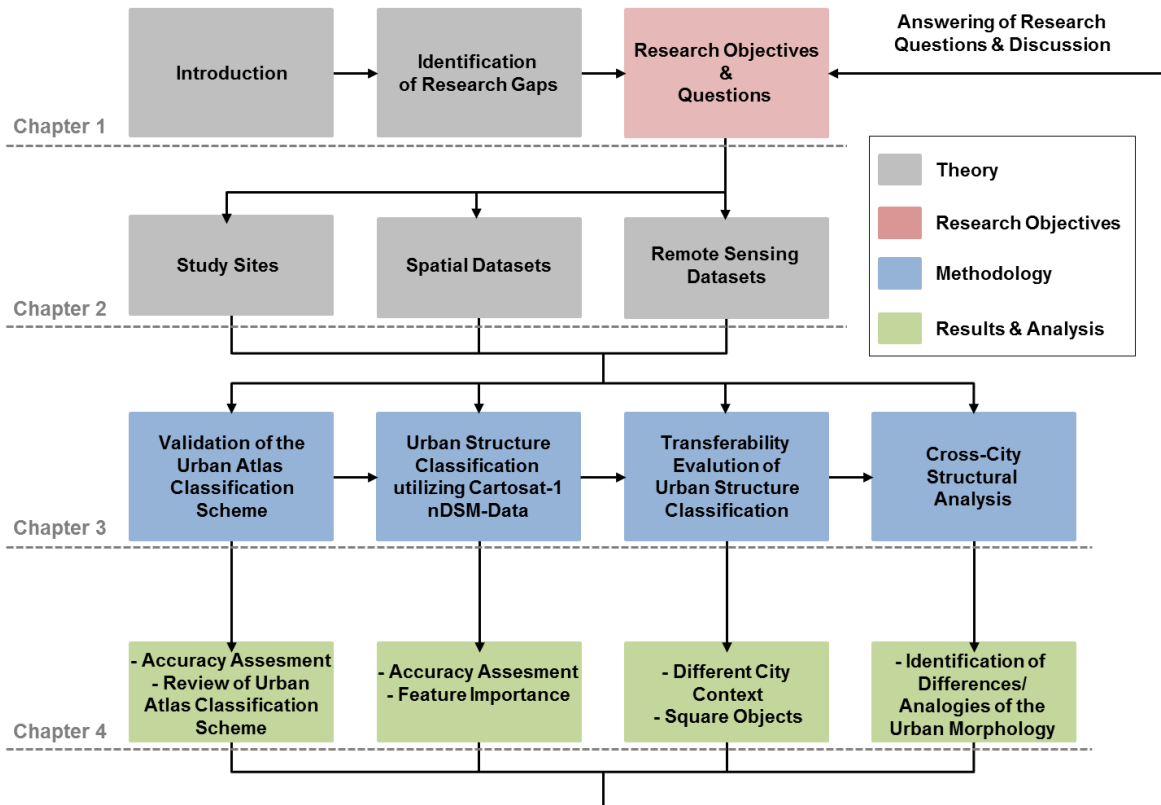


Figure 2: Outline of the thesis contents

## 2. STUDY SITES & DATA

Within this chapter, the selected study sites (2.1) as well as the utilized spatial (2.2) and remote sensing (2.3) datasets are introduced.

### 2.1 Study Sites

The two major aims of this study are the validation of the European Urban Atlas as well as the development of a methodology for urban structure classification using the Urban Atlas polygons and Cartosat-1 nDSM data. Urban Atlas data, as already mentioned in the previous chapter, is only available for European cities with more than 100,000 inhabitants (EEA 2010b). The nDSM data used within the scope of this study are taken over from (Klotz 2012; Taubenböck et al. 2013), who used these for the purpose of central business district delineation in London, England; Paris, France and Istanbul, Turkey. In order to be able to fulfill the research objectives of this study both, Urban Atlas as well as Cartosat-1 nDSM data need to be available for the cities to be analyzed. Thus, London and Paris are selected as study sites for this research. Although nDSM data is available for Istanbul, too, the city is not covered by the Urban Atlas and hence, not suited for the purpose of this research. In the following sections, the two selected study sites are briefly introduced.

#### 2.1.1 London, England

London is the capital of England and located in the United Kingdom at the south-eastern part of England. The Thames River runs through the city and splits it into a northern and a southern part. London is currently home for 10.2 million people (United Nations 2014: 26) and can therefore be categorized as megacity<sup>1</sup>.

London was established around 43 A.D. from the Romans under the name “Londinium”. After the Normans took over the city in 1066, London became the capital of the British Kingdom. In medieval times the city was a major center of English and continental networks of trade. (Keene 2000)

In 1666 large parts of London were destroyed by an event commonly named “the great fire”. Subsequently, a lot of plans were made for large-scale reconstructions. However, none of these was ever realized. During industrialization London experienced a tremendous expansion

---

<sup>1</sup> According to the United Nations (2012: 26), megacities can be defined as cities inhabiting more than 10 million people.

and became a major city of politics. Due to the city's spatial expansion beyond statutory city boundaries, it is often termed as "spreading city" which consists of a vast number of small houses. (Alter 2000)

Today's London is one of the leading world cities with regard to finance and commerce, communication, culture and knowledge (Simmie and Sennet 2001: 195).

### 2.1.2 Paris, France

Paris is the capital of France located in the Île-de-France region in the northern part of the country. The city is split by the Seine River which meanders through the whole city area. With around 10.8 million inhabitants (United Nations 2014: 26), Paris is, besides London, another European megacity.

In the mid of the 3<sup>rd</sup> century B.C. a small settlement named "Lutetia" was established on the Île-de la-Cité from the Keltic. This settlement was conquered by the Romans in 52 B.C., who subsequently established the city of Paris at that location. (Sohn 2000)

In the 17<sup>th</sup> century, under the rule of King Ludwig XIV, a lot of baroque buildings and boulevards were built within Paris who determined the appearance of the city henceforth. Beginning from 1768, during the French Revolution, the city increasingly gained importance as the center of France. Under Napoleon III, Haussmann revolutionized the urban development of Paris. Due to public safety, hygienic as well as imperial prestige reasons almost all medieval streets in the center and in the western part of Paris were replaced by new street networks and representative administration, transport as well as cultural buildings. In the scope of industrialization, the population of Paris experienced a rapid growth which was mainly absorbed by the suburb regions (Banlieues). (Wirsching 2000)

Today's Paris holds a unique position in France which, first under monarchy and later under successive republics, concentrates political, cultural and economic functions (Halbert 2006: 180).

## 2.2 Spatial Datasets

In the following sections the spatial datasets used within the scope of this study are introduced. These comprise the Urban Atlas (2.2.1) as well as building references for London (2.2.2) and Paris (2.2.3).

## 2. STUDY SITES & DATA

### 2.2.1 European Urban Atlas

The European Urban Atlas provides reliable, intercomparable, high-resolution landuse/landcover data for cities with more than 100,000 inhabitants in Europe for the reference year 2006 ( $\pm 1$  year). It is part of the Global Monitoring for Environment and Security (GMES)/Copernicus land monitoring service program and is distributed free of costs in vector/polygon format over the Internet by the European Environment Agency (EEA) (EEA 2010b; Prastacos et al. 2011: 261 Prastacos et al. 2012: 261; Sapena and Ruiz 2015: 1412).

**Table 2:** Urban Atlas nomenclature

Class Code	Nomenclature	Usage of Urban Built-up Areas
11100	Continuous Urban Fabric (Sealing Degree > 80%)	residential
11210	Discontinuous Dense Urban Fabric (Sealing Degree 50 - 80%)	residential
11220	Discontinuous Medium Density Urban Fabric (Sealing Degree 30 -	residential
11230	Discontinuous Low Density Urban Fabric (Sealing Degree 10 - 30%)	residential
11240	Discontinuous Very Low Density Urban Fabric (Sealing Degree <	residential
11300	Isolated structures	non-residential
12100	Industrial, commercial, public, military and private units	non-residential
12210	Fast transit roads and associated land	
12220	Other roads and associated land	
12230	Railways and associated land	
12300	Port Areas	non-residential
12400	Airports	non-residential
13100	Mineral extraction and dump sites	
13300	Construction Sites	non-residential
13400	Land without current use	
14100	Green urban Areas	
14200	Sports and leisure facilities	
20000	Agricultural areas, semi-natural areas and wetlands	
30000	Forests	
40000	Water	

Source: EEA 2010c : 8-9

The Urban Atlas datasets are equivalently provided in the scale 1:10,000 with a minimum mapping unit of 0.25 ha. The positional accuracy of the dataset is  $\pm 5\text{m}$  and the overall accuracy averagely amounts 80% for all classes (EEA 2010c: 1).

The Urban Atlas classification scheme differentiates 20 distinct landuse/landcover classes. 17 out of the total 20 classes can be considered as built/artificial urban classes (Prastacos et al. 2012: 261). However, only 10 of the 17 urban classes contain built-up structures (EEA 2010c: 12ff.) and can further be differentiated in “residential” and “non-residential” usage. These particular 10 classes are delineated on the level of building blocks. The Urban Atlas nomenclature for all classes is shown in Table 2.

The nomenclature of the Urban Atlas “Continuous” and “Discontinuous Urban Fabric” classes (see Table 2) is based on the CORINE land cover classes “Continuous Urban Fabric > 80%” and “Discontinuous Urban Fabric 30-80%”. Nevertheless, some refinements were made. While the class “Discontinuous Urban Fabric >80%” was retained, the class “Discontinuous Urban Fabric 30-80%” was subdivided into two classes. Additionally, two further classes were added to the Urban Atlas classification scheme, namely “Discontinuous Urban Fabric 10-30%” and “Discontinuous Urban Fabric <10%”. (Prastacos et al. 2012: 262)

The production of the Urban Atlas datasets has been carried out mainly on the basis of high-resolution (2.5m) satellite images (e.g. Spot 5, Quickbird, Formosat-2, Kompsat-2 and ALOS Data) in combination with topographic, land use and ancillary maps (EEA 2010c: 2; Stathakis and Tsilimigkas 2013: 127). The degree of sealing of the “Discontinuous” and “Continuous Urban Fabric” classes was derived using a soil sealing layer (EEA 2010c: 2). This layer provides a quantitative measure of the area covered by buildings, streets and other artificial objects. The production process of the Urban Atlas datasets involved a mix of classification and image-interpretation (Prastacos et al. 2012: 261) following uniform standards which are described in a specific mapping guide (EEA 2010c). Thus, the Urban Atlas datasets are permitting comparison of landuse/landcover between the participating European cities (EEA 2010b). In order to ensure a high quality of the Urban Atlas datasets, the production process further included a three-step validation. This comprised a project intern quality assessment, independent experts as well as a technical review by the European Topic Centre on Land Use and Spatial Information (Prastacos et al. 2012: 261).

The landuse/landcover information of the Urban Atlas datasets is provided based on exactly the same boundaries as used for the Urban Audit dataset (Prastacos et al. 2011: 2). The latter is a database containing a collection of statistical information on e.g. demography, social and economic aspects, environment, etc. of European cities (Seifert 2009: 232; Prastacos et al. 2011: 2). Hence, the analysis of the Urban Atlas datasets strongly benefits from having access to socioeconomic data of the Urban Audit database for the same areas and vice versa (Prastacos et al. 2011: 3). Regular continuations of the Urban Atlas datasets are planned for every three to five years, in the same time frame as the update frequencies of the Urban Audit datasets (Seifert 2009: 240; Prastacos et al. 2011: 3).

Due to the manifold advantages, the Urban Atlas allows for a wide range of urban analysis and applications (EEA 2010b). Within this context, a variety of research applications like urban heat island analysis (Fabrizio et al. 2011), analysis of urban development (Sapena and Ruiz 2015), land use modelling (Prastacos et al. 2011) and analysis of urban compactness (Stathakis and Tsilimigkas 2013) have already made use of the Urban Atlas. Nevertheless, the datasets are criticized for hiding information on the urban morphology (Prastacos et al. 2011: 2, 2012: 261) and therefore pose an obstacle to the application in the domain of physical urban structure research. However, this point of criticism has not yet been proved quantitatively and is one of the research aims of this study. Another aim is to develop a classification methodology to differentiate urban structures based on the Urban Atlas polygons and Cartosat-1 nDSM data.

With regard to the formulated research aims and to the selected study sites, Urban Atlas datasets of London, England and Paris, France were utilized within the scope of this research. Nevertheless, since the study focusses solely on urban structures, only polygons of the “residential” and “non-residential” Urban Atlas classes (see Table 2) were considered.

### 2.2.2 UKMap - Building Inventory of London

The UKMap building inventory is a comprehensive database which provides information on building footprints and their associated height in shapefile format covering the whole city area of London. Height and coverage attributes of the buildings are LIDAR-derived with a vertical accuracy of 95% and 0.5m confidence limits (Klotz 2012: 19). The dataset is openly available for teaching, learning and research aims (Kittmito et al. 2000: 1) and provided by the Geoinformation Group of the University of Manchester (UKMap building inventory © The Geoin-

formation Group 2012). Within the scope of this study, this data is utilized for the validation of the European Urban Atlas classification scheme, for the development of the urban structure classification methodology as well as for the cross-city structural analysis.

### 2.2.3 OpenStreetMap – Building Footprint Data of Paris

In recent years, the interest in volunteered geographic information (VGI) was growing rapidly (Goodchild 2007: 211). VGI is a specific version of crowd-sourcing, where participants create and contribute geographic facts to websites where these are stored in databases (Goodchild and Li 2012: 110). OpenStreetMap (OSM) is one example for VGI and represents an international work to create a cost-free source of map data by the collective effort of many volunteers. Within this context, OSM represents a valuable source of geographical information for different purposes. Nevertheless, quality and availability of the data are strongly dependent on the individual volunteers (Goodchild 2007: 213ff).

France is one of the countries providing free access to building footprint data in vector format. In this context, the OSM community already undertakes considerable activities to implement these data into the OSM database (Hecht et al. 2013: 1087). Thus, a large dataset of building footprints with good quality is provided within OSM especially for Paris. In this regard, OSM data (2012) is used for the purpose of transferability evaluation to another city context as well as for the cross-city structural analysis in this study.

### 2.3 Remote Sensing Datasets

In the following sections, the remote sensing datasets used within this study are introduced. These comprise Cartosat-1 nDSMs of London and Paris (2.3.1) as well as Global Urban Footprint (GUF) data of London (2.3.2).

#### 2.3.1 Cartosat-1 – normalized Digital Surface Model (nDSM)

Cartosat-1 nDSMs are the major datasets used for urban structure classification within the scope of this study. These data were taken over from (Klotz 2012; Taubenböck et al. 2013) who used it for the purpose of central business district delineation. The nDSMs were derived in a three-step process from Cartosat-1 stereo scenes. In the following, general and technical facts of the Cartosat-1 satellite as well as the particular procedures to derive the desired data are briefly outlined.

## 2. STUDY SITES & DATA

Cartosat-1 or IRS-P5 (Indian Remote Sensing Satellite P5) was launched from the Indian National Remote Sensing Agency on the 5<sup>th</sup> of May in 2005. The satellite orbits the Earth sun-synchronously in a height of 618km and captures the entire globe with a repeat cycle of 128 days. It carries two panchromatic cameras which record images in the spectral wavelength range 500-850nm (Gianinetto 2008: 300) in stereo mode. Within this context, one of the cameras is looking forward 26° and the other one is looking aft -5°. The stereo images feature a geometric resolution of 2.5m and are recorded at a relatively large swath width of 26km. (Jensen 2007: 229–231)

**Table 3:** Cartosat-1 stereo scenes of London and Paris

City	No. of stereo pairs	Aerial coverage (in km <sup>2</sup> )	Sensor	Date/Data source	Cloud cover	Path/Row	Product
London	2	1,521	Pan Fore	19 May 2010	<10%	86/162	Standard GeoTiff
			Pan Aft	/Euromap			
			Pan Fore	19 May 2010	<10%	86/163	Standard GeoTiff
			Pan Aft	/Euromap			
Paris	4	2,505	Pan Fore	29 June 2011	0%	104/174	Standard GeoTiff
			Pan Aft	/Euromap			
			Pan Fore	29 June 2011	<10%	104/175	Standard GeoTiff
			Pan Aft	/Euromap			
			Pan Fore	3 July 2011	0%	105/174	Standard GeoTiff
			Pan Aft	/Euromap			
			Pan Fore	3 July 2011	0%	105/175	Standard GeoTiff
			Pan Aft	/Euromap			

Source: Klotz 2012: 15

The satellite has already captured stereo images of large parts of the Earth’s surface including the European continent (Uttenthaler et al. 2013: 4). Due to the availability as well as the spatial and temporal coverage (revisiting rate = 5 days) of the images, Cartosat-1 is particularly suited to capture very large urban areas in a cost-effective manner (Wurm et al. 2014: 2). An overview of the Cartosat-1 stereo scenes used for the generation of the nDSM data for London and Paris is given within Table 3. The data has been provided within the scope of the DLR scientific data pool by the Euromap GmbH, which is responsible for the distribution of the Cartosat-1 data in Europe (Klotz 2012: 16).

The derivation of the nDSMs required the generation of DSMs in advance (*Step 1*). DSMs contain elevation information about all features of a landscape including buildings, vegetation and other structures (Jensen 2007: 335). Cartosat-1 stereo images are suited to generate DSMs with a geometrical resolution of 5m (dAngelo et al. 2008: 1137). The DSMs for London and Paris were derived from the Cartosat-1 stereo scenes presented within Table 3 by the German Remote Sensing Data Center (DFD) (Klotz 2012: 16). For that purpose, fully automatic semi-global image matching was applied (dAngelo et al. 2010: 2), using mutual information (Hirschmüller 2008: 329) of the respective stereo images of London and Paris.

Stereo matching in general finds corresponding pixels in image pairs and uses the known camera orientations (intrinsic and extrinsic) for triangulation. This in turn enables for 3D reconstruction of image objects. Local stereo image matching techniques use matching windows to find corresponding pixels in two or more overlapping images. However, images are locally very ambiguous. Global image matching techniques on the contrary, overcome this problem by matching pixels individually but require high computation effort. Semi-global image matching combines the concepts of local and global stereo methods successfully and matches the pixels individually with a low runtime. (Hirschmüller 2011: 174–175)

The semi-global matching method applied for derivation of the DSMs of London and Paris was evaluated by comparing DSMs generated from stereo images of 18 test sites in Europe with independent ground truth data. The tests confirmed an average horizontal accuracy of 6.7m and an average vertical accuracy of 5.1m. (dAngelo et al. 2010: 3–4)

In order to be able to derive the desired nDSM data, DTMs needed to be derived from the previously created DSMs (*Step 2*) (Klotz 2012: 34). DTMs contain only information of the Earth's surface without the influence of vegetation, buildings or other structures (Jensen 2007: 335). The DTMs used for the generation of the nDSMs of London and Paris were derived using a morphological opening approach (Haralick et al. 1987) from the field of mathematical morphology (Klotz 2012: 34). The algorithm is based on a sequence of *erosion (minimum)* and *dilation (maximum)* filter. The kernel window-based filter operation firstly substitutes each pixel of the DSMs with the filter minimum. The resulting interim image is subsequently filtered again using the same kernel window, but this time substituting each pixel with the filter maximum (Bochow 2010: 57). In order to smooth the DTM surface a median filter was applied subsequently (Klotz 2012: 36).

Since the results of the morphological filtering are sensitive to the size of the kernel filter (Arefi et al. 2009: 3), several kernel sizes were tested (Klotz 2012: 34). The best results could be achieved with a kernel window with a size of 10x10 pixels which was thus used for the generation of the DTMs of London and Paris.

In a last step (*Step 3*), the final nDSMs were derived by calculating the difference between the DSMs and the DTMs (see Figure 3). The nDSMs contain solely height information of vegetation, buildings and other objects above ground without the influence of the Earth's surface elevation. Maps showing the derived nDSMs of London and Paris can be found in Appendix 3 and Appendix 4.

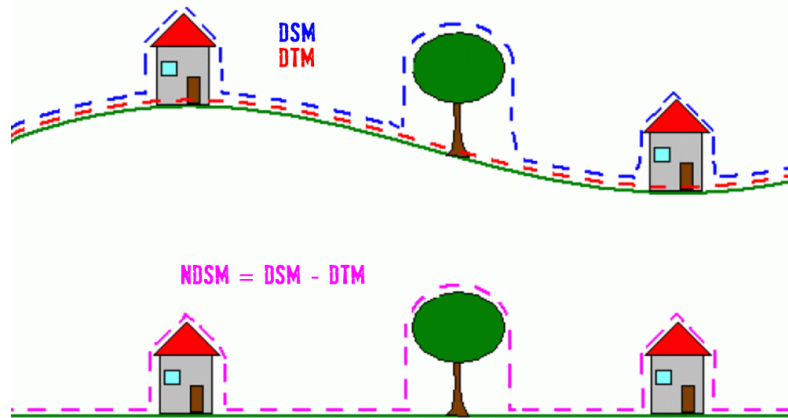


**Figure 3:** Schematic representation of nDSM calculation (Brüsshaber et al. 2010: 4)

The final nDSMs feature a geometric resolution of 5m and can therefore be categorized as high resolution products (Taubenböck et al. 2012: 162). This resolution is yet too coarse in order to allow for the extraction of single buildings (Taubenböck et al. 2013: 395). Nevertheless, using the single pixels of the nDSMs as building substitute allows for the detection of physical urban structures as proved in the context of central business district delineation from Taubenböck et al. (2013). Besides, as already mentioned above, Cartosat-1 nDSMs are very cost-effective and cover large areas due to the large swath width. Thus, the data represents a valuable source for urban structure classification as intended within this study.

### 2.3.2 TerraSAR-X & TanDEM-X – Global Urban Footprint (GUF)

New missions like the German TerraSAR-X and TanDEM-X sensors allow for deriving urbanized areas with high spatial detail. In this regard, the German Remote Sensing Data Center

(DFD) of the German Aerospace Center (DLR) has developed a fully automated processing chain (Urban Footprint Processor) for the global delineation of human settlements based on radar data of the two satellites (Esch et al. 2013: 1617). In the following, general facts of the TerraSAR-X and TanDEM-X satellites as well as the processing stages of the “Urban Footprint Processor” are briefly outlined.

TerraSAR-X was launched on the 15<sup>th</sup> of June in 2007, implemented by a public-private-partnership between the DLR and EATS Astrium GmbH. The satellite circles the Earth in a sun-synchronous orbit at 514km. The main recording device on board of the satellite is a modern X-band radar sensor, a so-called “Synthetic-Radar-Aperture” (SAR), which is recording at a frequency of around 9.65 GHz, corresponding to a wavelength of 3cm. The sensor enables different modes (Spotlight, Stripmap and ScanSAR) of operation which in turn allow capturing radar images with different swath width (10, 30 and 100km), geometric resolutions (1, 12 and 30m) and polarisations. Since TerraSAR-X carries an active system, it is independent from sun-illumination and weather conditions. This enables to record images around the clock and even of areas which are covered by clouds. TerraSAR-X images can be used for both, scientific and commercial applications and have already been applied in a variety of fields like geology, climate research, urban research, etc. (DLR 2009; Buckreuss et al. 2009)

The TanDEM-X (TerraSAR-X add-on for Digital Elevation Measurements) mission serves as an extension of the TerraSAR-X satellite and was again implemented by a public-private-partnership between DLR and EATS Astrium GmbH. The TanDEM-X Satellite was launched on the 21<sup>st</sup> of June in 2010 and orbits sun-synchronously in a height of 514km. The satellite is a replica of the TerraSAR-X satellite with only few modifications and thus, enables to record in Spotlight, Stripmap and ScanSAR mode, too. The two satellites are flying in a unique formation with a distance of 250 up to 500m between each other. Thereby, two operation modes are possible. On the one hand, both satellites can operate independently in monostatic mode and on the other, synchronously in bi-static mode. Within this context, the bi-static mode serves as the basis for the generation of a worldwide, consistent, timely, and high-precision Digital Elevation Model (DEM), which is the primary objective of the TanDEM-X mission. Within one year, the whole surface of the Earth can be recorded twice with radar imagery of the TerraSAR-X and TanDEM-X satellites. (Moreira et al. 2004; Krieger et al. 2007; Esch et al. 2012)

Besides using the radar data of the two satellites for DEM generation, these are also utilized for the derivation of a global human settlement layer (Felbier et al. 2014: 4816). For identification and delineation of urban areas, single-polarized very high resolution (3-5m) SAR imagery, recorded independently by both satellites in the years 2011 and 2012, is used (Esch et al. 2012: 5). In order to classify these data automatically the DFD-DLR has developed the fully automatic “Urban Footprint Processor” which comprises three main processing stages (Esch et al. 2013: 1617) (see Figure 4).

The *first stage* is devoted to feature extraction. Within this step, a specific texture measure is calculated which enables to point out highly structured and heterogeneous built-up areas on the radar imagery (Esch et al. 2013: 1618). In the *second step*, an unsupervised classification approach on Pixel level is conducted. This uses the previously calculated texture information as well as local backscattering characteristics in order to generate a binary mask, discriminating between “built-up” and “none built-up” areas (Esch et al. 2013: 1619). With regard to this, high texture and backscattering values of the pixels are associated with built-up structures while low values correspond to none urbanized areas (Felbier et al. 2014: 4816). In the *third step*, post-editing and mosaicking of the binary masks generated in the classification process is carried out (Esch et al. 2013: 1619).

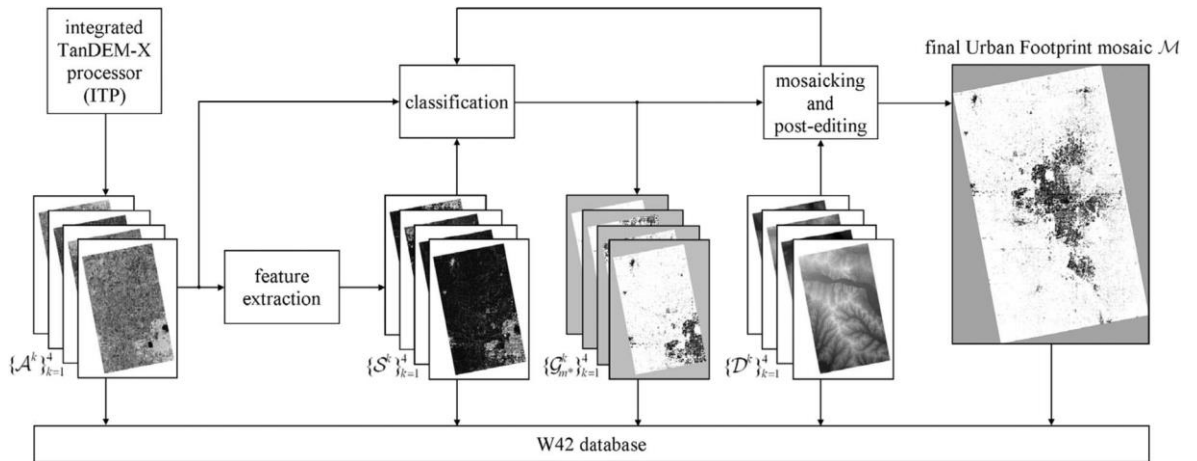


**Figure 4:** Schematic representation of the process chain of the "Urban Footprint Processor" (Esch et al. 2013: 1618)

The utilization of the “Urban Footprint Processor” enabled already to derive human settlement classifications covering the whole globe from around 180.000 radar images of the TerraSAR-X and TanDEM-X satellites. This Global Urban Footprint (GUF) is available in two

## 2. STUDY SITES & DATA

---

different resolutions, namely 12m (high resolution) and 75m (medium resolution). (Felbier et al. 2014: 4816)

Within this study, an extract of the high resolution GUF of London (see Appendix 5), derived from radar data of the year 2011, was utilized in the context of urban structure classification using an independent reference unit of square objects. This allowed for generating square objects only for areas which are classified as “built-up” in the GUF dataset.

### 3. METHODOLOGY

The workflow of this study comprises four methodological steps which are presented briefly in the following:

(1) The *first step* is concerned with the validation of the Urban Atlas classification scheme. This is done using the city of London as an example. The reference dataset for the validation is a high resolution 3D city model (UKMap building inventory). Initially, some preprocessing steps are conducted in order to correct inconsistencies of the UKMap building inventory and of the Urban Atlas dataset. From the corrected 3D model physical parameters such as building size and density are calculated on Urban Atlas building block level. By comparing the calculated parameters with the particular Urban Atlas classes, the Urban Atlas classification scheme can be reviewed concerning its accuracy on the one hand and on whether it contains distinct information on urban structures on the other.

(2) In the *second step*, an object-based classification methodology is developed to extract information on urban structures utilizing Cartosat-1 nDSM data. The Urban Atlas building block level (initially implemented for the example of London) provides the spatial level. At the beginning, the physical parameters, calculated on Urban Atlas level within the first step, are used to delineate urban structures and create reference classifications. Subsequently, a mixture of spatial and textural features is computed for the spatial entities of building blocks. In the next step, Random Forest classification models are developed and applied on the Cartosat-1 nDSM dataset in London. Finally, the accuracy of the resulting classifications is assessed in order to gain confidence on their correctness and on the performance of the different classification models.

(3) The next and *third step* is concerned with the transferability evaluation of the previously developed urban structure classification methodology. On the one hand, it is evaluated whether the classification models developed based on the city structure of London do perform similar in another urban context. This is tested for the city of Paris in France. On the other hand, it is examined if equal classification results can be gained by substituting the Urban Atlas building blocks by an artificial reference unit of square objects, to evaluate if the classification can be conducted independently from the Urban Atlas dataset. This is tested for the city of London. By comparing the classification results on Urban Atlas level of Paris and on square

### 3. METHODOLOGY

---

---

object level of London with those on Urban Atlas level of London (see second working step) the transferability of the urban structure classification methodology can be evaluated.

(4) In the *fourth step*, a cross-city structural analysis is conducted based on the urban structures of London and Paris in order to demonstrate that information on the urban morphology allows for detailed urban analysis. Within this context, analogies and differences between the urban morphology – by means of physical parameters – of the two cities are identified depending on the distance to the respective city center.

A graphical outline of the methodological workflow is presented within Figure 5.

### 3. METHODOLOGY

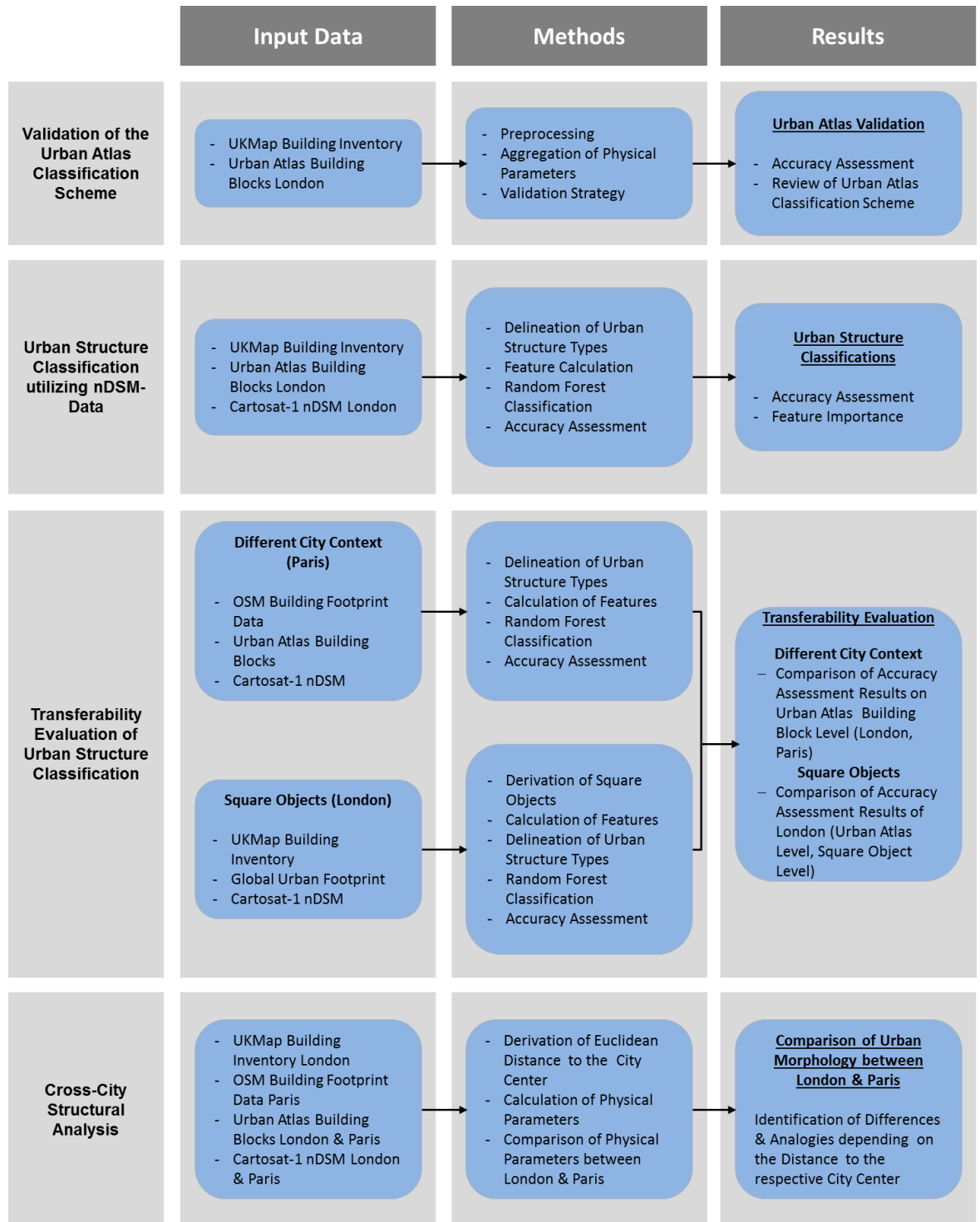


Figure 5: Methodological workflow of the study

#### 3.1 Validation of the Urban Atlas Classification Scheme

As indicated in the introduction (see *1.4 Research Objectives*), although the European Urban Atlas datasets allow for detailed urban analysis based on landuse/landcover information, these are criticized for hiding information on the morphology of cities (Prastacos et al. 2011: 2). At the first glance, the Urban Atlas classification scheme mainly comprises information on the landuse/landcover of urban areas and only few characteristics on the urban structure by means of the different degree of sealing ranges – given within the class descriptions of the “Continuous” and “Discontinuous Urban Fabric” classes. Nevertheless, it may be possible that the “Continuous” and “Discontinuous Urban Fabric” classes as well as the other Urban Atlas classes under consideration reveal further information on urban structures and urban morphologies although not explicitly mentioned.

The *UKMap building inventory* is a comprehensive database which provides information on building footprints and their associated height covering the whole city region of London. The building parameters allow for aggregating information on the physical spatial structure of cities – by means of physical parameters – on Urban Atlas building block level. Comparing the structural information with the class descriptions of the Urban Atlas classes on Urban Atlas building block level enables to examine whether or not the Urban Atlas dataset reveals distinct information on the horizontal and vertical structure of cities. Besides, those parameters can be utilized to validate the accuracy of the sealing degree ranges of the “Discontinuous” and “Continuous Urban Fabric” classes.

In the following sections the preprocessing steps as well as the derivation of physical parameters is described gradually. Eventually, a strategy for the validation of the European Urban Atlas classification scheme is introduced.

##### 3.1.1 Data Preprocessing

In order to be able to generate preferably accurate reference datasets for the aggregation of physical parameters a few preprocessing tasks need to be carried out.

###### UKMap Building Inventory

The UKMap building inventory in itself is not fully consistent and features some errors. These are polygons which were falsely classified as buildings – mainly encompassing green and forest areas. Since those expanses would distort the calculation of physical parameters and lead to an

overestimation of e.g. building densities, the incorrect building footprints need to be eliminated in advance. This is done by visually checking the dataset against Google Earth up-to-date satellite imagery (Google Inc. 2013). Thereby, incorrect polygons can be identified and removed manually.

The calculation of physical parameters requires the utilization of the parameters building height, building area as well as floor count values. However, the UKMap building inventory does only comprise information on the height and area of buildings. The number of floors, and in the case of some buildings even the height values, are missing. Hence, these values need to be modeled beforehand based on obtainable information.

The derivation of the floor counts is done as follows. The facades of around 70 buildings are visually checked, using Google Street View in order to count the number of floors and to generate a representative database with known accuracy. Within this context, attention is paid, to an equal spatial distribution of the buildings over the city area as well as to the coverage of the full range of building heights occurring in the UKMap dataset.

Subsequently, a linear regression is performed, which enables to determine the influence of an independent variable on a dependent variable (Wurm 2013: 148). The regression equation expresses the correlation between dependent and independent variables in mathematical terms. The robustness of the correlation between the independent and the dependent variables can be evaluated by means of the determination coefficient  $r^2$ . This is a measure which describes the explained variance of a dependent variable utilizing a specific regression model. In the best case  $r^2$  is alike 1/-1 and therefore enables to derive every dependent variable utilizing the respective independent variable within the regression equation. On the contrary, an  $r^2$  equal 0 means that there is no correlation at all between the considered data. (Bahrenberg et al. 1999: 136–148)

The linear regression carried out to model the floor counts is based on the correlation between the floor counts of the previously inquired buildings and their corresponding building height information. The regression analysis is done using the statistical software R (R Core Team 2014). Building height values are converted to floor counts by the following equation:

$$Y = -0.0032x^2 + 0.312x + 0.0021 \quad (1)$$

where  $Y$  is the dependent variable (floor counts) and  $x$  is the independent variable (building height).

The missing height values are derived performing a linear regression, too, but this time employing the correlation between the building area and building height. The derived equation used to model the missing height values reads as follows:

$$Y = (4E^{-10}x^3) - (3E^{-06}x^2) + 0.0105x + 9.8757 \quad (2)$$

where  $Y$  is the building height to be derived and  $x$  is the building area.

#### **Urban Atlas Dataset**

Another problem is given by a non-linear distortion of the Urban Atlas dataset of London. To overcome resulting positional inaccuracies of averagely 6m the dataset is newly geo-referenced. For this purpose, a topographic map provided within the “*Basemap Function*” of the ArcGIS Software (ESRI 2013) is utilized as reference data. Around 100 control points, equally distributed over the whole extent of the Urban Atlas dataset and precisely identifiable on both, the Urban Atlas dataset and the topographic map, are set. Subsequently, an affine transformation is executed in order to correct the distortions as far as possible.

#### **3.1.2 Aggregation of Physical Parameters**

The validation of the Urban Atlas classification scheme requires, first and foremost the generation of a database which allows for a systematical structural analysis. Therefore, a certain number of physical parameters need to be selected and calculated in advance.

Many authors consider the building density as one of the most important parameters when describing the physical structure of a city (e.g. Acioly Jr. and Davidson 1996: 6; OECD 2012: 27; Fina et al. 2014: 180). It measures the proportional area of a building block which is covered by buildings and is therefore suited to describe the horizontal urban structure. Nevertheless, in order to capture the holistic morphology of a city, the vertical component of urban objects has to be considered, too (Wurm and Taubenböck 2010b: 67). In this regard, Wurm and Taubenböck (2010a: 98) have stated that the size and height of buildings as well as their integration in the urban structure are valuable physical parameters to quantify the physical spatial structure of a city. The integration of building structures in the urban structure is among others definable by the previously mentioned building density and by the floor space

### 3. METHODOLOGY

density. The floor space density is an index which measures the total floor area of buildings within a building block as a share of the total area of that considered building block.

To calculate physical parameters describing the structure of a city, spatial reference areas are needed (Taubenböck et al. 2010: 87). Since the Urban Atlas dataset provides information on the basis of building blocks, these are used as reference units for physical parameter aggregation. In order to implement information on the size and height of buildings on building block level, the mean building volume as well as the mean height present suitable measures in addition to the building density and floor space density. Thus, these four physical parameters are selected for the purpose of Urban Atlas validation within the scope of this study.

In order to derive the chosen physical parameters, the building parameters of the UKMap building inventory are aggregated on Urban Atlas building block level using the equations described in Table 4. Nevertheless, since the spatial coverage of the Urban Atlas exceeds that of the UKMap building inventory, the building blocks that do not contain buildings of the latter are initially excluded from the calculation. This is done in order to avoid zero values of the physical parameters which do not necessarily mirror the actual urban structure of the building blocks, but are rather an outcome of the different spatial extents of the two datasets.

As a result, a data basis containing the four physical parameters on Urban Atlas building block level is created.

**Table 4:** Overview of the selected physical parameters with the respective equations

Physical parameter	Equation	Variables
Building Density (in %)	$BD = \frac{\sum_{n=1}^{n_{Ru}} B_{a_n}}{R_{ua}}$	(3) $R_u$ = Building Block $R_{ua}$ = Building Block Area
Floor Space Density	$FSD = \frac{\sum_{n=1}^{n_{Ru}} (B_{f_n} \times B_{a_n})}{R_{ua}}$	(4) $B_a$ = Building Area $B_h$ = Building Height $B_f$ = Floor Count per Building
Mean Building Volume (in m <sup>3</sup> )	$\overline{Vol} = \frac{\sum_{n=1}^{n_{Ru}} (B_{h_n} \times B_{a_n})}{n_{Ru}}$	(5) $n$ = Number of Buildings
Mean Building Height (in m)	$\overline{Hgt} = \frac{\sum_{n=1}^{n_{Ru}} B_{h_n}}{n_{Ru}}$	(6)

#### 3.1.3 Validation Strategy

The validation of the Urban Atlas classification is carried out by comparing the values of the previously calculated physical parameters with the Urban Atlas classes on Urban Atlas building block level utilizing boxplots. Boxplots are graphical figures that enable to interpret the distribution and position of data values. A Boxplot consists of a box with two whiskers on the upper and lower side of it. The box itself is a representation of the interquartile range between the first and third quartile, containing 50% of all occurring values. The whiskers display the 1.5-fold interquartile distance. Additionally, the median can be inferred by means of the line within the box (see Figure 6). (Wurm 2013: 83)

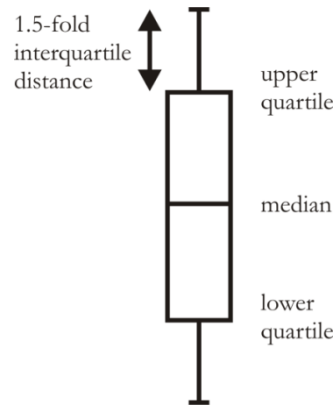


**Figure 6:** Schematic illustration of a boxplot

With the help of boxplots the value ranges of the different physical parameters on building block level per Urban Atlas class can be identified. Outliers are neglected since these are not representative and would lead to an erroneous representation of the upper and/or lower class limits. The sufficiency of the Urban Atlas classification scheme to characterize horizontal and vertical urban structures requires that the classes reveal a certain degree of homogeneity. Furthermore, the between-class variability should be significant enough in order to allow differentiation between the considered Urban Atlas classes. Thus, the validation of the Urban Atlas classification scheme is done by comparing the particular value ranges of the physical parameters on within-class level as well as on between-class level. The homogeneity of the classes is a measure for the homogeneity of the urban structure these represent. Besides, the more clearly the separability between the Urban Atlas classes with regard to the considered physical parameters, the more appropriate are the classes to represent specific urban structures and to describe a city's morphology. Thus, the within-class and between-class evaluation of the consid-

ered Urban Atlas classes enables to evaluate whether the Urban Atlas classification scheme contains distinct information on urban structures or not.

A further concern of this study is to assess the accuracy of the “Discontinuous” and “Continuous Urban Fabric” classes. In order to do this, the degree of sealing ranges of the “Discontinuous” and “Continuous Urban Fabric” classes were compared with the building densities aggregated on block level of the same classes utilizing boxplots. The correspondence between the density ranges, given in the description of the “Discontinuous” and “Continuous Urban Fabric” classes of the Urban Atlas, and the degree of sealing ranges prevalent on the building blocks of the same classes, is used for assessing the accuracy. Within this context, it should be noted that the building density values are averagely smaller than the respective sealing degree values given in the Urban Atlas class descriptions. This is caused by the fact that the degree of sealing values were derived using a soil sealing layer (EEA 2010c: 2) which measures the percentage of sealing of a building block, considering buildings, streets and other artificial objects. The building density on the contrary was aggregated – as the name already indicates – solely on the basis of buildings.

#### **3.2 Urban Structure Classification utilizing Cartosat-1 nDSM-Data**

The central hypothesis of this study states that the Urban Atlas classes only partially contain distinct information on urban structures. However, in order to describe a city’s morphological composition information on the horizontal and vertical city structure is an obligatory prerequisite (Wurm and Taubenböck 2010b: 67). These information on urban structures serve as a valuable information basis (Anas et al. 1998: 1426) in order to gain comprehensive knowledge and support intelligent decisions for a sustainable urban growth (Herold et al. 2003: 1443).

The nDSM data generated based on stereo images of Cartosat-1 provide a reliable data source to implement 3D information by means of the height values of the single pixels. Furthermore, although the geometrical resolution of 5m does not allow the extraction of individual buildings, pixels with a height value exceeding 0m can be seen as a generalized representation of urban objects (Taubenböck et al. 2013: 395). Therefore, information on the 2D coverage of urban objects above ground – even though accompanied by a certain degree of information loss (Klotz 2012: 36) – can be derived from the nDSM-datasets, too.

Taking into account this prior knowledge, a methodology towards urban structure delineation – by means of urban structure types – based on the Cartosat-1 nDSM dataset is to be devel-

oped. In this regard, one necessary requirement to derive urban structure types based on remotely sensed data is the employment of reference units. The Urban Atlas datasets provide such information in terms of the individual building blocks and are therefore utilized as the spatial entities to be classified. Since the individual building blocks are composed of several pixels of the Cartosat-1 nDSM dataset an object-based method is applied within the scope of this study.

Object-based image analysis uses a two-step process comprising image segmentation and classification. However, these are further composed of many intermediate processes (Campbell and Wynne 2011: 371). The stepwise procedure of the object-based approach applied within this study is described in the following sections.

#### 3.2.1 Delineation of Urban Structure Types

A commonly used approach to describe the physical face of a city is the delineation of smaller entities in classes with similar structural characteristics, the so-called urban structure types. However, no compulsory and generally accepted scheme for the delineation of urban structure types exists so far, so that their definition is always case specific, mainly depending on the area under study and the objective of an analysis (Banzhaf and Höfer 2008: 131).

Thus, in order to automatically derive information on the physical spatial structure of cities, appropriate urban structure type classes need to be defined in advance (Voltersen et al. 2014: 194). This definition can be done using physical parameters which are suitable to describe the physical spatial structure of cities, for instance the amount and/or arrangement of urban objects like buildings within the spatial reference units (Bochow et al. 2010: 1796).

The physical parameters aggregated based on the building parameters of the UKMap building inventory (see section *3.1.2 Aggregation of Physical Parameters*) meet the requirements to represent the physical spatial structure of a city on the basis of spatial reference entities, namely the Urban Atlas building blocks of London. Particularly, the mean building height and the building density are measures which are suitable to characterize the 3D and 2D urban structure, respectively. Therefore, urban structure type delineation is conducted on Urban Atlas building block level utilizing building density and mean height for the differentiation purpose.

However, one of the later working steps of this study tests the performance of the classification methodology in a different city context, namely Paris in France. Thus, the LiDAR-derived

height values of the UKMap building inventory need to be substituted by height information of the Cartosat-1 nDSM dataset of London. Only the Cartosat-1 nDSMs are available for entire Europe (Uttenthaler et al. 2013: 4) and provide compared to the sparsely available LIDAR data consistent coverage. Thus, using the height information of the Cartosat-1 data allows for generating a transferable urban structure type classification scheme. Using the respective equations given in Table 4 (see section 3.1.2 *Aggregation of Physical Parameters*) the mean height is aggregated on Urban Atlas level, but this time using the Cartosat-1 height information. Within this context, it should be noted that the areal coverage of the Cartosat-1 nDSM of London is smaller than that of the Urban Atlas dataset of London (see Appendix 3). Therefore, only those Urban Atlas building blocks as well as those buildings of the UKMap building inventory that are located within the area covered by the nDSM data are taken into consideration for urban structure type delineation.

In order to utilize the chosen physical parameters for the delineation of urban structure types, both, the building density and the mean height range on Urban Atlas building block level need to be divided into preferably meaningful classes. This requires the definition of an appropriate number of classes in advance.

The Urban Atlas “Discontinuous” and “Continuous Urban Fabric” classes are partitioned into five classes, each corresponding to a specific sealing degree range. However, taken together the complete range of sealing degrees of the Urban Atlas “Discontinuous” and “Continuous Urban Fabric” classes is larger than that of the building densities aggregated on Urban Atlas level. This results from the fact that the first measures the degree of sealing per building block, including buildings, streets and other artificial objects while the latter considers buildings only. Thus, the number of classes was reduced from five to a maximum of three and a minimum of two. The three classes are supposed to be representatives for high, medium and low building densities respectively mean heights. Additionally, the binary approach is chosen in case the Cartosat-1 nDSM dataset proves to be insufficient to extract more differentiated information. In this context, the two classes are representatives of high and low building densities respectively mean heights.

The class breaks are defined utilizing the Jenks Natural Breaks algorithm. The algorithm derives class limits in order that within-class differences are minimized and between-class differences are maximized (ESRI 2014). Resulting from the previously defined number of classes as

### 3. METHODOLOGY

well as from the derived class breaks, respectively two building density and mean height classification schemes are generated. These are shown in Table 5.

**Table 5:** Class-breaks of physical parameters for different numbers of classes

	Class description	Building density (in %)	Mean height (in m)
<b>3 Classes</b>	low	$\leq 24$	$\leq 7.5$
	medium	$> 24 - \leq 40$	$> 7.5 - \leq 11.3$
	high	$> 40$	$> 11.3$
<b>2 Classes</b>	low	$\leq 29.7$	$\leq 8.8$
	high	$> 29.7$	$> 8.8$

In order to meet the requirements of a classification methodology suitable to extract information on the horizontal and vertical physical structure of cities simultaneously, the urban structure type classes need to contain both, 2D and 3D information. Hence, the building density and the mean height classification schemes were further combined in every possible way. Thereby, four different urban structure type classification schemes are derived. One example is shown in Table 6.

**Table 6:** Example of urban structure type classification key

Class number	Class description
<b>1 1</b>	<b>low low</b>
<b>1 2</b>	<b>low high</b>
<b>2 1</b>	<b>medium low</b>
<b>2 2</b>	<b>medium high</b>
<b>3 1</b>	<b>high low</b>
<b>3 2</b>	<b>high high</b>
<b>Building density</b>	
<b>Mean height</b>	

Both, the four urban structure type as well as each of the two building density and the mean height classification schemes are applied on Urban Atlas building block level. As a result, eight

reference classifications – containing information on the 2D and 3D urban structure in combined and separate form – are generated.

#### **3.2.2 Feature Calculation**

Thematic classification of image objects based on remotely sensed data is normally conducted using a multitude of properties – within this study referred to as features – which enable to discriminate different thematic classes. These features are not synonymous with geographical features but statistical characteristics of the image objects in numerical form (Campbell and Wynne 2011: 341; Lillesand et al. 2004: 551). In order to be able to distinguish the individual classes of the different reference classifications based on the Cartosat-1 nDSM dataset, some suitable features need to be selected and calculated.

#### **Selection of appropriate Features**

In the scope of this research, urban structure type classification schemes are derived based on spatial characteristics – building density and mean height – of the Urban Atlas building blocks. Those spatial properties, as stated by Bochow et al. (2010: 1796), can be assessed from images by calculating spatial features. In the scope of urban structure type classification based on remotely sensed data, a variety of studies have already successfully applied spatial features for object-based differentiation of urban structures (Wurm et al. 2010; Bochow et al. 2010; Voltersen et al. 2014; Hermosilla et al. 2014; Heinzl and Kemper 2015; Taubenböck et al. 2013). Features used within this context were among others, building density, floor space density as well as height and volume parameters.

Another important characteristic which can be used to assess information from remotely sensed data is texture. Textural features contain information about the spatial distribution of tonal variations within an image or image object (Haralick et al. 1973: 611–612). There are several ways to calculate textural features (Herold et al. 2003: 993). Nevertheless, most commonly these are derived utilizing Grey-Level Co-occurrence Matrices (GLCM) introduced by Haralick et al. (1973). The GLCM statistically describe the relationship of neighboring pixels within an image or image object, and can be calculated for different angles and distances between pixels (Haralick et al. 1973: 612; Haralick 1979: 791). With the help of GLCM several textural features like dissimilarity, entropy, contrast etc. can be derived which were applied in a variety of studies concerned with landuse/landcover classifications in urban environments

### 3. METHODOLOGY

achieving promising results (e.g. Herold et al. 2003; Pacifici et al. 2009; Mahmoud et al. 2011; Mhangara and Odindi 2013).

Taking into consideration the above mentioned advantages, a set of ten spatial features (see Table 7) and eight textural features after Haralick et al. (1973) (see Table 8) is selected for the purpose of urban structure type classification based on the Cartosat-1 nDSM dataset of London within this study.

**Table 7:** Pixel-based equations of selected spatial features

Feature	Pixel-based Equation	Variables
Building Density	$BD = \frac{\sum_{n=1}^{n_{R_u}} P_{a_n}}{R_{ua}}$	(7) $R_u =$ Building Block $R_{ua} =$ Building Block Area
Floor Space Density	$FSD = \frac{\sum_{n=1}^{n_{R_u}} (P_{f_n} \times P_{a_n})}{R_{ua}}$	(8) $P_a =$ Pixel-based Area $P_h =$ Pixel-based Height
Mean Height	$\overline{Hgt} = \frac{\sum_{n=1}^{n_{R_u}} P_{h_n}}{n_{R_u}}$	(9) $P_f =$ Pixel-based Floor Count $n =$ Number of Built-up Pixels
Maximum Height	$Hgt_{max} = \max_{n \in R_u} (P_{h_n})$	(10)
Median Height	$Hgt_{med} = \text{med}_{n \in R_u} (P_{h_n})$	(11)
Quantile90 Height	$Q_{90} = Q_{90}_{n \in R_u} (P_{h_n})$	(12)
Standard Deviation Height	$Hgt_{std} = \text{std}_{n \in R_u} (P_{h_n})$	(13)
Volume	$Vol = \sum_{n=1}^{n_{R_u}} (P_{h_n} \times P_{a_n})$	(14)
Mean Volume	$\overline{Vol} = \frac{\sum_{n=1}^{n_{R_u}} (P_{h_n} \times P_{a_n})}{n_{R_u}}$	(15)
Normalized Volume	$Vol_{norm} = \frac{\sum_{n=1}^{n_{R_u}} (P_{h_n} \times P_{a_n})}{R_{ua}}$	(16)

### 3. METHODOLOGY

**Table 8:** Description of selected Haralick texture features

Feature	Description	Source
Angular 2nd Moment	Measures the homogeneity of pixel values	Trimble GmbH 2014b: 377
Contrast	Measures the amount of local pixel value variations	Trimble GmbH 2014b: 375-376
Correlation	Measures the linear dependency between neighboring pixel values	Trimble GmbH 2014b: 379
Dissimilarity	Measures the contrast of pixel values	Trimble GmbH 2014b: 376
Entropy	Measures the distribution of GLCM elements	Trimble GmbH 2014b: 377
Homogeneity	Measures the amount of local pixel value variations opposite to contrast	Trimble GmbH 2014b: 375
Mean	Measures the average co-occurrence of pixel values	Trimble GmbH 2014b: 378
Standard Deviation	Measures the dispersion of pixel values around the mean	Trimble GmbH 2014b: 378

#### **Feature Calculation**

Feature calculation is carried out within the object-based image analysis software eCognition Developer (Trimble GmbH 2014b) on the basis of a top-down segmentation approach, adapted and modified after Klotz (2012: 35 ff.).

The derivation of spatial features is done utilizing the Cartosat-1 nDSM dataset of London. As already mentioned in the beginning of this chapter, the pixel size of the nDSM data does not allow extracting single buildings (Taubenböck et al. 2013: 395). Therefore, spatial features are calculated using the pixels as substitutes for urban objects as conducted by Klotz (2012) and Taubenböck et al. (2013), who employed the same dataset for central business district delineation.

For the purpose of calculating textural features the height values of the Cartosat-1 nDSM are reclassified in order to minimize the computational effort as suggested by Jensen (2005: 423). This is done utilizing the reclassification key presented in Table 9.

### 3. METHODOLOGY

**Table 9:** Cartosat-1 nDSM reclassification key

Cartosat-1 nDSM heights (in m)	Reclassified value
0	0
1 - 8	1
9 - 23	2
24 - 38	3
39 - 53	4
54 - 68	5
69 - 83	6
84 - 98	7
99 - 113	8
114 - 128	9
> 129	10

The segmentation procedure is carried out on the basis of the Cartosat-1 nDSM which represents the pixel level. The lowest spatial scale is the Urban Atlas Level (L1) (see Figure 7) which is created by integrating the Urban Atlas dataset of London as a thematic layer into the segmentation procedure.

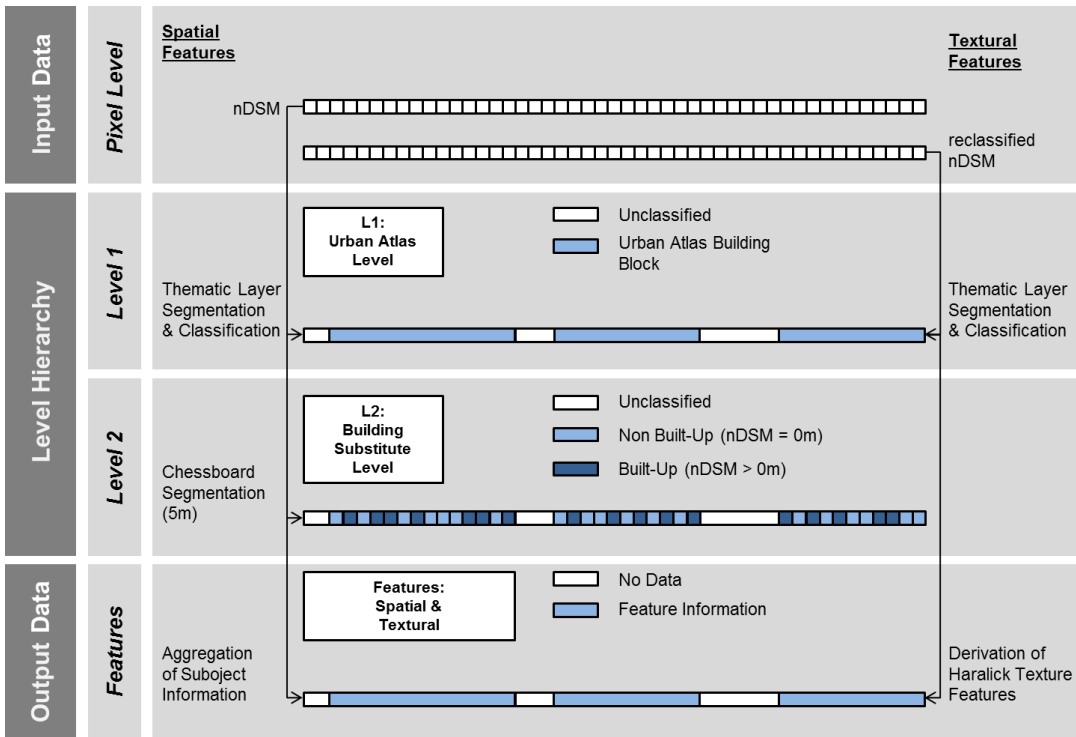


**Figure 7:** Top-down segmentation scheme – Urban Atlas level (modified after Klotz 2012)

In order to be able to calculate the selected spatial features a Building Substitute Level (L2) needs to be created, too. This is done by copying L1 and performing chessboard segmentation within the individual building blocks. The size of the square segments to be created is set to 25m<sup>2</sup> as this equals the pixel level of the Cartosat-1 nDSM. By classifying the pixels with height values greater than 0m into ‘built-up’ and that with height values alike 0m into ‘non-built-up’, a pixel-based representation of urban objects and surface area within each of the Urban Atlas building blocks (L1) is generated. Subsequently, the spatial features are calculated by aggregating the individual pixel values of the Building Substitute Level (L2) on the individual building blocks of the Urban Atlas Level (L1) employing relational features (Trimble GmbH 2014a: 280). Within this context, only the pixels classified as ‘built-up’ are of interest since these present the substitute for urban objects above ground. The ten selected spatial features are derived using the pixel-based equations presented within Table 7.

Nevertheless, one of the spatial features to be calculated is the floor space density which requires a pixel-based floor count substitute to be modeled in advance. This is done by linear regression based on the correlation between the floor counts of the previously inquired buildings (see section 3.1.1 *Data Preprocessing*) and their corresponding Cartosat-1 nDSM height information. The Cartosat-1 nDSM height values are converted into floor counts utilizing the following equation:

$$P_f = -0.0081x^2 + 0.4402x + 0.1849 \quad (17)$$

where  $P_f$  is the pixel-based floor count to be modeled and  $x$  the corresponding Cartosat-1 nDSM height value of the pixels classified as ‘built-up’.

In order to derive the eight selected textural features after Haralick et al. (1973) GLCM are utilized. The GLCM are computed for all building blocks of the Urban Atlas Level (L1) in all directions – this means considering all neighboring pixels in the directions 0°, 45°, 90° and 135° (Trimble GmbH 2014a: 374) – based on the reclassified nDSM. The name as well as a short description of the employed textural features is presented in Table 8.

Resulting from the calculations of the ten spatial features and eight textural features an 18-dimensional feature vector is generated. This contains the numerical values of the spatial and textural features for each building block on Urban Atlas Level (L1).

#### 3.2.3 Random Forest Classification

When information on class membership as well as on feature values of the objects to be classified is available, classification can be conducted following a supervised approach. In supervised classification this prior knowledge is used to develop classification models in order to subsequently be able to classify data of unknown identity (Campbell and Wynne 2011: 349). A variety of classifiers is available for supervised classification. Some of these are machine learning<sup>2</sup> algorithms like artificial neural networks, support vector machines, decision trees and ensemble learning classifiers (Rodríguez-Galiano et al. 2012b: 94).

In recent years, ensemble learning classifiers have increasingly been proved successful (Waske et al. 2009: 17). These are sets of single classifiers whose individual decisions are combined to classify new data (Pal 2005: 217). Advantages of the ensembles are that they utilize the strength of individual classifiers on the one hand while avoiding their weaknesses on the other (Ghimire et al. 2010: 46; Rodríguez-Galiano et al. 2012b: 94). Thus, ensembles generate more accurate results and are more robust to noise in comparison to conventional classification methods (Breiman 1996: 124; Rodríguez-Galiano et al. 2012b: 94).

Random Forest is an ensemble learning classifier based on a combination of decision trees and was first introduced by Breiman (2001). The classifier has shown promising results in a variety of remote sensing applications (e.g. Pal 2005; Guo et al. 2011; Rodríguez-Galiano et al. 2012a; Rodríguez-Galiano et al. 2012b). Advantages of the classifier in the field of remote sensing are, that it runs fast on large datasets, can handle high-dimensional feature spaces, estimates which of the features mostly contribute to the classification, has an inherent error measure and is robust against overfitting, noise and outliers (Rodríguez-Galiano et al. 2012b: 95–96). Furthermore, Fernández-Delgado et al. (2014) who reviewed the performance of a large number of classifiers on a variety of datasets, have found that Random Forest performed best in the majority of tested applications.

Under consideration of the explanations presented above a Random Forest approach is selected for the purpose of urban structure type classification within the scope of this study.

---

<sup>2</sup> “Machine learning is an area of artificial intelligence and generally refers to the development of methods that optimize their performance by iteratively learning from the data (Waske et al. 2009: 4).”

#### **Theoretical Background of the Random Forest Algorithm**

The Random Forest algorithm combines bagging with decision trees (Breiman 1996) and a random feature selection method (Breiman 2001).

In bagging different sample subsets – the bootstrap samples or bags – are created from the original training dataset (Guo et al. 2011: 60). This is done using a technique called bootstrap aggregating (Rodriguez-Galiano et al. 2012b: 96) which randomly resamples the training data with replacements (Rodriguez-Galiano et al. 2012a: 95; Breiman 2001: 11). Within this context, some of the samples of the original training dataset are considered when creating a bootstrap sample – altogether around 2/3 of the total count - while others are completely discarded (Rodriguez-Galiano et al. 2012b: 96). In order to train the classifier, a decision tree is independently grown from each of the different bootstrap samples (Liaw and Wiener 2002: 18; Guo et al. 2011: 60).

In addition to bagging, Random Forest changes how the decision trees are constructed (Liaw and Wiener 2002: 18). The classifier uses a randomly selected subset of features at each node to find the best split and not like conventional tree-methods all input features (Rodriguez-Galiano et al. 2012a: 95) and therefore adds a further layer of randomness to bagging (Liaw and Wiener 2002: 18).

For the classification itself Random Forest utilizes the entire tree ensemble. Each of the trees gives a unit vote at each of the input samples to be classified. In accordance with the principle “the winner takes it all” the final class for each of the samples is determined by the majority vote of all trees (Guo et al. 2011: 60). An overview of the work flow of the Random Forest training and classification is presented in Figure 8.

The samples that are not considered when creating the bootstrap samples – the remaining 1/3 of the original training data – form the so-called Out-Of-Bag (OOB) subsets (Guo et al. 2011: 60) which are independently created for every tree (Rodriguez-Galiano et al. 2012b: 96). These are not considered when training the classifier and can therefore be used to assess the Random Forest ensemble performance (Rodriguez-Galiano et al. 2012a: 95).

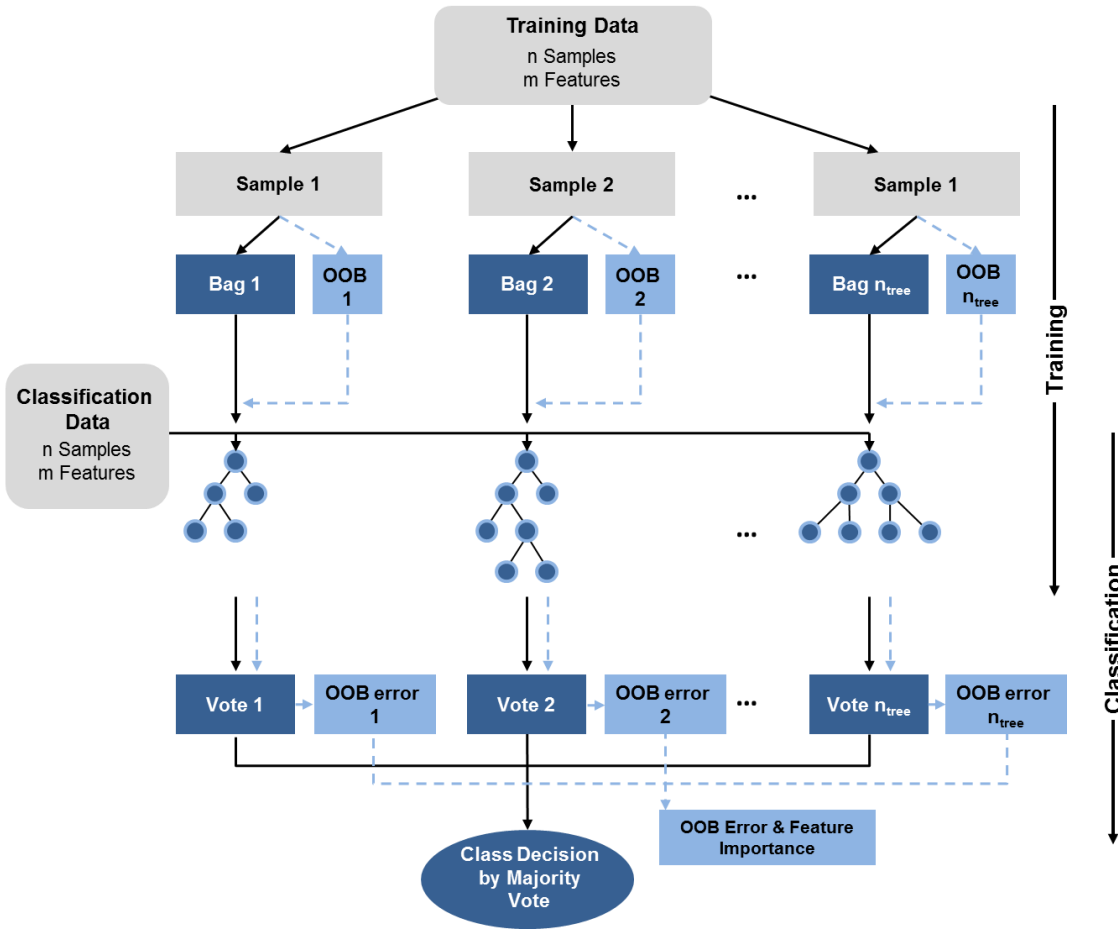


Figure 8: Random Forest (RF) work flow (modified after Guo et al. 2011)

One parameter to measure the model performance is the OOB error. By classifying each of the OOB samples utilizing only the classification trees which did not use the respective sample for training, every single sample of the total OOB samples has averagely been run through 1/3 of the total number of trees (Breiman 2001: 11). The majority vote of the considered trees – a smaller ensemble version of the Random Forest model – decides the class membership of the respective sample. The OOB error is then expressed by the proportion between the misclassifications and the total number of OOB samples and provides an unbiased estimation of the generalization error (Rodriguez-Galiano et al. 2012b: 96).

Based on the OOB subsets the relative feature importance can be calculated, too. Therefore, each of the features is successively switched while keeping the remaining features constant. The importance of each feature is calculated for every tree by measuring the difference between misclassifications before and after the exclusion of the considered feature. In order to gain information on the importance of each feature within the total Random Forest classifier

ensemble, the importance measures of the single trees are averaged for each feature, respectively (Breiman 2001: 23–24; Rodriguez-Galiano et al. 2012b: 96).

The application of the Random Forest algorithm is very user-friendly by means that only two parameters need to be defined when developing a classification model. These are the number of bootstrap samples  $n_{\text{tree}}$  and the number of features to be randomly selected at each node  $m_{\text{Try}}$  (Breiman 2002: 3; Guo et al. 2011: 60; Rodriguez-Galiano et al. 2012b: 97).

#### **Implementation of Random Forest Classification**

The Random Forest classification models for urban structure type classification are derived using the “randomForest” Package (Liaw and Wiener 2015) within the statistical software R (R Core Team 2014).

Classification models are developed based on the four different urban structure type as well as based on each of the two building density and mean height reference classifications (see section 3.2.1 *Delineation of Urban Structure Types*). On the one hand, this experimental setup is chosen in order to test whether or not, and if possible to what extent respectively level of detail urban structures can be classified based on the Cartosat-1 nDSM-dataset. On the other hand, the utilization of the classifications containing information solely on either the 2D or 3D urban structure enables to evaluate the performance of the classifier in extracting information on the building density and mean height, respectively based on the Cartosat-1 nDSM-dataset, too.

The Urban Atlas building block dataset contains the information on the class membership – in accordance to the considered classification scheme – as well as on the corresponding feature values for each building block, respectively. Since a supervised classification approach is conducted, some of the building blocks are used for training the classifier respectively for deriving the classification model. Training samples are selected using a stratified random sampling approach which considers the prior knowledge about the classification by means of class membership of the samples and class frequencies (Congalton and Green 1999: 23; Campbell and Wynne 2011: 399). In total, 10% of the Urban Atlas building blocks of each class per considered classification scheme are randomly selected out of the total dataset. Thus, the resulting training datasets represent a 10% share of the respective reference classification while maintaining the occurring frequencies of the classes. The remaining 90% of the data not utilized for training are used for classification and a subsequent accuracy assessment which is described in detail within the next section.

The development of classification models based on the Random Forest algorithm requires the number of features to be randomly selected at each node  $m_{\text{Try}}$ , and the number of bootstrap samples  $n_{\text{tree}}$  to be defined in advance. In order to select the optimal values of these parameters two different procedures are conducted.

In general, the Random Forest algorithm is not too sensitive concerning  $m_{\text{Try}}$  and therefore the default value of  $\sqrt{p}$  – where  $p$  is the number of features – is often maintained since it gives near optimum results in many cases (Breiman 2002: 3). Nevertheless, a parameterization of the  $m_{\text{Try}}$  values for all classification models is yet done in the scope of this study utilizing the “TuneRF” function integrated within the “randomForest” Package. The function searches, beginning from the default value the optimal number for  $m_{\text{Try}}$  with respect to the decrease of the OOB error (Liaw and Wiener 2015: 26).

The number of bootstrap samples or trees  $n_{\text{tree}}$  is the second parameter to be defined. A step-wise increase of the number of trees improves the classification until at some point the classifiers performance converges (Rodriguez-Galiano et al. 2012a: 98). However, Random Forest does not overfit as more trees are added (Breiman 2001: 7). Hence, increasing the number of trees after the point of convergence is reached, neither leads to a decrease nor to an increase of the generalization error (Rodriguez-Galiano et al. 2012b: 97). However, it requires a higher computational effort. A good estimator for the generalization error depending on the number of trees is the OOB error (Rodriguez-Galiano et al. 2012b:97). In order to identify the point of convergence the classification models are repeatedly trained constantly keeping the optimal number of  $m_{\text{Try}}$  while changing the  $n_{\text{tree}}$  values. The optimal number of  $n_{\text{tree}}$  corresponds to the point of convergence and therefore the point where the OOB error not significantly changes anymore.

#### 3.2.4 Accuracy Assessment

The information derived by classification of remote sensing data can only be considered reliable and correct after its accuracy has been assessed. Accuracy assessment is normally conducted by evaluating the correspondence between predicted class membership and reference class membership of objects or pixels and therefore, gives an impression to which degree the classification result agrees with reality or ‘truth’ (Foody 2002: 186).

One straightforward option to computationally evaluate the accuracy of classifications is the so-called confusion or error matrix. It allows establishing a relation between reference entities

### 3. METHODOLOGY

– pixels or objects of known identity – and the class of the same entities assigned by the utilized classification model. Within this context, the number of columns and rows of the confusion matrix equals the number of informational categories to be classified (Campbell and Wynne 2011: 417; Lillesand et al. 2004: 586). A scheme of the confusion matrix is exemplified within Figure 9.

		Reference Data				
		A	B	C	D	Σ
Classification Data	A	$n_{AA}$	$n_{AB}$	$n_{AC}$	$n_{AD}$	$n_{A+}$
	B	$n_{BA}$	$n_{BB}$	$n_{BC}$	$n_{BD}$	$n_{B+}$
	C	$n_{CA}$	$n_{CB}$	$n_{CC}$	$n_{CD}$	$n_{C+}$
	D	$n_{DA}$	$n_{DB}$	$n_{DC}$	$n_{DD}$	$n_{D+}$
	Σ	$n_{+A}$	$n_{+B}$	$n_{+C}$	$n_{+D}$	$n$

**Figure 9:** Schematic representation of a confusion matrix (modified after Foody 2002)

The confusion matrix allows identifying and specifying classification errors (Foody 2002: 187), the so-called errors of commission and errors of omission. The commission error – derivable from each row of the matrix – is a specification for pixels or objects which were included in the false class. The omission error – derivable from each column of the matrix – is a measure for pixels or objects which were excluded from the class they belong to (Congalton and Green 1999: 10; Richards and Jia 2006: 314).

Analogously to the error measures the classification accuracy can be assessed from the confusion matrix. In this context, the most prominent measure is the overall accuracy (OA) which can be calculated by dividing the total number of correct classified entities by the total number of reference entities (see equation 18).

$$OA = \frac{\sum_{i=1}^k n_{ii}}{n} \quad (18)$$

with  $k$  being the number of classes,  $n_{ii}$  being the number of correct classified samples and  $n$  the total number of reference samples (Congalton and Green 1999: 48).

The accuracy of the individual classes of interest can be evaluated by computing the User's Accuracy (UA) and the Producer's Accuracy (PA) (Congalton and Green 1999: 10). The UA

---



---

### 3. METHODOLOGY

---



---

can be calculated by dividing the total number of correct classified entities of one class ( $n_{ii}$ ) by the total number of entities of the same class ( $n_{i+}$ ) – the row totals – and is therefore the counterpart of the commission error (see equation 19) (Congalton and Green 1999: 48)

$$UA = \frac{n_{ii}}{n_{i+}} \quad (19)$$

The PA on the contrary, can be calculated by dividing the total number of correct classified entities of one class ( $n_{jj}$ ) by the total number of reference entities of the same class ( $n_{+j}$ ) – the column totals – and is therefore the counterpart of the omission error (see equation 20) (Congalton and Green 1999: 48).

$$PA = \frac{n_{jj}}{n_{+j}} \quad (20)$$

One obstacle in the context of accuracy assessment with the parameters described above is that they do not accommodate the effects of chance agreement (Foody 2002: 188). Some of the entities to be classified may be allocated to the right category during classification process but simply by chance. The Kappa Coefficient is a measure which considers all the elements of the confusion matrix and thereby overcomes the obstacle of chance agreement (Congalton and Green 1999: 59). A further advantage of the Kappa is that it constitutes an adequate measure when comparing results of different classifications (Foody 2002: 188) – as desired within the frame of this research. The equation to compute the Kappa reads as follows:

$$Kappa = \frac{N \sum_{i=1}^r x_{ii} - \sum_{i=1}^r (x_i + x_{+i})}{N^2 \sum_{i=1}^r (x_i + x_{+i})} \quad (21)$$

where  $N$  is the total number of samples,  $r$  is the total number of rows,  $x_{ii}$  the value of row  $i$  as well as column  $i$  and  $x_{+i}$  and  $x_i$  the totals of the columns and rows (Congalton and Green 1999: 50).

The resulting Kappa values range between 0 and 1, where a value of 1 indicates a total agreement between classification and reference data while a value of 0 means that there is no agreement respectively only chance agreement (Congalton and Green 1999: 50). Within this context, Landis and Koch (1977) developed an interpretation key which can be utilized when scoring the resulting Kappa values and thus, evaluating the classification performance.

**Table 10:** Interpretation key for Kappa Values

Kappa Value	Agreement
0	no/chance agreement
0.01 – 0.20	slight
0.21 – 0.40	fair
0.41 – 0.60	moderate
0.61 – 0.80	substantial
0.81 – 1.00	almost perfect

Source: modified after Landis and Koch 1977

In the scope of this study, the above introduced accuracy measures are calculated for all classification results – the four urban structure type classifications as well as the four building density and mean height classifications – and thereby allows for evaluating the performance of the urban structure type derivation utilizing the Random Forest classifier based on the Cartosat-1 nDSM dataset.

### 3.3 Transferability Evaluation of Urban Structure Type Classification

Within the previous chapter, the development of a classification methodology to automatically detect urban structures based on the Cartosat-1 nDSM dataset was introduced. Within this context, urban structure classification schemes were derived on the basis of physical parameters aggregated from the building parameters of London using the UKMap building inventory on Urban Atlas building block level. The urban structure type classification itself was further done by using the individual Urban Atlas building blocks as reference units.

The physical parameters as well as the class breaks for the purpose of urban structure delineation are derived solely based on the urban structure of London. Nevertheless, the structure of other cities may be completely different in order that the defined categories might not be present or differ in some way. Furthermore, Urban Atlas datasets are only available for cities with more than 100,000 inhabitants in Europe (EEA 2010b) and thus, constitute an obstacle when someone seeks to analyze the morphological structure of smaller cities or cities on another continent. Moreover, structural comparison between different urban areas is limited to the available Urban Atlas datasets, too.

Taking into account the considerations mentioned above, the transferability of the developed urban structure type classification methodology has to be examined. On the one hand, it is evaluated whether the classification models developed based on the city structure of London do perform similar in another urban context, which is tested for the city of Paris in France. On the other hand, it is examined if equal classification results can be gained by substituting the Urban Atlas building blocks by an artificial reference unit of square objects – to become independent from other than earth observation datasets.

The transferability is tested roughly following the same procedure introduced within chapter *3.2 Urban Structure Classification utilizing Cartosat-1 nDSM-Data*, but with some context-specific adaptations which are going to be presented in the next sections. Within this context, only those three classification models that performed best in urban structure type classification based on the Urban Atlas building blocks and the Cartosat-1 nDSM data of London are considered for transferability evaluation of the classification methodology.

#### **3.3.1 Different City Context**

For the application of the urban structure type classification methodology in Paris, Urban Atlas building blocks, a dataset containing building footprints as well as a Cartosat-1 nDSM dataset were required. Unlike the Urban Atlas and the nDSM data, no dataset comparable to the UKMap building inventory of London is available for Paris. Therefore, building footprints provided by OSM - OpenStreetMap (2012) are utilized. The extent of the Urban Atlas and the OSM dataset are adjusted to that of the nDSM dataset since the latter – equal to the situation in London – does not cover the whole city area.

Initially, the height information of the Cartosat-1 nDSM is assigned to the OSM building footprints. Subsequently, building density and mean building height are aggregated on Urban Atlas building block level based on the building parameters of the OSM dataset – building area and height – utilizing the respective equations presented in Table 4 within section *3.1.2 Aggregation of Physical Parameters*. As already mentioned above, only three classification models – those that performed best in urban structure type classification in London – are utilized for testing the transferability. Therefore, only the respective three urban structure delineation schemes are applied on the Urban Atlas building blocks – based on the aggregated building density and mean height values – in order that three reference classifications on Urban Atlas block level of Paris are resulting.

In the next step, the selected spatial and textural features are calculated following the same procedure as presented within section 3.2.2 *Feature Calculation*. Nevertheless, in this context the Cartosat-1 nDSM and the Urban Atlas dataset from Paris are utilized. Reclassification of the nDSM dataset for the purpose of textural feature derivation is done using the reclassification key presented in Table 9. The Urban Atlas dataset of Paris – containing information on urban structure type class membership as well as the numerical values of the spatial and textural features of the individual building blocks – builds the input data for classification. The dataset is classified using the three Random Forest classification models that performed best on the London dataset. Additionally, it is used to develop three new classification models and subsequently conduct a classification following the procedure presented within section 3.2.3 *Random Forest Classification*. This is done in order to be able to compare performance variations between different classification models, too. On the one hand trained based on another city structure and on the other hand trained based on the structure of the city to be classified.

The performance of urban structure type classification utilizing different classification models within Paris is assessed by calculating accuracy measures – presented within section 3.2.4 *Accuracy Assessment* – for the different classifications results. Within this context, especially the Kappa values are taken into consideration for evaluation since these are particularly suited when comparing results of different classifications (Congalton and Green 1999: 59; Foody 2002: 188). The transferability is evaluated by comparing the accuracy measures on Urban Atlas building block level of Paris with the accuracy measures of the same classification schemes on Urban Atlas building block level of London.

#### 3.3.2 Square Objects

The transferability of the urban structure type classification methodology utilizing an artificial reference unit of square objects is tested based on the city structure of London. Data used within this context are the Cartosat-1 nDSM, the reclassified nDSM and the UKMap building inventory, while the Urban Atlas building blocks are substituted by square objects. However, the latter are not available in advance and therefore need to be created during segmentation. In order to derive square units only for areas which actually feature urban structures, the Global Urban Footprint extract of London derived from data of the TerraSAR-X/TanDEM-X sensors (Esch et al. 2012) is implemented in the process, too. The top-down segmentation procedure is conducted following the same approach as utilized by Klotz (2012: 35 ff.):

The lowest spatial scale is presented by the Urban Footprint Level (L1) (see Figure 10) which is generated by implementation of the Global Urban Footprint extract of London into the segmentation. The Building Block Level (L2) is created by copying L1 and conducting chessboard segmentation within the Urban Footprint area. The size of the square segments to be created is set to 40,000m<sup>2</sup>. The value is based on a suggestion of Taubenböck et al. (2013: 396), since they considered this size appropriate to capture urban alignment and structure. The Building Substitute Level (L3) is created based on the Building Block Level (L2) by copying the latter and performing chessboard segmentation within the individual building block segments – setting the size of square segments to be created to 25m<sup>2</sup> which equals the nDSM pixel level. Subsequently, feature calculation is carried out on Building Block Level (L2) following the same procedure as presented within section 3.2.2 *Feature Calculation*.

After segmentation and feature calculation, mean height values and building density values are derived for the individual square objects (L2) by aggregating the building parameters of the UKMap building inventory (see section 3.1.2 *Aggregation of Physical Parameters*). However, the spatial coverage of L2 exceeded that of the UKMap building inventory and therefore, square segments not containing buildings of the latter are excluded in order to avoid erroneous zero values. Based on the physical parameters the three urban structure type classification schemes under consideration are applied on L2.

Subsequently, Random Forest classification models are developed utilizing the class information of the considered reference classifications as well as the numerical feature values following the approach presented within section 3.2.3 *Random Forest Classification*.

Finally, accuracy measures – see section 3.2.4 *Accuracy Assessment* – are calculated for the resulting classifications in order to be able to quantitatively evaluate the performance of the classifiers on square object level. The transferability is evaluated by comparing the accuracy measures on square object level of London with the accuracy measures of the same classification schemes on Urban Atlas building block level of London.

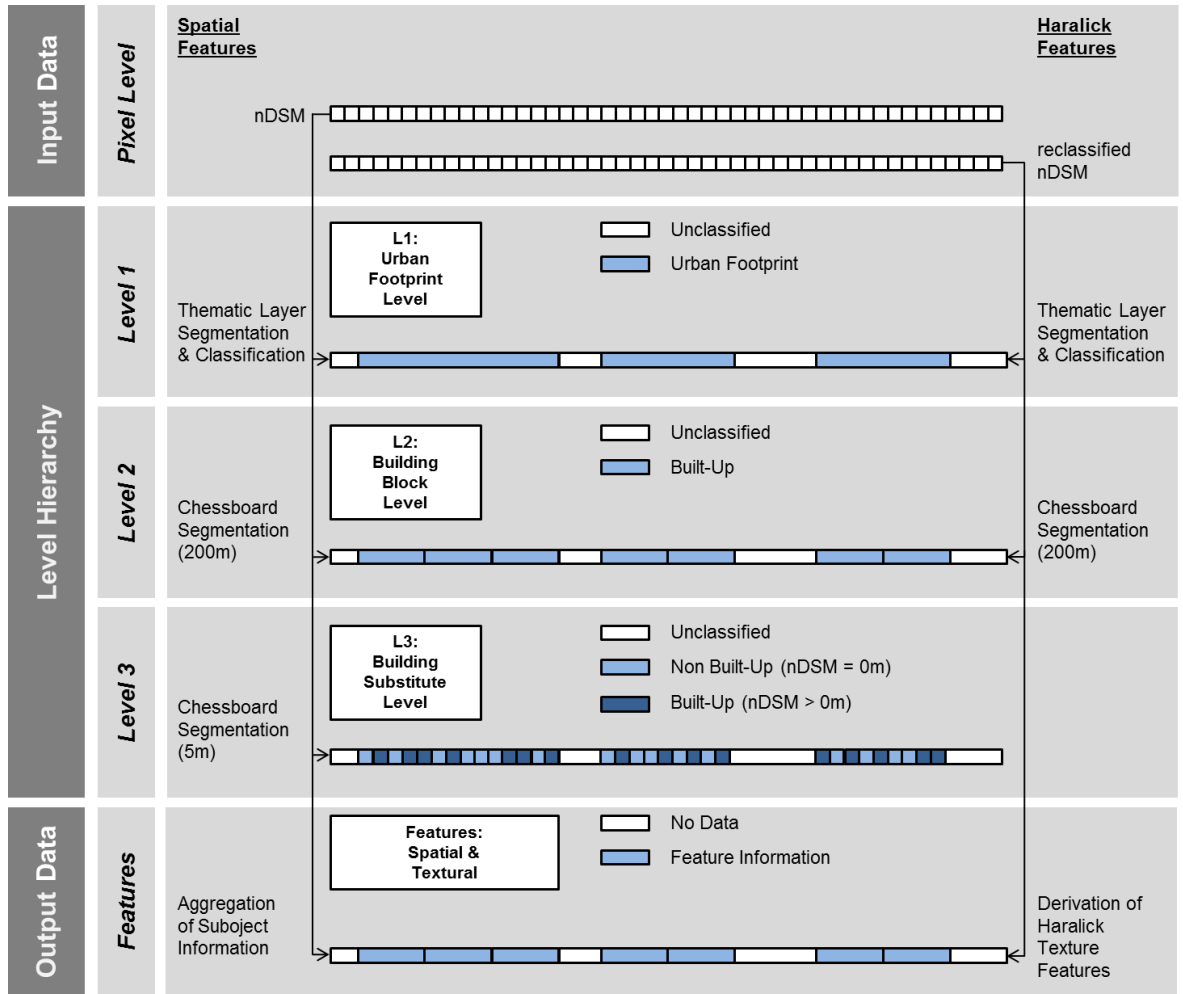


Figure 10: Top-down segmentation scheme – square object level (modified after Klotz 2012)

### 3.4 Cross-City Structural Analysis

The morphology of cities can be quantified by parameters capable to capture horizontal and vertical characteristics of urban structures. In the scope of this study, morphological properties – by means of physical parameters – were derived for the individual Urban Atlas building blocks of London and Paris. Those parameters are suitable to describe the structure of urban areas and therefore allow identifying analogies and differences of the urban morphology between different cities, as targeted within the fourth research objective.

Luck and Wu (2002: 327) stated that morphology and growth of urban areas were subjects of investigation for geographers, economists and social scientists for a long time. Within this context, a variety of theories on the spatial and temporal composition of cities has been developed (e.g. Thünen 2011; Burgess 1984; Christaller 1933). The concentric zone model introduced by Burgess (1984) is among the classic theories of urban morphology and understands

### 3. METHODOLOGY

---

the city as a composition of concentric rings around a central business district. Although this model cannot be seen as the absolute reality, it is assumable that the physical face of cities might change beginning from the center to the fringe.

Some studies have already conducted urban analysis depending on the distance to the city center. Luck and Wu (2002) have examined how land used types change with increasing distance from the city center in the Phoenix metropolitan region. Furthermore, Wurm et al. (2015a) have presented an approach to discriminate city centers in Germany depending on the correlation between the perceived distance of citizens from their home to a central point and changing morphological characteristics with increasing distance from that central point.

Within this study, the approach of analyzing the urban morphology depending on the distance from the city center is taken up. Therefore, analogies and differences between London and Paris are identified based on physical parameters on Urban Atlas building block level and their alteration with increasing distance from the city center. The physical parameters considered within this context are the building density, the floor space density as well as the mean height. However, for the purpose of comparability the floor space density and mean height values calculated based on Cartosat-1 nDSM height information are utilized, since only these are available for both cities under consideration.

In order to be able to derive distance values central points need to be defined within each of the city areas in advance. These are set to the church of Notre Dame in Paris and the St. Paul's cathedral in London, because both are located in the historic center of the respective city. Subsequently, the Euclidean distance from the individual Urban Atlas building blocks to the respective city center is calculated. Within this context, only those building blocks located within a distance of 12km around the respective city center are taken into consideration for the subsequent analysis. This is done because the areal coverage of the building blocks within London is limited to that extent. Figure 11 exemplarily contrasts the calculated distance values on Urban Atlas building block level in London beginning from the city center with the building density values for the same building blocks.

### 3. METHODOLOGY

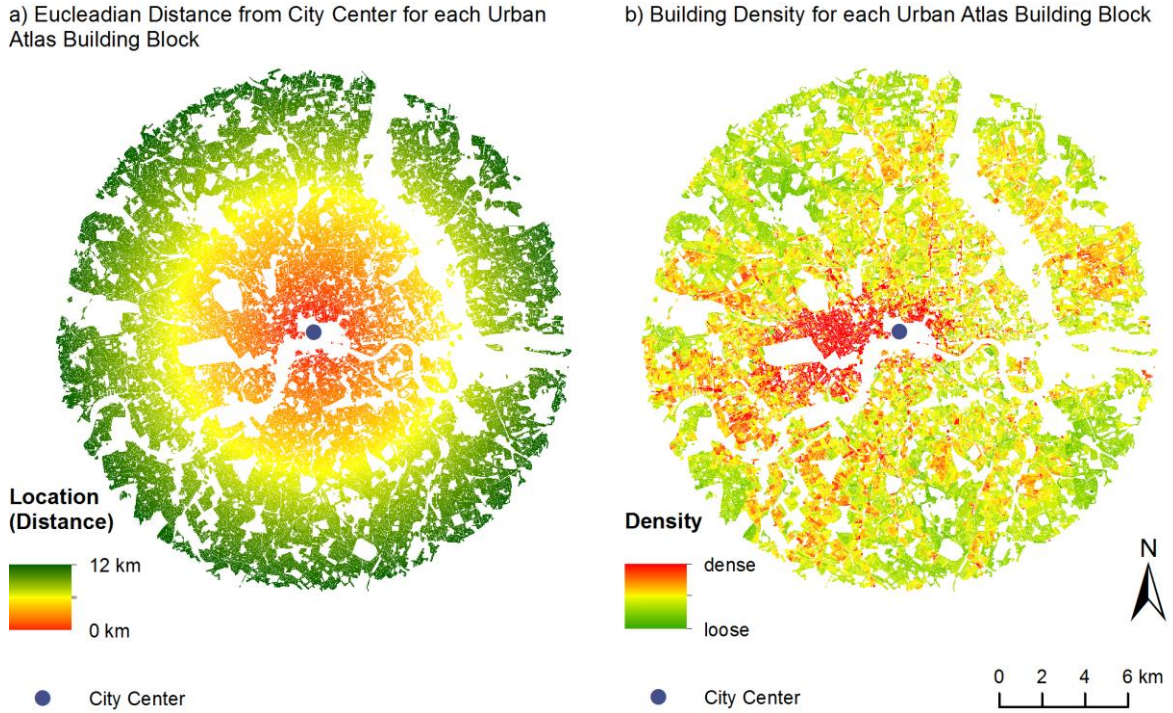


**Figure 11:** Location and building density of London on Urban Atlas level (modified after Wurm et al. 2015b)

For the purpose of analyzing the alteration of the urban morphology with increasing distance from the city center, the individual Urban Atlas building blocks are classified according to their distance to the city center by intervals of 1km. As a result of this step, a composition of eleven concentric rings around the city center is created for each city. The blocks being located in a distance of up to 1km around the central point are classified as city center. The value ranges of the particular physical parameters are visualized as boxplots respectively for each of the concentric rings and the city center of Paris and London. This allows for analyzing the morphological composition of each city depending on the distance to the city center.

Furthermore, the three considered physical parameters of the individual Urban Atlas building blocks are averaged for each of the eleven concentric rings and for the city center utilizing the equations presented within Table 11.

For the purpose of comparability between Paris and London the averaged parameters are normalized by the dimension of the largest resulting value of the respective city. For the comparative structural analysis, the alteration of the normalized parameters with increasing distance from the city center of London and Paris are respectively contrasted using line charts.

### 3. METHODOLOGY

**Table 11:** Ring-based equations of physical parameters

Physical parameter	Equation	Variables
Averaged Building Density (in %)	$\overline{BD} = \frac{BD}{n_{R_u}}$ (22)	BD = Building Density per Urban Atlas Building Block (see equation 3)
Averaged Floor Space Density	$\overline{FSD} = \frac{FSD}{n_{R_u}}$ (23)	FSD = Floor Space Density per Urban Atlas Building Block (see equation 4)
Averaged Mean Height (in m)	$\overline{HGT} = \frac{HGT}{n_{R_u}}$ (24)	HGT = Mean Height per Urban Atlas Building Block (see equation 6) n = Number of Building Blocks R <sub>u</sub> = Concentric Ring

## 4. RESULTS & ANALYSIS

Within this chapter the results gained during this study are presented and analyzed in the context of the research objectives. This includes (4.1) the validation of the Urban Atlas classification scheme, (4.2) the assessment of the correctness and performance of the urban structure classification methodology, (4.3) the evaluation of the transferability of the urban structure classification methodology and (4.4) the cross-city structural analysis. Subsequently, the results are summarized briefly in order to answer the research questions (4.5). Eventually, the outcomes gained during the study are discussed with regard to limitations of the applied methodological approaches and the used data (4.6).

### 4.1 Validation of Urban Atlas Classification Scheme

In the following sections the validation results of the Urban Atlas classification scheme are presented. These include the accuracy assessment of the ‘Discontinuous’ and ‘Continuous Urban Fabric’ classes and the review of Urban Atlas classes in terms of structural information.

#### 4.1.1 Accuracy Assessment

The accuracy of the Urban Atlas classification scheme is assessed by comparing the density ranges of the ‘Discontinuous’ and ‘Continuous Urban Fabric’ classes with the aggregated building densities on Urban Atlas block level utilizing boxplots (see Figure 12).

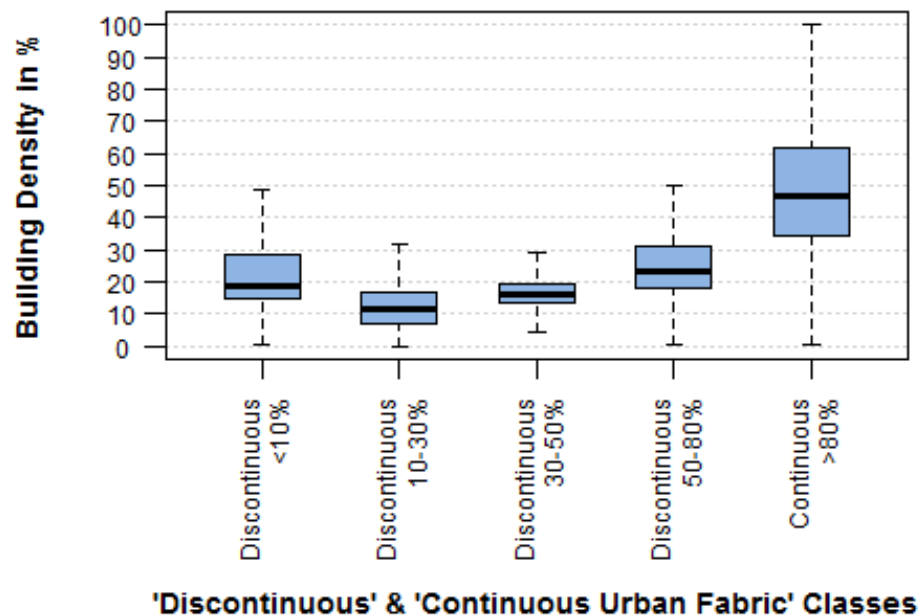


**Figure 12:** Boxplots displaying building densities of the “Discontinuous” and “Continuous Urban Fabric” classes

In general, the boxplots reveal that the degree of sealing ranges of the ‘Discontinuous’ and ‘Continuous Urban Fabric’ classes correspond to the building densities calculated from the 3D city model. However, in detail, the results display misclassifications of the Urban Atlas dataset, too.

With the exception of the class ‘Discontinuous <10%’, the boxplots of the remaining classes reveal constantly increasing building densities beginning from the class ‘Discontinuous 10-30%’. The interquartile ranges of the classes under consideration can clearly be differentiated with only small overlaps. This reflects by tendency an agreement with the descriptions of the respective Urban Atlas classes.

Nevertheless, as already indicated above, building densities of the class ‘Discontinuous <10%’ are not consistent with the class description. The density values of the majority of the blocks – around four fifths - exceed the 10% limit. Within this context, it should be noted that the blocks featuring building density values larger 10% mainly feature building structures like detached, semi-detached and row houses. Visually checking these blocks against Google Earth Imagery from 2006 – this date equals the production date of the Urban Atlas dataset – reveals that those building structures already existed during that time. A misclassification caused by construction of the building structures after the production date of the Urban Atlas is therefore excluded.

A view at the upper and lower class limits – displayed by the staple lines at the upper and lower end of the whiskers – further reveals that there are more or less high within-group variances of building densities among the different classes. The greatest variation of absolute values can be found within the ‘Continuous >80%’ class where building densities range from 0 up to 100%. In contrast to that, the class ‘Discontinuous 30-50%’ exhibits the lowest within-group variability and therefore a higher degree of homogeneity in terms of building densities. The building density values of the respective building blocks range only from approximately 5 up to 30%. However, comparing the ranges of all classes reveals that almost all of them are overlapping. Therefore, a clear distinction between the classes based on building densities is not possible.

Concluding, the accuracy of the Urban Atlas classes can only be considered partially correct. Although, a right tendency in terms of agreement between the degree of sealing and the aggregated building density values is given, no clear differentiation between the classes - as indi-

cated by the Urban Atlas class descriptions – is possible due to low between-class variability of the building densities. Furthermore, the class ‘Discontinuous <10%’ does nearly not correspond with the class description given in the Urban Atlas. Concluding, the degree of sealing of the Urban Atlas ‘Discontinuous’ and ‘Continuous Urban Fabric’ classes is not consistent with the building density. Thus, the degree of sealing ranges of the considered Urban Atlas classes do not allow for drawing conclusion on the underlying building structures.

### 4.1.2 Review of Urban Atlas Classification Scheme

The sufficiency of the Urban Atlas classification scheme to characterize horizontal and vertical urban structures requires that the classes reveal a certain degree of homogeneity. Furthermore, the between-class variability should be significant enough in order that a differentiation between the classes is possible. Therefore, the Urban Atlas classes are subsequently reviewed in terms of their within-class and between-class variability based on the selected physical parameters – building density, floor space density, mean volume and mean height – utilizing boxplots (see Figure 13).

*Building Density/ Floor Space Density (see Figure 13 – a/b):* An almost identical picture of the within-class and between-class distribution arises when looking at the building density and floor space density ranges of the different Urban Atlas classes. The ‘Discontinuous’ and ‘Continuous Urban Fabric’ classes reveal – with the exception of the ‘Discontinuous <10%’ class – an increase of building densities and floor space densities beginning from the ‘Discontinuous 10-30%’ class. However, due to more or less low between-class variances a clear separability between the classes is not possible. A closer look on the remaining Urban Atlas classes shows that the variability of building/floor space densities on block level of the classes ‘Industrial’, ‘Port Areas’ and ‘Construction Sites’ is considerably larger than these of the classes ‘Airports’ and ‘Isolated Structures’. This indicates a higher degree of within-class homogeneity with regard to building/floor space densities of the latter. Furthermore, building/floor space density values of the classes ‘Airports’ and ‘Isolated Structures’ are generally lower, owing to the typical scattered development of the respective building blocks. However, the between-class variability is not sufficient enough for physical differentiation. The building blocks of ‘Industrial’, ‘Port Areas’ and ‘Construction Sites’ can by tendency be distinguished from that of ‘Airports’ and ‘Isolated Structures’ but reveal high similarities with regard to building/floor space densities among each other. Besides, analogies to the ‘Discontinuous’ and ‘Continuous Urban Fabric’ classes are present, too. The building/floor space densities on block level of the classes

## 4. RESULTS & ANALYSIS

‘Airports’ and ‘Isolated Structures’ are for instance very similar to that of the ‘Discontinuous 10-30%’ class. Furthermore, the lower and upper class limits of almost all classes reveal more or less distinctive overlaps resulting in separation difficulties between the classes.

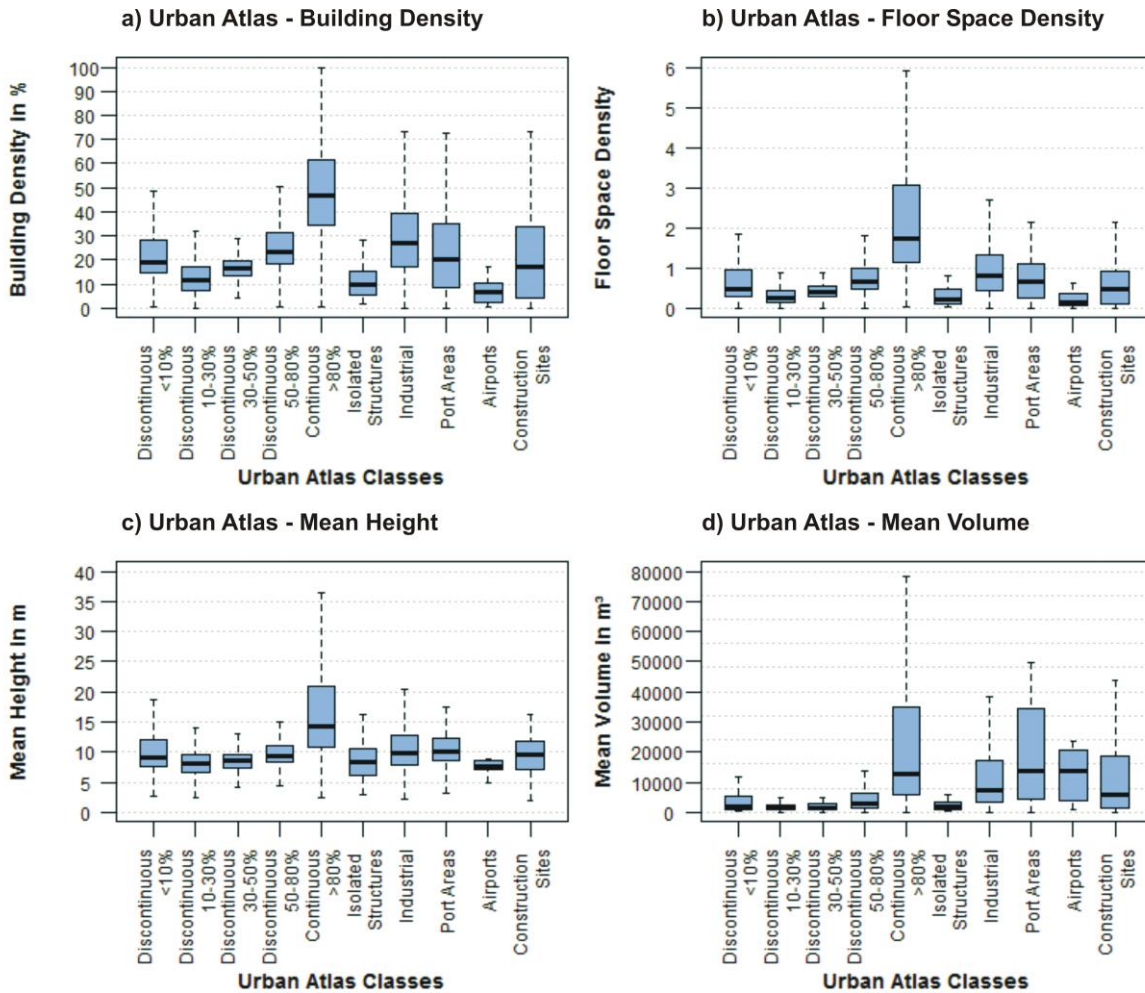


**Figure 13:** Boxplots displaying a) building densities, b) floor space densities, c) mean heights and d) mean volumes of the Urban Atlas classes

*Mean Height (see Figure 13 - c):* The mean height ranges of the different Urban Atlas classes under consideration display a very homogenous distribution. Within this context, considerable differences can only be identified on block level between the classes ‘Airports’ and ‘Continuous >80%’. Building blocks of the class ‘Airports’ exhibit the lowest within-class variances and therefore feature the highest degree of homogeneity in terms of the mean height values. Similar to the building/floor space density, the building blocks of the ‘Continuous >80%’ class reveal the highest within-class variability. Besides, the mean height values of ‘Airports’ are

considerably lower than that of the building blocks of the ‘Continuous >80%’ class. The remaining classes show more or less equal distributions on both, within-class and between-class level and can therefore physically hardly be separated in terms of the height. A closer look on the ‘Discontinuous’ and ‘Continuous Urban Fabric’ classes reveals that – again with the exception of the ‘Discontinuous <10%’ class – mean height values by tendency increase starting from the ‘Discontinuous 10-30%’ class. However, this tendency is much lesser distinct than noticeable with respect to building density and floor space density.

*Mean Volume (see Figure 13 - d):* With regard to the mean volume ranges the Urban Atlas classes can be delineated into two groups. The first group exhibits relatively high within-class variances and comprises the classes ‘Continuous >80%’, ‘Industrial’, ‘Port Areas’, ‘Airports’ and ‘Construction Sites’. The second group on the contrary reveals relatively low within-group variances – indicating a higher degree of homogeneity in terms of building volumes – and comprises the remaining classes. Furthermore, mean building volumes within the second group are considerably lower than that within the first. Therefore, structural differences in terms of the mean building volume are prevalent between the two groups. Nevertheless, the between-class variability among the classes of the two different groups is too low in order that a differentiation on class level is not possible.

Summarizing, the outcomes of the validation of the Urban Atlas classification scheme support the central hypothesis of the first research objective. The Urban Atlas classes under consideration do only partially contain information building structures. The ‘Discontinuous’ and ‘Continuous Urban Fabric’ classes exhibit – with the exception of the ‘Discontinuous <10%’ class – an increase of the physical parameters in accordance with the respective class description. However, only with regard to building density, floor space density and mean height. This characteristic is not visible with respect to the mean volume. Nevertheless, clear physical separability between the ‘Discontinuous’ and ‘Continuous Urban Fabric’ classes is not possible due to the insufficient between-class variability which leads to overlaps of the upper and lower class limits. The remaining classes do not reveal distinct structural information in terms of the physical parameters. Although some of them can be assembled into groups of similar structural characteristics and therefore differentiated on between-group level, per-class delineation based on structural information is hardly possible.

## 4.2 Urban Structure Classification utilizing Cartosat-1 nDSM Data

Within this section the results of the different classification schemes are presented and analyzed in order to review the performance of the *Random Forest classifier* in deriving structural information from the Cartosat-1 nDSM data. Eventually, the features used for the classification are evaluated regarding their explanatory power for classification.

### 4.2.1 Accuracy Assessment

The accuracy of the different classification scheme results is assessed in order to gain confidence on the *correctness* of the classification results and to determine the classifier *performance*.

**Table 12:** Results of the accuracy assessment of the different classification schemes

	Classification Scheme	Classification Scheme ID	Overall Accuracy	Kappa Value	Interpretation of Kappa Value
<b>Urban Structure Types</b>	3-Class Density/ 3-Class Height	D3H3	0.45	0.30	fair
	3-Class Density/ 2-Class Height	D3H2	0.50	0.31	fair
	2-Class Density/ 3-Class Height	D2H3	0.56	0.39	fair
	2-Class Density/ 2-Class Height	D2H2	0.64	0.41	moderate
<b>Building Density</b>	3-Class Density	D3	0.54	0.26	fair
	2-Class Density	D2	0.69	0.33	fair
<b>Mean Height</b>	3-Class Height	H3	0.79	0.63	substantial
	2-Class Height	H2	0.91	0.75	substantial

As the results reveal (see Table 12), the Random Forest classifier performs better in differentiating and extracting height information than building density information based on the Cartosat-1 nDSM data. In terms of the classification schemes which contain separate information on the building density respectively mean height, considerably better classification results could be achieved for the mean height classifications. Within this context, overall accuracies of the mean height classification results are relatively high, ranging from 0.79 up to 0.91. Furthermore, with Kappa values equal/greater than 0.63, both mean height classification outcomes can be regarded substantial with respect to their accuracy. On the contrary, the results of the density classification schemes are considerably poorer. Overall accuracies of the classifi-

cations remain on a mediocre level. In accordance to that, the Kappa values of 0.26 respectively 0.33 indicate only “fair” classification outcomes, which are just slightly better than chance agreement. In general, these results allow for the conclusion that the Cartosat-1 nDSM is a valuable dataset for classification of building heights while it – at least for the tested method - is not appropriate for the derivation of building densities.

In terms of the urban structure type classification schemes the classification precisions remain thoroughly on a mediocre level (see Table 12). For all classification schemes overall accuracies ranging from 0.45 up to 0.64 were achieved. The respective Kappa values reveal that solely the result of the D2H2 classification scheme – combination of 2-class building density and 2-class mean height – can be rated moderately. The outcomes of the other urban structure type classification schemes are slightly worse and remain – equal to the results of the building density classification schemes – on a fair level.

With regard to the results presented above, the best classification outcomes could be achieved for the H2; H3 and D2H2 classification schemes (see Table 12). Nevertheless, taking a look at the confusion matrix of the D2H2 classification scheme (see Table 13 – a) reveals that omission and commission errors are very high for the classes being composed of a low-high mixture of building density and mean height, 0.65 and 0.78 respectively 0.52 to 0.62. As a result of this, User’s and Producer’s accuracies of the respective classes are very poor, too. Within this context, it is particularly striking that omission and commission occurred primarily among the classes being composed of the same mean height but different density ranges. These shortcomings are a consequence of the only mediocre performance of the classifier in differentiating building density information based on the Cartosat-1 nDSM data. The best classification results could be achieved for the classes which are composed of ‘high/high’ respectively ‘low/low’ building density and mean height ranges. A similar picture to that identified for the D2H2 classification arises when viewing the confusion matrices of the remaining urban structure type classification schemes (see Appendix 6 – a-c).

In terms of the mean height classification schemes the omission and commission errors are considerably lower (see Table 13 – b/c). This reversely results in higher User’s and Producer’s accuracies in comparison to the D2H2 classification scheme. Within this context, the highest error values of 0.39 respectively 0.32, occur on the ‘Medium height’ class of the H3 classification scheme. With User’s and Producer’s accuracies constantly exceeding 0.83 respectively

## 4. RESULTS & ANALYSIS

0.76 the 'Low Height' and 'High Height' classes are well distinct within both, the H2 as well as the H3 classification scheme.

**Table 13:** Confusion matrices of a) D2H2 classification, b) H3 classification and c) H2 classification of London on Urban Atlas level

		Reference Data					
Prediction	a) D2H2	<i>1 1</i>	<i>1 2</i>	<i>2 1</i>	<i>2 2</i>	Row Total	
		<i>1 1</i>	13,191	708	4,710	541	19,150
		<i>1 2</i>	259	<b>563</b>	116	524	1,462
		<i>2 1</i>	2,391	262	<b>2,772</b>	305	5,731
		<i>2 2</i>	357	1,074	267	<b>3,667</b>	5,365
		Column Total	16,199	2,607	7,865	5,037	<b>31,708</b>
	Omission Error	0.19	0.78	0.65	0.17	<i>Density Height</i>  1 = Low 2 = High	
	Producer's Accuracy	0.81	0.22	0.35	0.73		
	Commission Error	0.31	0.62	0.52	0.32		
	User's Accuracy	0.69	0.38	0.48	0.68		

		Reference Data				
Prediction	b) H3	<i>1</i>	<i>2</i>	<i>3</i>	Row Total	
		<i>1</i>	16,502	3,097	80	19,679
		<i>2</i>	1,856	<b>5,700</b>	844	8,400
		<i>3</i>	44	583	<b>3,003</b>	3,630
		Column Total	18,402	9,380	3,927	<b>31,709</b>
		Omission Error	0.10	0.39	0.24	<i>Height</i>  1 = Low 2 = Medium 3 = High
	Producer's Accuracy	0.90	0.61	0.76		
	Commission Error	0.16	0.32	0.17		
	User's Accuracy	0.84	0.68	0.83		

Reference Data				
Prediction	c) H2	1	2	Row Total
	1	22,944	1,678	24,622
	2	1,120	5,967	7,087
	Column Total	24,064	7,645	31,709
	Omission Error	0.05	0.22	<i>Height</i> 1 = Low 2 = High
	Producer's Accuracy	0.95	0.78	
	Commission Error	0.07	0.16	
	User's Accuracy	0.93	0.84	

Summarizing, the classifier performed best in deriving height information within the scope of the H2 and H3 classification schemes achieving substantial results. The performance of the classification models in extracting information on building density is significantly poorer. The results remain thoroughly on a mediocre level never exceeding fair rankings. As a consequence of the poor differentiation ability of building densities, the outcomes of the urban structure type classifications remain on a mediocre level, too. The best but only moderate ranked result could be achieved for the D2H2 scheme which is also the third-best result in terms of all classification schemes under consideration. Nevertheless, relatively high omission and commission errors occur. Concluding, Cartosat-1 nDSMs reveal to be a substantial Earth observation dataset for classification of building heights but fail to add information on the building density.

### 4.2.2 Classification Results

A visual comparison of reference classifications and prediction results of the three best-ranked classification schemes – D2H2, H3 and H2 – is presented within Figure 14, Figure 15 and Figure 16.

The visual presentations reveal that the H3 and H2 classification results agree quite well with the respective reference classifications. The largest but still minor deviations can be observed on building blocks belonging to the ‘Medium Height’ class of the H3 classification scheme. In accordance with the accuracy assessment presented within the previous section differentiation problems occurred primarily between the ‘Medium Height’ and ‘Low Height’ class.

The visual agreement between reference classification and classification result of the D2H2 classification scheme is significantly poorer. The high omission and commission errors of the ‘High Density/Low Height’ and ‘Low Density/High Height’ classes (see Table 13 – a) are clearly reflected in the classification outcome. The majority of the building blocks belonging to those classes were falsely delineated during classification. As a result a clear underrepresentation of the blocks of the ‘High Density/Low Height’ and ‘Low Density/High Height’ classes is apparent when comparing the classification result with the reference (see Figure 14).

## 4. RESULTS & ANALYSIS

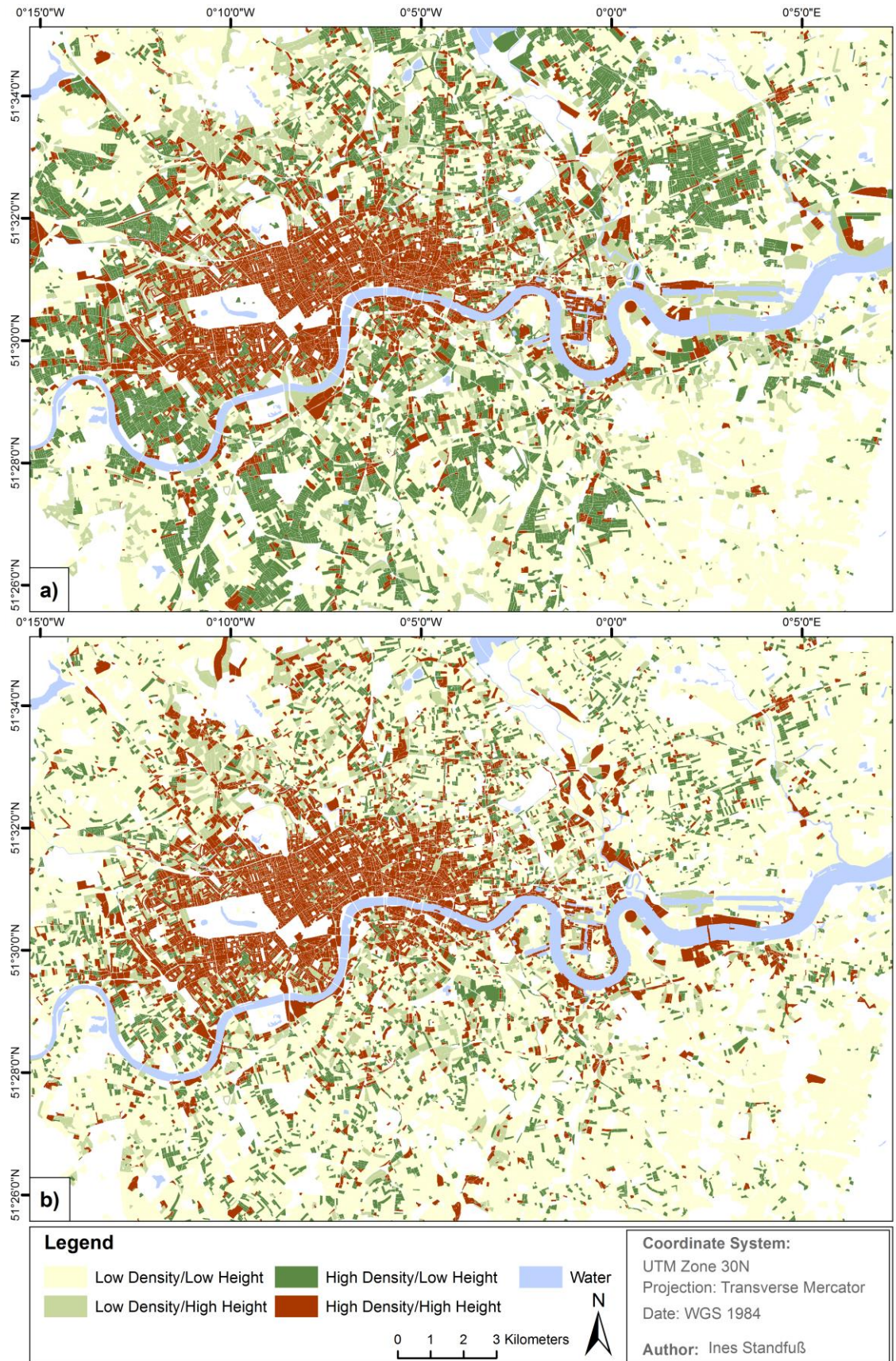
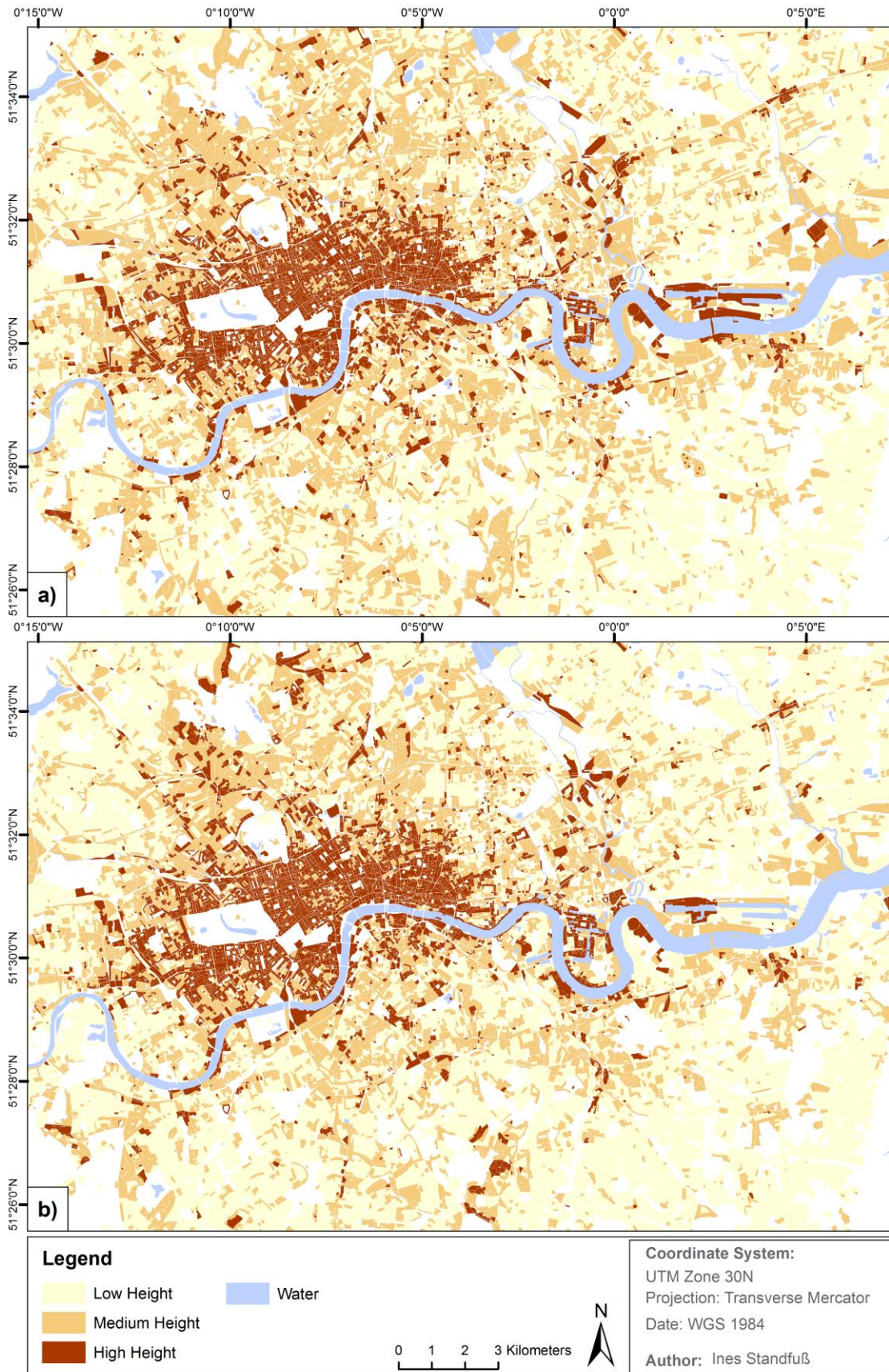


Figure 14: D2H2 classification of London on Urban Atlas level: a) reference data and b) classification result

## 4. RESULTS & ANALYSIS



**Figure 15:** H3 classification of London on Urban Atlas level: a) reference data and b) classification result

## 4. RESULTS & ANALYSIS

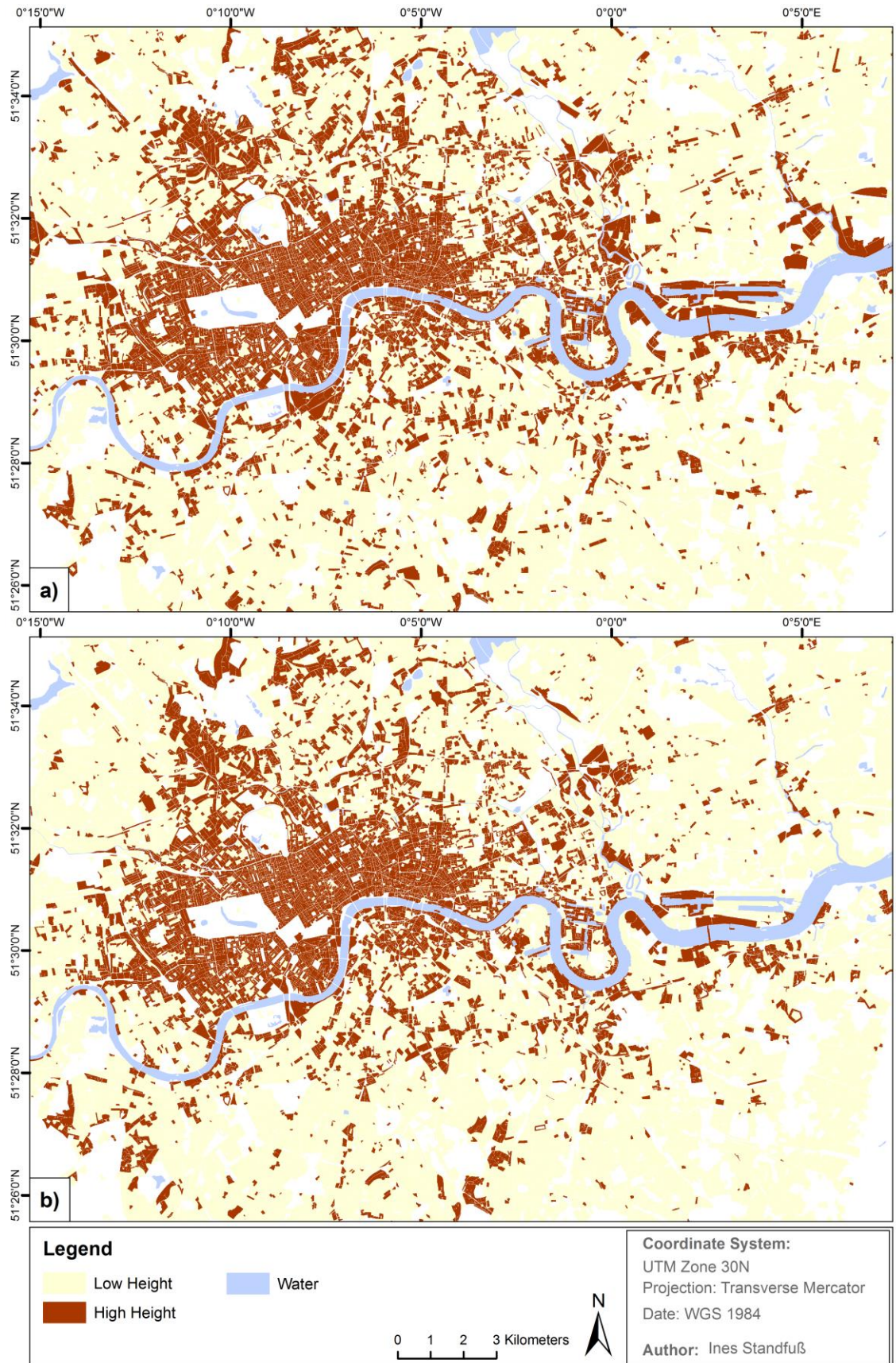


**Figure 16:** H2 classification of London on Urban Atlas level: a) reference data and b) classification result

4.2.3 Evaluation of Feature Importance

In the scope of this study an 18-dimensional feature vector comprising spatial and textural features was used for classification. The relative importance of each feature was automatically assessed within the Random Forest classification process (see section 3.2.3 *Random Forest Classification*). The results of the feature importance assessment for the three best-ranked classification schemes - H3, H2 and D2H2 - are presented in terms of a feature importance ranking within Figure 17.

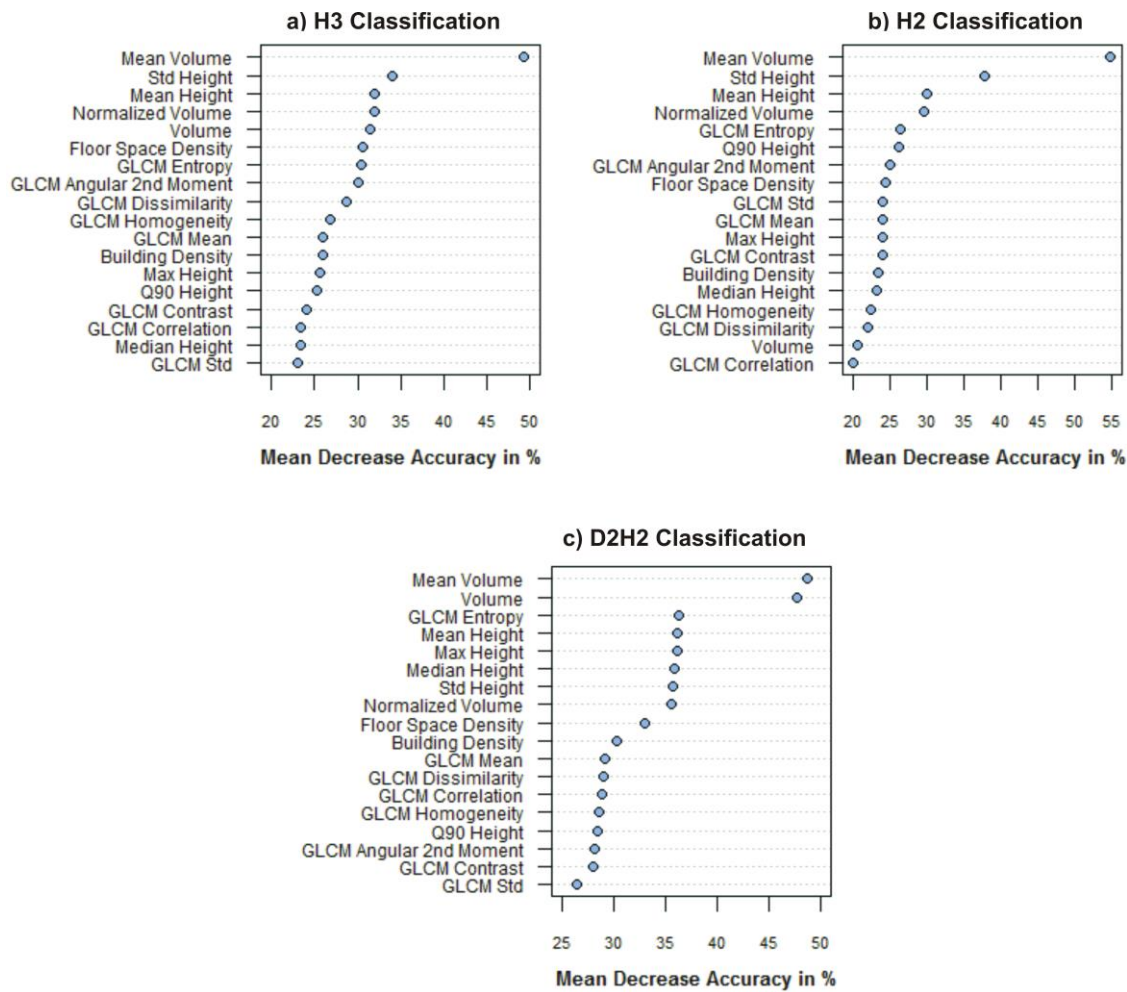


Figure 17: Feature importance ranking of a) H3 classification, b) H2 classification and c) D2H2 classification of London

With regard to the H3 and H2 – mean height – classification schemes (see Figure 17 – a/b) three spatial features have the highest explanatory power for classification. These are in both cases ‘Mean Volume’, ‘Standard Deviation Height’ and ‘Mean Height’. Excluding these fea-

tures would result in a mean decrease of classification accuracy ranging from 30 up to 55%. However, the largest decrease would be recorded for ‘Mean Volume’ with 50 respectively 55%. The mean increase of the other two features would be significantly lower. The best-ranked textural feature in the frame of the H3 and H2 classification is ‘GLCM Entropy’. Nevertheless, although not all spatial features contribute equivalently to the classification process, spatial features clearly have a greater influence on the classification success than textural features.

In the scope of the D2H2 – combination of 2-class building density and 2-class mean height – classification scheme (see Figure 17 – c), two spatial features and one textural feature are among the three best-ranked features. These are namely ‘Mean Volume’, ‘Volume’ and ‘GLCM Entropy’. Nevertheless, while the two spatial features would cause a mean decrease of accuracy of around 50% each, the loss of accuracy in terms of the textural feature is substantially lower and amounts only around 36%. Equal to the H2 and H3 classification scheme, spatial features have a greater influence on the classification success than textural features in terms of the D2H2 classification scheme.

### 4.3 Transferability Evaluation of Urban Structure Classification

The transferability of the urban structure classification was tested by applying the classification methodology in a different city context as well as on square reference units which act as substitutes of the Urban Atlas building blocks. In the following sections the results of the accuracy assessment are presented in order to gain confidence about the correctness of the classifications and to determine the transferability of the urban structure classification methodology.

#### 4.3.1 Different City Context

In order to review the performance of the urban structure classification in a different city context, the three best-ranked classification schemes – D2H2, H3 and H2 – were applied on urban Atlas building block level within Paris, France. The classification was conducted by applying the Random Forest classification models on a Cartosat-1 nDSM dataset of Paris. In this context, classification models trained with a subset of the London data as well as classification models trained with a subset of the Paris data were used. Within Table 14 the overall accuracies (OA) as well as the Kappa values of the different classification outcomes on Urban Atlas building block level of London and Paris are compared.

## 4. RESULTS & ANALYSIS

**Table 14:** Comparison between classification results of London on Urban Atlas level and classification results of Paris on Urban Atlas level (Paris trained/London trained)

Classification Scheme	London			Paris (London trained)			Paris (Paris trained)		
	OA	Kappa	Kappa Key	OA	Kappa	Kappa Key	OA	Kappa	Kappa Key
<b>D2H2</b>	0.64	0.41	moderate	0.64	0.45	moderate	0.69	0.51	moderate
<b>H3</b>	0.79	0.63	substantial	0.77	0.63	substantial	0.79	0.67	substantial
<b>H2</b>	0.91	0.75	substantial	0.88	0.74	substantial	0.88	0.75	substantial

The overall accuracies of the D2H2 classification outcomes, with 0.64 in London and 0.64 respectively 0.69 in Paris, are relatively constant across the two cities. The Kappa values - as more robust indicators when comparing the results of different classifications - of 0.45 respectively 0.51 in Paris are even slightly better compared to 0.41 in London. Nevertheless, all Kappa values of the D2H2 classifications indicate moderate classification outcomes.

With regard to the H3 and H2 classification schemes the overall accuracies of Paris are equal respectively just slightly poorer in comparison to that of London (see Table 14). The respective Kappa values are indicating substantial results across the two cities.

Spatial precision deficits, in terms of per-class omission and commission errors, are relatively constant among the different classification schemes across Paris and London. Figure 18 exemplarily shows a visual comparison of reference classification and prediction result of the H3 classification model trained with London data in Paris. The classification result agrees well with the reference classification. Nevertheless, deviations are observable on the building blocks belonging to the ‘Medium Height’ class as a result of the omission and commission errors of 0.43 respectively 0.32 (see Appendix 7 – b). These values are very similar to the omission and commission errors of 0.39 and 0.32, identified for the same class in the context of the H3 classification of London (see 4.2.1 *Accuracy Assessment*). With regard to the per-class spatial precision of the D2H2 and the H2 classification scheme, equal magnitudes of omission and commission errors are noticeable among the two cities, too (see Table 13 – a/c and Appendix 7 – a/c)

## 4. RESULTS & ANALYSIS

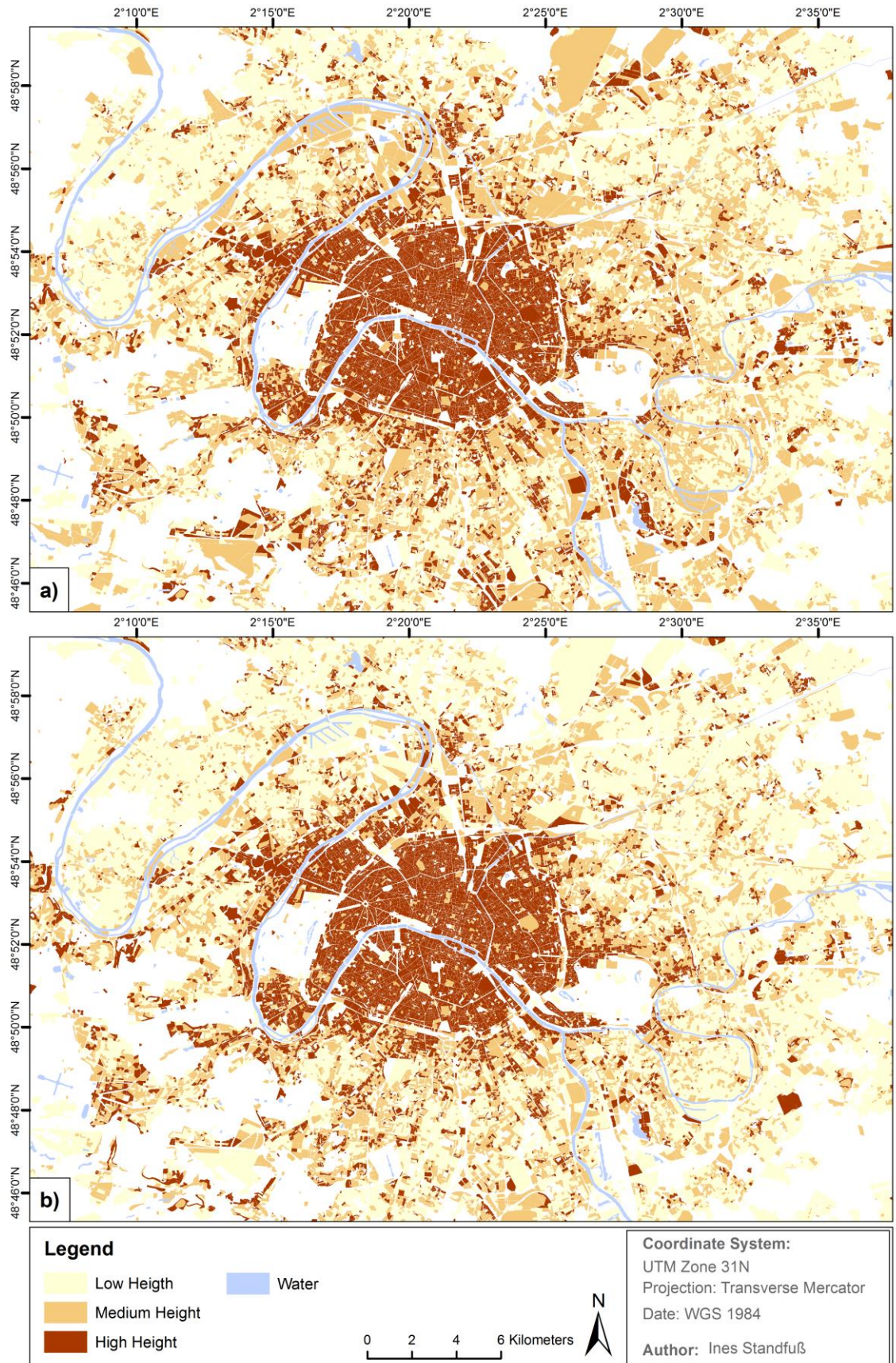


**Figure 18:** H3 classification of Paris on Urban Atlas level: a) reference data and b) classification result

Summarizing, the overall accuracies as well as the Kappa values constantly remain on an equal level across Paris and London. The per-class spatial precisions of the different classification schemes are very similar across the two cities, too. Furthermore, the classification accuracies in Paris utilizing the classifiers trained with Paris data are only slightly better in comparison to that trained with London data. Therefore, no significant improvement is noticeable. Concluding, the consistent results of the classification accuracies across London and Paris confirm the transferability of the methodology to a different city context.

### 4.3.2 Square Objects

The availability of Urban Atlas building block information is spatially limited to European cities with more than 100,000 inhabitants (EEA 2010b). Thus, it was tested whether the classification methodology is applicable on artificial spatial units of square objects with a size of 40,000m<sup>2</sup>. In order to review the transferability of the urban structure classification, the D2H2, H3 and H2 classification schemes were applied on this particular square object level. The classification was conducted by training the respective Random Forest classification models with the information available on this square object level. Subsequently, classification was carried out based on the Cartosat-1 nDSM dataset of London. The overall accuracies (OA) as well as the Kappa values of the different classification outcomes on Urban Atlas building block and on square object level of London are compared within Table 15.

**Table 15:** Comparison between classification results of London on Urban Atlas level and classification results of London on square object level

Classification Scheme	London (Urban Atlas Building Blocks)			London (Square Objects)		
	OA	Kappa	Kappa Key	OA	Kappa	Kappa Key
D2H2	0.64	0.41	moderate	0.80	0.41	moderate
H3	0.79	0.62	substantial	0.79	0.56	moderate
H2	0.91	0.75	substantial	0.91	0.65	substantial

With regard to the D2H2 classification Scheme, the overall accuracy of 0.80 on square object level is considerably better than that of 0.64 on Urban Atlas building block level. However, the Kappa value is identical on Urban Atlas and square object level, indicating moderate classification outcomes. Within the context of the D2H2 classification on square object level, the most precise class, in terms of accuracy and spatial precision, is ‘Low Density/Low height’. Omission

sion and commission errors of that class are very low, resulting in very high producer's and user's accuracies (see Appendix 10 – a). It is particularly striking that a share of around 70% of the total amount of square objects belongs to that class, explaining the high overall accuracy of the D2H2 classification on square object level. Nevertheless, omission and commission errors of the remaining classes of the D2H2 classification scheme on square object level are considerably larger. These are ranging from 0.53 up to 0.99 respectively 0.34 up to 0.72 (see Appendix 10 – a). Particularly the omission error of the 'High Density/High Height' class, is with 0.53 on square object level clearly higher than that of 0.17 (see Appendix 10 – a and Table 13 – a) on Urban Atlas level. With the exception of the square reference units, the same datasets applied on Urban Atlas level were used on square object level for classification purpose, too. Therefore, the shortcomings in terms of spatial precision – especially of the 'High Density/High Height' class – are clearly an outcome of the selection of square objects as reference units.

The overall accuracies of the outcomes of the H3 and H2 classification schemes are identical among square object and Urban Atlas level. However, the Kappa values of 0.56 and 0.65 on square object level are poorer than that of 0.62 and 0.75 on Urban Atlas level (see Table 15). With regard to the interpretation of those values, the H3 classification outcome on square object level can only be ranked moderate and is therefore worse than the substantial result on Urban Atlas level. The results of the H2 classification on square object and Urban Atlas level are both substantial. The per-class accuracies of the H2 and H3 classification results on square object and Urban Atlas level are relatively similar with the exception of 'High Height' classes (see Appendix 10 – b/c and Table 12 – b/c). With 0.38 and 0.39 the respective omission errors on square object level are considerably higher than that on Urban Atlas level, amounting only 0.22 and 0.24. Again, as already identified above, clearly an outcome of the choice of square objects as reference units.

Figure 19 exemplarily shows a visual comparison of reference classification and prediction result of the H3 classification on square object level. In general, the classification result mainly agrees with the reference data. However, the shortcomings in terms of the per-class spatial precision are visible. The 'Medium Height' and the 'High Height' classes are partially underrepresented in the classification outcome.

## 4. RESULTS & ANALYSIS

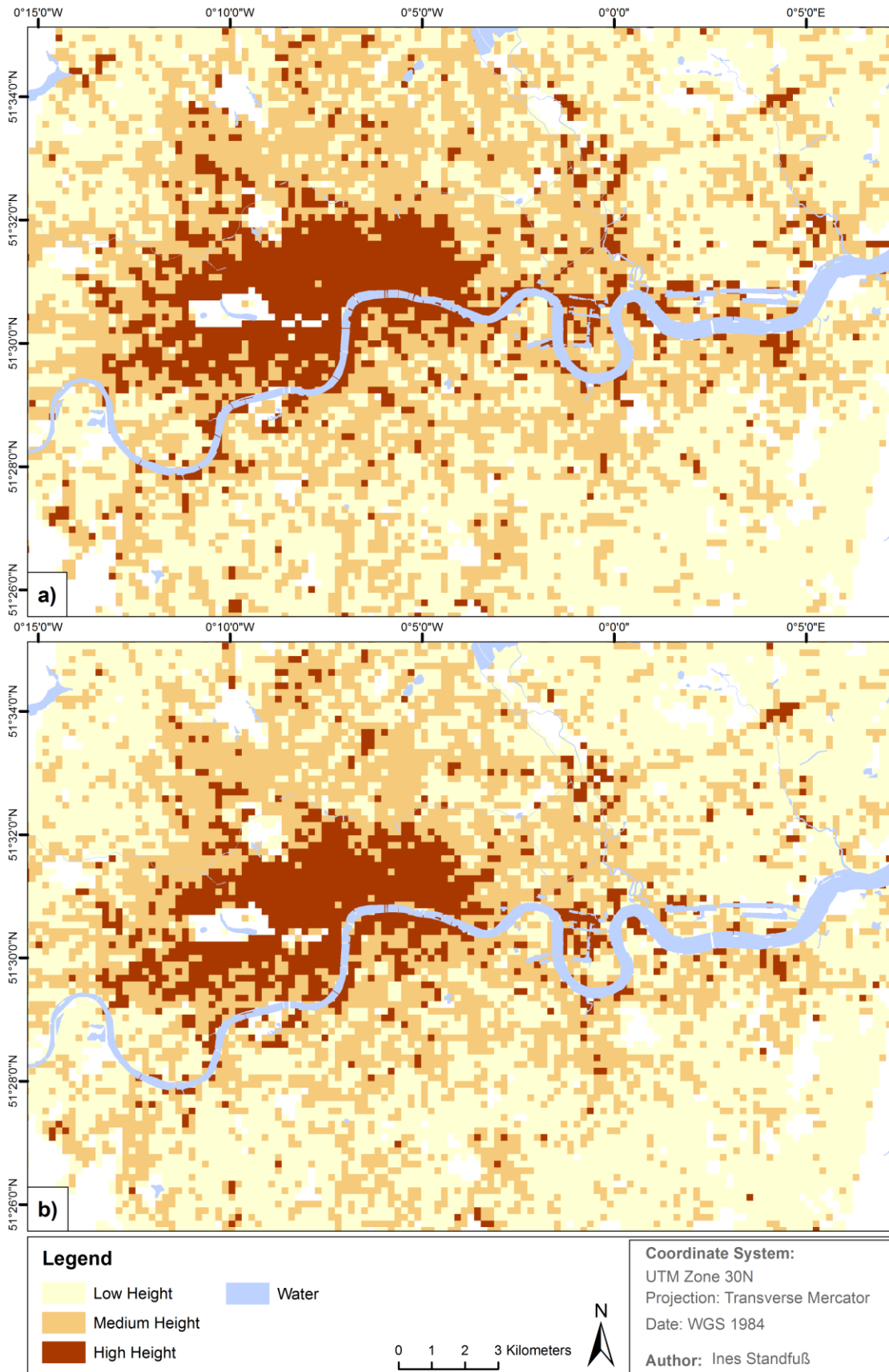


**Figure 19:** H3 classification of London on square object level: a) reference data and b) classification result

Summarizing, the classification outcomes on square object level are poorer in comparison to that achieved on Urban Atlas building block level. This is particularly the result of the inferior per-class spatial precision caused by the coarser spatial scale of the square objects and the artificial location of the square units often including a mixture of classes within the spatial extent. However, the still moderate and substantial rankings of the classification results confirm that the methodology is transferable to square objects. This allows to overcome spatial limitations and to derive information on urban structures independently from additional spatial data sources, on continental and even global scale. Nevertheless, precision limitations on square object level are more pronounced.

### 4.4 Cross-City Structural Analysis

One aim of this study was to compare the urban morphology of two European megacities – namely Paris, France and London, England. The morphological characteristics of London and Paris were derived on Urban Atlas building block level depending on the distance to the respective city center. In this context, the urban morphology was quantified by the physical parameters building density, floor space density and mean height. The results are displayed for each parameter and each of the considered cities utilizing boxplots within Figure 20. Based on these outcomes differences and analogies of the morphological characteristics between London and Paris are going to be identified.

The results reveal that Paris is denser and building heights are higher towards the city center compared to London. The absolute values of the considered physical parameters are on average higher than those of London (see Figure 20). The majority of the considered building blocks in Paris exhibit high building/floor space density and mean height values. The building blocks in London on the contrary feature a mixture of high and low values of the considered parameters in the city center respectively nearby.

Furthermore, the variability of the physical parameters on block level differs between London and Paris depending on the distance to the city center. The variability reaches their maximum within London in the city center respectively nearby up to a distance of 3km. Further outward, variances decrease constantly and the building blocks become more homogeneous, in order that the value ranges of the considered parameters decline. The variability of building/floor space densities and mean heights on building block level in Paris is lower close to the city center up to a distance of 3km compared to London. Nevertheless, it constantly increases begin-

## 4. RESULTS & ANALYSIS

ning from 3 to 4km distance until it starts dropping again at 6km respectively 7km from the city center. Therefore, building blocks within Paris are more homogeneous in the city center respectively nearby. In a distance of around 4km to 6km the building blocks become very heterogeneous in terms of the value ranges of the considered physical parameters. Starting from a distance of around 6 to 7km the homogeneity increases again. On the contrary, building blocks within London are very heterogeneous at the city center respectively nearby and become more homogeneous with increasing distance from the city center.

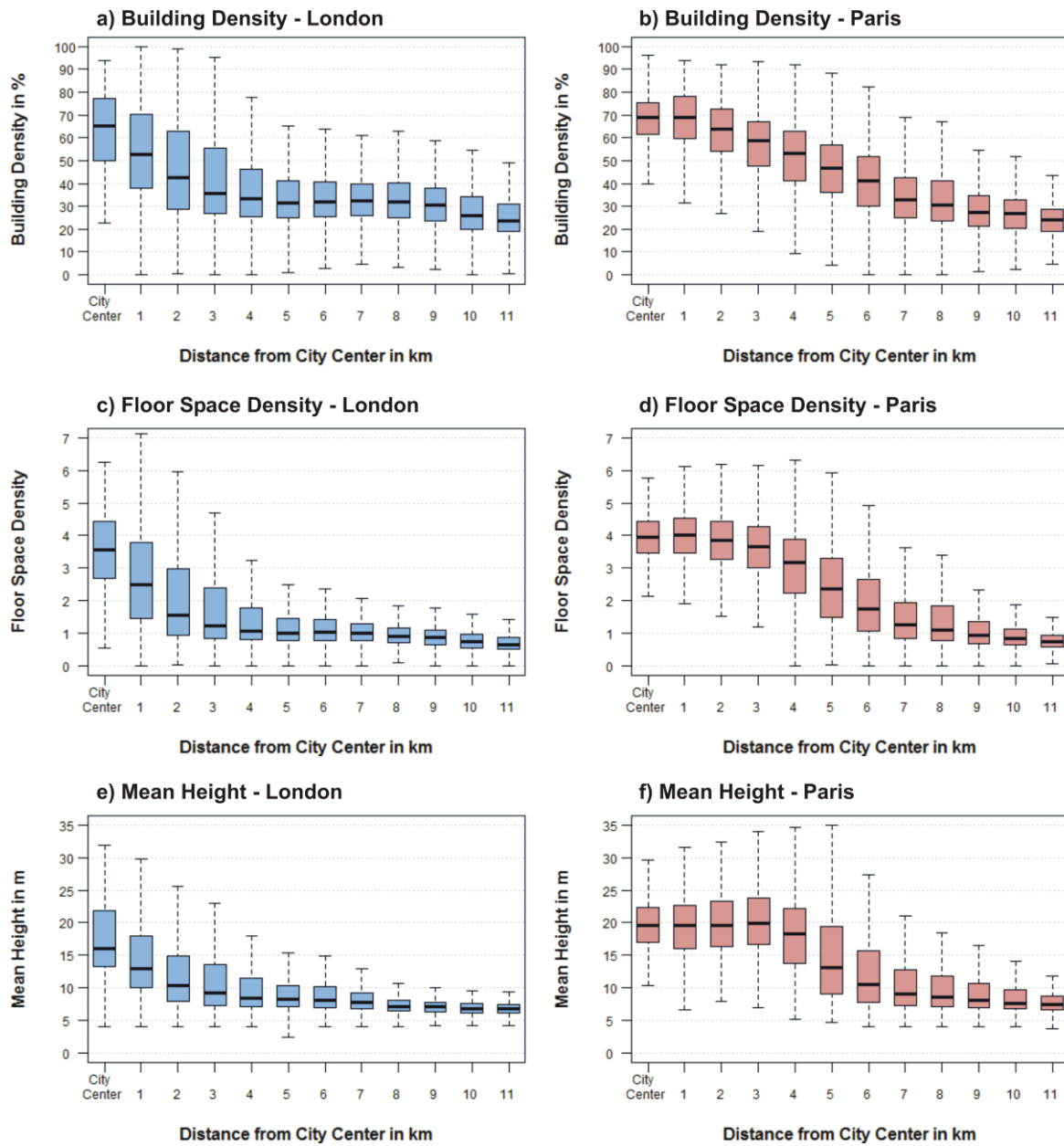


**Figure 20:** Boxplots displaying alteration of a/b) building density, c/d) floor space density and e/f) mean height in London and in Paris depending on the distance to the city center

Furthermore, building density, floor space density and mean height in London have their peak directly in the city center and are constantly decreasing beginning from that point. Paris on the contrary features several peaks. Building/floor space densities exhibit a slight decrease until 1km distance to the city center. Besides, the mean height values on building block level even increase up to a distance of 4km from the city center, before they start decreasing. Therefore, the physical parameters under consideration increase directly beginning from the city center in London while they exhibit a slight increase before they start dropping in Paris.

Differences between London and Paris are further noticeable with regard to the saturation points of the parameters. The saturation level in London – regardless of the physical parameter – is reached at 4km distance from the city center. Values of the considered parameters remain relatively similar and decrease only slightly starting from that distance. On the contrary, the saturation level in Paris is reached at a larger distance from the city center, at 6km in terms of the mean height and at 7km with regard to building/floor space density. The decrease of the parameters in Paris becomes therefore just slighter in a larger distance from the city center compared to London.

In the light of the foregoing considerations, analogies in the urban morphology of London and Paris can only be identified in the outskirts, starting from a distance of around 6 up to 7km from the city center. From then onwards, the physical parameters are relatively similar, with regard to their quantity, their decrease rate and variability, across the two cities.

A direct comparison of the normalized average building density, floor space density and mean height on building block level of London and Paris depending on the distance to the city center is displayed within Figure 21. The comparison displays the previously identified differences and analogies between the urban morphology of the two cities in a distinct and simplified manner. The course of the lines of London and Paris is considerably different in a distance of 1km up to approximately 7km from the city center. The line of Paris displays a clear curvature resulting from the increase of the physical parameters under consideration. On the contrary, the line of London reveals a concave shaping being a consequence of the decrease of the physical parameters. Only further outwards, in a distance of approximately 7km from the city center, the morphologies of London and Paris start to resemble and hence, reveal analogies. This is clearly identifiable by the converging lines of the two cities beginning from the considered distance.

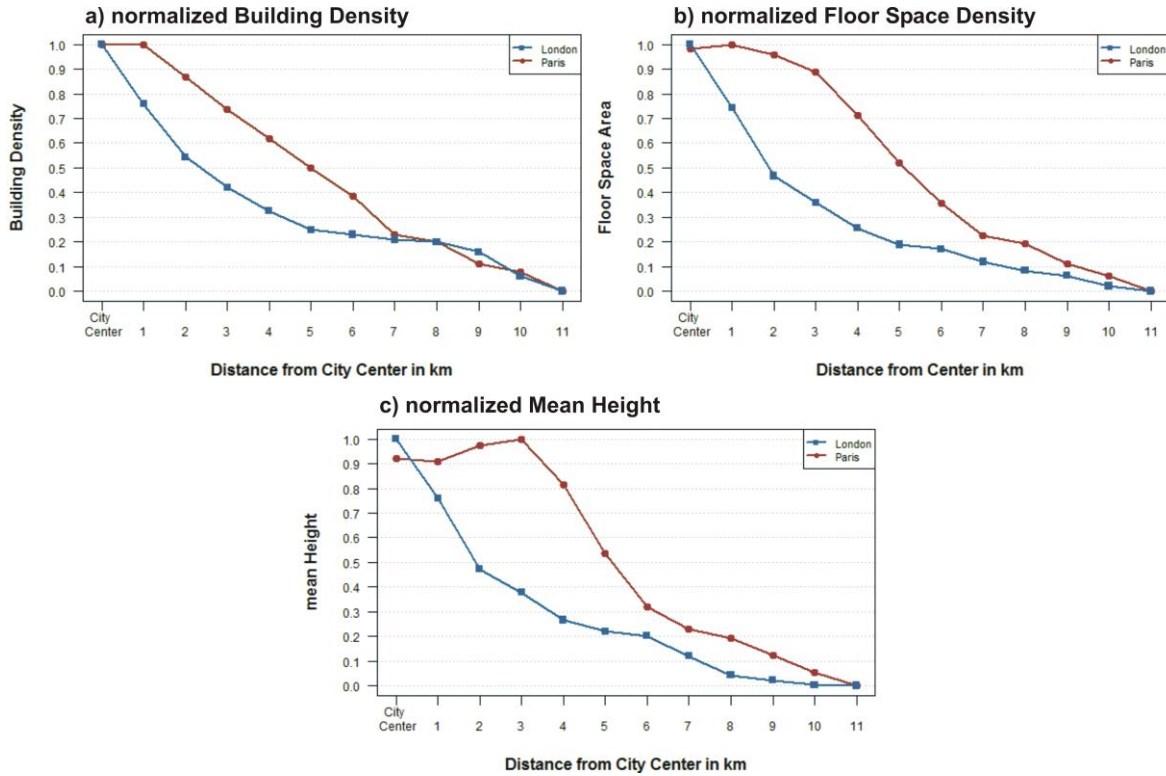


**Figure 21:** Direct comparison between normalized average a) building density, b) floor space density and c) mean height of London and Paris depending on the distance to the city center

#### 4.5 Results in the Context of the Research Objectives

In the following, the results gained in the scope of this study are summarized briefly in the view of the research questions posed under the different research objectives.

##### 1) Validation of Urban Atlas Classification Scheme

1.1) *Are the density ranges of the Urban Atlas ‘Discontinuous’ and ‘Continuous Urban Fabric’ Classes accurate?*

The accuracy of the ‘Discontinuous’ and ‘Continuous Urban Fabric’ classes in the European Urban Atlas can only be considered partially correct. A right tendency in terms of agreement between the Urban Atlas degree of sealing and the aggregated building density derived from a 3D building model can be identified. Nevertheless, no clear differentiation between the classes - as indicated by the Urban Atlas class descriptions - is possible due to low between-class variability of the building densities. Furthermore, the class “Discontinuous <10%” does nearly not correspond with the class description given in the Urban Atlas. Concluding, the ‘Discontinuous’ and ‘Continuous Urban Fabric’ classes do not hold distinct information on the build-

ing density and thus, do not allow for drawing conclusion on the underlying building structures.

### *1.2) Do the Urban Atlas classes feature information on urban structures?*

The ‘Discontinuous’ and ‘Continuous Urban Fabric’ classes exhibit – with the exception of the ‘Discontinuous <10%’ class – an increase of the physical parameters in accordance with the respective class description and do therefore contain structural information. However, only with regard to building density, floor space density and mean height. This characteristic is not visible in terms of the mean volume. Nevertheless, clear separability between the ‘Discontinuous’ and ‘Continuous Urban Fabric’ classes is not possible regardless of the physical parameter. This is caused by an insufficient between-class variability which leads to overlaps of the upper and lower class limits. The remaining classes do not reveal distinct structural information in terms of the physical parameters under consideration. Although some of them can be assembled into groups of similar structural characteristics and therefore differentiated on group level, per-class delineation based on structural information is hardly possible.

*Hypothesis: The Urban Atlas classes do only partially contain information on the horizontal and vertical structure of cities.*

The outcomes of the validation of the Urban Atlas classification scheme support the central hypothesis of this study. The classes under consideration do only partially contain structural information by means of the ‘Discontinuous’ and ‘Continuous Urban Fabric’ classes. The remaining classes under consideration do not contain distinct structural information, at least not on class level.

### **2) Urban Structure Classification utilizing Cartosat-1 nDSM Data**

#### *2.1) Is it possible to automatically derive information on urban structures from Cartosat-1 nDSM datasets?*

In the scope of this study a classification methodology to automatically derive information on urban structures based on Cartosat-1 nDSM data has been developed. The classification models enable to automatically derive height information achieving substantial results. However, the performance of extracting information on building density is significantly poorer. The results remain thoroughly on a mediocre level never exceeding fair rankings. As a consequence of the poor differentiation ability of building densities, the outcomes of the urban structure type classifications remain on a mediocre level, too. The best but only moderately ranked re-

sult could be achieved for only one urban structure type classification scheme. Nevertheless, spatial precision and accuracy of some classes of the urban structure type classification scheme are very poor. Therefore, it is possible to automatically derive urban structure information from Cartosat-1 nDSM data but in varying quality. While substantial results are achievable when extracting height information, only mediocre classification outcomes can be attained with regard to building density and urban structure classification. Concluding, Cartosat-1 nDSMs reveal to be a substantial Earth observation dataset for classification of building heights but fail to add information on the building density.

### *2.2) Which features have the highest explanatory power for classification of urban structures?*

The relative feature importance for classification has been assessed for the three best-ranked classification outcomes. With regard to the considered classification schemes, the five features having the highest explanatory power for urban structure classification are namely ‘Mean Volume’, ‘Standard Deviation Height’ ‘Mean Height’, ‘Volume’ and ‘GLCM Entropy’. Excluding these features would lead to a decrease of classification accuracy ranging from 30 up to 55%. Nevertheless, the highest decrease would be caused when omitting ‘Mean Volume’ – ranging from 50 up to 55% – which is therefore the feature with the highest explanatory power for all classification schemes under consideration. Besides, although not all spatial features used for classification contribute equivalently to the process, spatial features clearly have a higher explanatory power for urban structure classification than textural features.

### **3) Transferability Evaluation of Urban Structure Classification**

#### *3.1) Is the developed urban structure classification methodology transferable...?*

##### *a) ...to another city context?*

In order to review the transferability of the urban structure classification to another city context, the classification results on Urban Atlas block level of Paris were compared with that on Urban Atlas block level of London. The overall accuracies as well as the Kappa values of the classification outcomes constantly remain on an equal level across Paris and London. Furthermore, the per-class spatial precisions and accuracies of the different classification schemes are very similar across the two cities, too. Concluding, the consistent quality of classification outcomes across London and Paris confirms the transferability of the methodology to a different city context.

*b) ...to an independent spatial unit of square objects?*

Transferability of the urban structure classification to an independent spatial unit of square objects has been evaluated by comparing the classification outcomes on square object level of London with that on Urban Atlas building block level of London. The classification results on square object level are poorer in comparison to that achieved on Urban Atlas building block level. However, the outcomes are still ranked moderately respectively even substantial. Thus, the results confirm that the methodology is transferable to square objects, too. This allows to overcome spatial limitations and to derive information on urban structures independently from additional spatial data sources, on continental and even global scale. Nevertheless, limitations in terms of the per-class spatial precision and accuracy on square object level are more pronounced caused by the coarser spatial scale of the square units.

#### **4) Cross-City Structural Analysis**

*4.1) Are there differences and/or analogies between the urban morphology – by means of the horizontal and vertical urban structure – of London, England and Paris, France?*

Differences and analogies of the urban morphology exist between London and Paris and were identified depending on the distance to the respective city center. Within this context it was found, that the building morphology of Paris is denser und higher towards the city center compared to London. The buildings in Paris are more homogeneous within the building blocks close to the center and become more heterogeneous with increasing distance. On the contrary, building blocks in London are very heterogeneous with regard to building structures close to the center and become more homogeneous with increasing distance from the center. Furthermore, the physical parameters under consideration decrease directly beginning from the city center in London while they exhibit a slight increase before they start dropping in Paris. Within London, the saturation level of the decrease of the physical parameters is reached in a closer distance to the city center compared to Paris. Analogies in terms of the urban morphology between London and Paris can only be identified in the outskirts. Quantity, decrease rate and variability of the parameters are relatively similar there across the two cities.

### 4.6 Discussion

With the results at hand, the research questions were answered and the central hypothesis of this study was proved. Nevertheless, the outcomes need to be discussed with regard to restraints of the used data and of the applied methodology.

*Validation of Urban Atlas Classification Scheme:* In order to validate the Urban Atlas classification, physical parameters were aggregated based on the building parameters of the UKMap building inventory on Urban Atlas building block level. However, the UKMap dataset itself was not fully consistent and required some preprocessing steps. Firstly, data cleansing was necessary to remove polygons not representing building structures. Within this context, correction was done manually and thus, it cannot be guaranteed that falsely classified polygons have been removed completely. Some of these might have been missed during the cleansing process, leading to an overestimation of building densities of the concerned building blocks in return. However, the 3D model represents the urban morphology of London in the best and most complete way known and published.

Furthermore, floor counts and missing height values of the building footprints were modelled by linear regression. For the model purpose, correlations between floor counts and building height as well as between building height and building area have been utilized. The strength of the correlation between the considered variables, and therefore the potential to model the missing values, has been assessed using the coefficient of determination  $r^2$ . The correlation between floor counts and building height can be considered fairly robust with  $r^2=0.77$ . On the contrary, the correlation between building height and building area is sparsely solid with  $r^2=0.21$ . Performance and results of the regression analysis are therefore considerably better in terms of the floor counts than with regard to building height. Nevertheless, the applied regression was the only possibility to derive missing height values. Although not perfect, this approach is preferable to neglecting the missing values completely. With regard to the conducted preprocessing steps, it is assumable that the UKMap building inventory does not fulfill the claim of being 100% accurate. Nevertheless, using the different methods it was tried to generate a preferably realistic representation of the urban structure in London, suitable to validate the European Urban Atlas.

The accuracy of the Urban Atlas ‘Continuous’ and ‘Discontinuous Urban Fabric’ classes was assessed by comparing the degree of sealing ranges given in the respective class description

with the aggregated building densities on Urban Atlas building block level. In this context, it should be noted that the building density values are averagely smaller than the respective degree of sealing values given in the Urban Atlas class descriptions. The Urban Atlas sealing degrees were derived using a soil sealing layer (EEA 2010c: 2) which measures the proportional area of a building block which is sealed, considering buildings, streets and other artificial objects. The building density on the contrary was aggregated – as the name already indicates – solely on the basis of buildings using the UKMap building inventory. Although building density and Urban Atlas sealing degree values might display deviations due to differing calculation inputs, they yet allowed for evaluating the accuracy by tendency. Furthermore, they enabled to reveal that the European Urban Atlas is not suited to conduct analyses on the basis of building densities which is one of the most important urban parameters (Fina et al. 2014). Thus, the employment of the two differing parameters (building density and degree of sealing) can be considered sufficient for the purpose this study.

Another fact to discuss in terms of the accuracy assessment is the temporal difference of the acquisition dates of the Urban Atlas dataset and the UKMap building inventory. The Urban Atlas provides information on landuse/landcover in London of the year 2006. On the contrary, building footprints of the UKMap building inventory were acquired at a later time, namely in 2012. This temporal difference might have resulted in variations between the building densities aggregated on the basis of UKMap building information and the degree of sealing values given in the Urban Atlas class description. Particularly in terms of the accuracy assessment, variations between Urban Atlas sealing degree and aggregated building density were judged as failure of the Urban Atlas dataset. Nevertheless, some of these might have been simply an outcome of differences between the built-up structures at 2006 and 2012. However, 3D building datasets covering entire city areas are seldom and thus, it is pragmatically to utilize those despite of temporal uncertainties.

*Urban Structure Classification utilizing Cartosat-1 nDSM Data:* In the scope of this study, a methodology to automatically derive urban structures from Cartosat-1 nDSM data has been developed. For that purpose, reference classification schemes containing distinct information on the classes were derived in advance. Within this context, delineation of urban structures has solely been based on physical parameters. Therefore, it is not possible to draw conclusion on the underlying landuse. With regard to the Urban Atlas classification scheme it is the other way around. The classes mainly contain information on landuse/landcover and, as proved

during this study, only partially information on urban structures. However, a classification scheme considering both, structural and landuse information is desirable since those information provide the basis for an effective city management (Voltersen et al. 2014: 200). For that purpose, the exclusive utilization of nDSM data is not sufficient but requires additional socioeconomic information. Such data was not available within the scope of this study and therefore poses a limitation in terms of the developed methodology.

Furthermore, limitations of the utilized Cartosat-1 nDSM datasets need to be discussed with regard to the developed classification methodology. Firstly, Cartosat-1 DSMs respectively the thereof derived nDSMs are not suited to detect single buildings (Sirmacek et al. 2012: 7; dAngelo et al. 2008: 1341). Thus, as suggested by Taubenböck et al. (2013: 395), pixels exceeding a height of 0m were selected as building substitutes. Nevertheless, these are only a generalized representation of the built-up reality and therefore cause information loss (Klotz 2012: 64). Within this context, particularly the 5m geometrical resolution has been too coarse for the purpose of building density extraction with substantial accuracies. This might have been a reason for the inferior classifier performance and the mediocre classification outcomes in terms of the building density and urban structure type classification schemes.

Another limitation poses the spatially differing quality of the DSMs (Klotz 2012: 16) which were used for nDSM derivation. On the one hand, no height information is available for image areas covered by clouds. Hence, resulting gaps were filled with data from the Shuttle Radar Topography Mission (SRTM) with the delta fill algorithm introduced by Groham et al. (2006). However, with a geometrical resolution of 30m the SRTM data is considerably coarser compared to the 5m resolution of the Cartosat-1 DSMs. On the other hand, image resolution is impaired by induced artefacts causing building borders to be blurry (Sirmacek et al. 2012: 66). Both sources of error might have caused spatially varying performance of the classifiers.

Furthermore, Cartosat-1 DSMs generally underrate building heights (Wurm et al. 2014: 2). Within the scope of this study, physical parameters for urban structure delineation were derived on the basis of Cartosat-1 nDSM height information. This was done in order to guarantee transferability of the classification schemes to another city context, namely Paris. The Cartosat-1 nDSMs were the only source of height information available for both cities, London and Paris, within the scope of this study. Nevertheless, using the Cartosat-1 heights already for the purpose of delineation might have caused overall classification accuracies to be artificially

improved. In case of a delineation based on, for instance LIDAR-derived height information, the underrating of building heights by Cartosat-1 data might have influenced the classification and most probably resulted in lower classification accuracies.

The DTMs used for nDSM generation within the scope of this study were derived using a morphological filtering approach with a kernel window of 10x10 pixel. With regard to this dataset, quality limitations are also present. Klotz (2012: 64), who assessed the accuracy of the DTMs, has identified height deviations ranging from -14m up to 12m resulting in a Root Mean Square Error (RMSE) of 2.81. Nevertheless, although not perfect, too, he rated the data sufficient enough for the representation of the building volume.

Concluding, the data limitations presented above might have caused the mediocre performance in extracting building density and urban structure type information. However, Cartosat-1 data are a valuable data source to extract urban structure information of large city regions due to their large aerial coverage, despite the fact that the quality of the classification outcomes is varying.

*Transferability Evaluation of Urban Structure Classification:* The urban structure classification methodology was applied on Urban Atlas level in Paris achieving results with equal quality than gained for London. Thus, it was proved that the methodology is transferable to another city context. Nevertheless, the urban fabric of Paris is very similar to that of London. This in turn means that the physical face of cities located in other cultural backgrounds might be completely different. Therefore, the methodology can only be considered transferable to other cities featuring similar urban structures than London. In order to generate a statement concerning the universal transferability to other cities, the methodology needs to be tested in urban environments of different cultural backgrounds.

With regard to the square reference units, the classification methodology is yet transferable but with inferior results than achievable on Urban Atlas building block level. The artificial reference units are not particularly suited to render the urban structure caused by the uniform size and the unnatural shape. However, with regard to availability of data, square units pose the only possibility to derive urban structures independently without relying on other datasets such as the Urban Atlas.

*Cross-City Structural Analysis:* The results gained by the cross-city structural analysis need to be discussed with regard to the selection of the respective city center as well as the Cartosat-1 height

information used for deriving the physical parameters. First of all, the choice of the two city centers was subjective. The centers were set to a point/monument located in the historic center of the two cities. Although, the church of Notre Dame and the St. Paul's cathedral are accepted center points of the respective city, the choice is subjective and alternates could easily be found. Other characteristics which may be typical for city centers were not taken into account in terms of the choice. However, placing the centers to other points might have resulted in different outcomes of the structural analysis.

Furthermore, the physical parameters for the analysis were calculated using the Cartosat-1 nDSM heights. Within these datasets, as already mentioned above, building heights are underrated leading to deviations from reality of the mean height as well as of the floor space values. Nevertheless, the height information provided by Cartosat-1 exhibits, although underrated, a right tendency of height compositions and is therefore suitable for a comparison of urban structures between the two cities. Despite the points of criticism, it could be proved that the morphological composition of London and Paris exhibits both, differences and similarities. Thus, the accuracy of the dataset is considered sufficient for the purpose of the cross-city structural comparison. The added value of horizontal and structural information for urban analysis could be displayed within the scope of this study.

### 5. CONCLUSION & OUTLOOK

The main objectives of this study were the validation of the European Urban Atlas classification scheme and the development of a classification methodology towards urban structure delineation utilizing Cartosat-1 nDSM data.

In the scope of the European Urban Atlas validation, it was found that the Urban Atlas classes do only partially contain distinct information on physical urban structures. The “Discontinuous” and “Continuous Urban Fabric” classes are by tendency correct and exhibit an agreement between the considered physical parameters and the respective class description. However, the degree of sealing given in the class description of the considered classes is not consistent with the aggregated building density. Furthermore, distinct between-class discrimination is not possible regardless of the physical parameter. The remaining Urban Atlas classes under consideration can be assembled into groups of similar structural characteristics and therefore differentiated on between-group level. Nevertheless, discrimination of the single classes is hardly possible, too. Concluding, the European Urban Atlas classification scheme does not allow for drawing conclusion on the underlying building structures on class-level and thus, as a matter of fact, does not contain holistic information on the morphology of urban areas.

The developed classification methodology enables to derive urban structure information on European Urban Atlas building block level from Cartosat-1 nDSM data but in varying quality. In this regard, substantial results are achievable when extracting height information. However, the performance of the classification models in extracting information on building density as well as simultaneously on height and building density (urban structure types) is significantly poorer. In this context, only mediocre classification outcomes are attainable. Hence, Cartosat-1 nDSMs reveal to be a substantial remote sensing dataset for large area classification of building heights but fail to add information on the building density.

The classification methodology proves transferability to another city context as well as to an artificial reference unit of square objects. Nevertheless, while the classification quality remains on an equal level when applied on Urban Atlas building block level to another city context, it is inferior when utilized on square object level. The latter is attributed by the coarser spatial scale and the artificial location of the square objects within the spatial extent often including a mixture of urban structures. Nevertheless, the approach works independently from other ref-

---

---

erence units (e.g. Urban Atlas building blocks) and thus, allows for urban structure classification on continental and even global scale without additional geodata.

Besides the European Urban Atlas validation and the development of the urban structure classification methodology, the study at hand proves that information on the horizontal and vertical structure of cities allows for detailed analysis of urban morphologies. In this context, differences and analogies of the morphology – in terms of building density, floor space density and mean height on building block level – between the sample cities of London and Paris could be identified depending on the distance to the respective city center. The quantity, decrease rate and variability of the physical parameters on building block level are considerably different towards the city center of London and Paris. An equalization of the considered parameters and thus, analogies between the two cities, could only be identified in the outskirts.

As indicated in the discussion, there is still a need for improvement and enhancement of the urban structuring approach applied within the scope of this study. On the one hand, delineation of structures should be done considering both, structural as well as socioeconomic information. Such an approach would be more sophisticated and thus, would meet the requirements to provide a sufficient database for an effective city management. A suitable database for the implementation of socioeconomic data is presented by the Urban Audit dataset which provides the desired information on the exact same boundaries as the Urban Atlas (see section 2.2.1 *European Urban Atlas*). On the other hand, the implementation of another dataset – preferably at low costs and with a large areal coverage – should be tested in order to overcome the limitations in terms of extraction of building densities as identified within the context of the approach solely based on Cartosat-1 nDSM data. Besides, a variety of ensemble learning classifiers for supervised classification exist to-date. Thus, it should be tested whether better results are achievable when applying other classification models.

**BIBLIOGRAPHY**

- Acioly Jr., C.; Davidson, F. 1996: Density in urban development. In: *Building Issues*, Vol. 8, No. 3: 3–25
- Alter, P. 2000: London in der Neuzeit. In: Sohn, A.; Weber, H. (Eds.): *Hauptstädte und Global Cities an der Schwelle zum 21. Jahrhundert*. Herausforderungen, Bd. Bd. 9. Bochum: Dr. D. Winkler, 57–79
- Anas, A.; Arnott, R.; Small, K. A. 1998: Urban Spatial Structure. In: *Journal of Economic Literature*, Vol. 36, No. 3: 1426–1464
- Arefi, H.; dAngelo, P.; Mayer, H.; Reinartz, P. 2009: Automatic Generation of Digital Terrain Models from Cartosat-1 Stereo Images. In: ISPRS (Ed.): *Proceedings of the International Society for Photogrammetry and Remote Sensing workshop 2009*, 1–6
- Avelar, S.; Zah, R.; Tavares-Corrêa, C. 2009: Linking socioeconomic classes and land cover data in Lima, Peru: Assessment through the application of remote sensing and GIS. In: *International Journal of Applied Earth Observation and Geoinformation*, Vol. 11, No. 1: 27–37
- Bahrenberg, G.; Giese, E.; Nipper, J. 1999: *Statistische Methoden in der Geographie*. Teubner-Studienbücher Geographie. 4., überarb. Aufl. Stuttgart [u.a.]: Teubner
- Banzhaf, E.; Höfer, R. 2008: Monitoring Urban Structure Types as Spatial Indicators With CIR Aerial Photographs for a More Effective Urban Environmental Management. In: *IEEE Journal of Selected Topics in Applied Earth Observations and Remote Sensing*, Vol. 1, No. 2: 129–138
- Baud, I.; Kuffer, M.; Pfeffer, K.; Sliuzas, R.; Karuppanan, S. 2010: Understanding heterogeneity in metropolitan India: The added value of remote sensing data for analyzing sub-standard residential areas. In: *International Journal of Applied Earth Observation and Geoinformation*, Vol. 12, No. 5: 359–374
- Bochow, M. 2010: *Automatisierungspotential von Stadtbiotopkartierungen durch Methoden der Fernerkundung*. PhD-Thesis. Osnabrück
- Bochow, M.; Taubenböck, H.; Segl, K.; Kaufmann, H. 2010: An automated and adaptable approach for characterizing and partitioning cities into urban structure types. In: *IGARSS 2010 - 2010 IEEE International Geoscience and Remote Sensing Symposium*, 1796–1799
- Breiman, L. 1996: Bagging Predictors. In: *Machine Learning*, Vol. 24, No. 1: 123–140
- Breiman, L. 2001: Random Forests. In: *Machine Learning*, Vol. 45, No. 1: 5–32
- Breiman, L. 2002: *Manual on setting up, using, and understanding random forests V3.1*. Berkeley: University of California
- Brüsshaber, C.; Trosset, A. M.; Bucher, T. 2010: Possibilities and constraints in the use of very high spatial resolution UltraCamX airborne imagery and Digital Surface Models for classifi-

## BIBLIOGRAPHY

---

- cation in densely built-up areas – a case study Berlin. In: Michel, U.; Civco, D. L. (Eds.): Remote Sensing. SPIE Proceedings: SPIE, 783115–783115-12
- Buckreuss, S.; Werninghaus, R.; Pitz, W. 2009: The German satellite mission TerraSAR-X. In: IEEE Aerospace and Electronic Systems Magazine, Vol. 24, No. 11: 4–9
- Burgess, E. W. 1984: The Growth of the City: An Introduction to a Research Project. In: Park, R. E.; Burgess, E. W.; McKenzie, R. D. (Eds.): The City. Midway reprint. Chicago: University of Chicago Press, 47–62
- Campbell, J. B.; Wynne, R. H. 2011: Introduction to remote sensing. 5th ed. New York: Guilford Press
- Christaller, W. 1933: Central Places in Southern Germany. New Jersey: Prentice Hall; Englewood Cliffs
- Congalton, R. G.; Green, K. 1999: Assessing the accuracy of remotely sensed data: Principles and practices. Mapping science series. Boca Raton: Lewis Publications
- dAngelo, P.; Lehner, M.; Krauss, T.; Hoja, D.; Reinartz, P. 2008: Towards Automated DEM Generation from High Resolution Stereo Satellite Images. In: International Society for Photogrammetry and Remote Sensing (Ed.): The International Archives of the Photogrammetry, Remote Sensing and Spatial Information Sciences: ISPRS Conference 2008, Bd. XXXVII, 1137–1342
- dAngelo, P.; Uttenthaler, A.; Carl, S.; Barner, F.; Reinartz, P. 2010: Automatic Generation Of High Quality DSM Based On IRS-P5 CARTOSAT-1 Stereo Data. In: ESA (Ed.): Special Publication SP-686, 1–5
- DLR 2009: TerraSAR-X: The German Radar Eye in Space. Retrieved from [http://www.dlr.de/en/Portaldata/1/Resources/forschung\\_und\\_entwicklung/missionen/terrasar\\_x/TSX\\_brosch.pdf](http://www.dlr.de/en/Portaldata/1/Resources/forschung_und_entwicklung/missionen/terrasar_x/TSX_brosch.pdf) (retrieved on 6/18/2015)
- Donnay, J.-P.; Barnsley, M. J.; Longley, P. 2001: Remote sensing and urban analysis. GIS-DATA, No. 9. London: Taylor & Francis
- EEA 2010a: CORINE Land Cover database. Retrieved from <http://www.eea.europa.eu/data-and-maps/data/corine-land-cover-2000-clc2000-seamless-vector-database-5> (retrieved on 6/6/2015)
- EEA 2010b: Urban Atlas. Retrieved from <http://www.eea.europa.eu/data-and-maps/data/urban-atlas> (retrieved on 6/6/2015)
- EEA 2010c: Mapping Guide for a European Urban Atlas. Retrieved from <http://www.eea.europa.eu/data-and-maps/data/urban-atlas/mapping-guide> (Last changed on 8/26/2010, retrieved on 6/15/2015)
- Esch, T.; Marconcini, M.; Felbier, A.; Roth, A.; Heldens, W.; Huber, M.; Schwinger, M.; Taubenbock, H.; Muller, A.; Dech, S. 2013: Urban Footprint Processor—Fully Automated Processing Chain Generating Settlement Masks From Global Data of the TanDEM-X Mission. In: IEEE Geoscience and Remote Sensing Letters, Vol. 10, No. 6: 1617–1621

## BIBLIOGRAPHY

---

- Esch, T.; Schenk, A.; Ullmann, T.; Thiel, M.; Roth, A.; Dech, S. 2011: Characterization of Land Cover Types in TerraSAR-X Images by Combined Analysis of Speckle Statistics and Intensity Information. In: *IEEE Transactions on Geoscience and Remote Sensing*, Vol. 49, No. 6: 1911–1925
- Esch, T.; Taubenböck, H.; Heldens, W.; Thiel, M.; Wurm, M.; Geiß, Chr.; Dech, S. 2010: Urban Remote Sensing: How Can Earth Observation Support the Sustainable Development of Urban Environments? In: *Real CORP (Ed.): Proceedings*, 1–10
- Esch, T.; Taubenböck, H.; Roth, A.; Heldens, W.; Felbier, A.; Thiel, M.; Schmidt, M.; Müller, A.; Dech, S. 2012: TanDEM-X mission—new perspectives for the inventory and monitoring of global settlement patterns. In: *Journal of Applied Remote Sensing*, Vol. 6, No. 1: 1–20
- ESRI 2013: *ArcGIS Desktop*. Redlands, Canada: Environmental System Research Institute
- ESRI 2014: *ArcGIS Desktop Help 10.1*. Retrieved from [resources.arcgis.com/en/help/main/10.1](http://resources.arcgis.com/en/help/main/10.1) (retrieved on 4/2/2015)
- Fabrizio, R.; Santis, A. de; Gomez, A. 2011: Satellite and ground-based sensors for the Urban Heat Island analysis in the city of Madrid. In: *Stilla, U. (Ed.): JURSE 2011: 2011 Joint Urban Remote Sensing Event : proceedings : April 11-13, 2011, Munich, Germany*. [Piscataway, N.J.]: IEEE, 1–4
- Felbier, A.; Esch, T.; Heldens, W.; Marconcini, M.; Zeidler, J.; Rogan, J.; Klotz, M.; Wurm, M.; Taubenböck, H. 2014: The Global Urban Footprint: Processing Status and Cross Comparison To Existing Human Settlement Products. In: *IEEE International Geoscience and Remote Sensing Symposium (IGARSS), 2014: [held in conjunction with the] 35th Canadian Symposium on Remote Sensing (35th CSRS) ; 13 - 18 July 2014, Quebec City, Quebec, Canada ; proceedings*. Piscataway, NJ: IEEE
- Fernández-Delgado, M.; Cernadas, E.; Barro, S. 2014: Do we Need Hundreds of Classifiers to Solve Real World Classification Problems? In: *Journal of Machine Learning Research*, No. 15: 3133–3181
- Fina, S.; Krehl, A.; Siedentop, S.; Taubenböck, H.; Wurm, M. 2014: Dichter dran! Neue Möglichkeiten der Vernetzung von Geobasis-, Statistik- und Erdbeobachtungsdaten zur räumlichen Analyse und Visualisierung von Stadtstrukturen mit Dichteoberflächen und -profilen. In: *Raumforschung und Raumordnung*, Vol. 72, No. 3: 179–194
- Foody, G. M. 2002: Status of land cover classification accuracy assessment. In: *Remote Sensing of Environment*, Vol. 80, No. 1: 185–201
- Ghimire, B.; Rogan, J.; Miller, J. 2010: Contextual land-cover classification: incorporating spatial dependence in land-cover classification models using random forests and the Getis statistic. In: *Remote Sensing Letters*, Vol. 1, No. 1: 45–54
- Gianinetto, M. 2008: Automatic digital terrain model generation using Cartosat-1 stereo images. In: *Sensor Review*, Vol. 28, No. 4: 299–310

## BIBLIOGRAPHY

---

- Gill, S. E.; Handley, J. F.; Ennos, A. R.; Pauleit, S.; Theuray, N.; Lindley, S. J. 2008: Characterising the urban environment of UK cities and towns: A template for landscape planning. In: *Landscape and Urban Planning*, Vol. 87, No. 3: 210–222
- Gill, S.E; Handley, J.F; Ennos, A.R; Pauleit, S. 2007: Adapting Cities for Climate Change: The Role of the Green Infrastructure. In: *Built Environment*, Vol. 33, No. 1: 115–133
- Goodchild, M. F. 2007: Citizens as sensors: the world of volunteered geography. In: *GeoJournal*, Vol. 69, No. 4: 211–221
- Goodchild, M. F.; Li, L. 2012: Assuring the quality of volunteered geographic information. In: *Spatial Statistics*, Vol. 1, No. 1: 110–120
- Google Inc. 2013: Google Earth. Mountain View, Canada
- Griffiths, P.; Hostert, P.; Gruebner, O.; van der Linden, S. 2010: Mapping megacity growth with multi-sensor data. In: *Remote Sensing of Environment*, Vol. 114, No. 2: 426–439
- Groham, G.; Kroenung, G.; Strebeck, J. 2006: Filling SRTM voids: The delta surface fill model. In: *Photogrammetric Engineering and Remote Sensing*, No. 72: 213–216
- Guo, L.; Chehata, N.; Mallet, C.; Boukir, S. 2011: Relevance of airborne lidar and multispectral image data for urban scene classification using Random Forests. In: *ISPRS Journal of Photogrammetry and Remote Sensing*, Vol. 66, No. 1: 56–66
- Hahs, A. K.; McDonnell, M. J.; McCarthy, M. A.; Vesk, P. A.; Corlett, R. T.; Norton, B. A.; Clemants, S. E.; Duncan, R. P.; Thompson, K.; Schwartz, M. W.; Williams, N. S. G. 2009: A global synthesis of plant extinction rates in urban areas. In: *Ecology letters*, Vol. 12, No. 11: 1165–1173
- Halbert, L. 2006: The Paris Region: Polycentric Spatial Planning in a Monocentric Metropolitan Region. In: Hall, P.; Pain, K. (Eds.): *The polycentric metropolis: Learning from megacity regions in Europe*. London, Sterling, VA: Earthscan, 180–186
- Haralick, R. M. 1979: Statistical and structural approaches to texture. In: *Proceedings of the IEEE*, Vol. 67, No. 5: 786–804
- Haralick, R. M.; Shanmugam, K.; Dinstein, I. H. 1973: Textural Features for Image Classification. In: *IEEE Transactions on Systems, Man, and Cybernetics*, Vol. 3, No. 6: 610–621
- Haralick, R. M.; Sternberg, S. R.; Zhuang, X. 1987: Image Analysis Using Mathematical Morphology. In: *IEEE transactions on pattern analysis and machine intelligence*, Vol. PAMI-9, No. 4: 532–550
- Hecht, R.; Kunze, C.; Hahmann, S. 2013: Measuring Completeness of Building Footprints in OpenStreetMap over Space and Time. In: *ISPRS International Journal of Geo-Information*, Vol. 2, No. 4: 1066–1091
- Heinzel, J.; Kemper, T. 2015: Automated metric characterization of urban structure using building decomposition from very high resolution imagery. In: *International Journal of Applied Earth Observation and Geoinformation*, Vol. 35, No. 1: 151–160

- Hermosilla, T.; Palomar-Vázquez, J.; Balaguer-Beser, Á.; Balsa-Barreiro, J.; Ruiz, L. A. 2014: Using street based metrics to characterize urban typologies. In: *Computers, Environment and Urban Systems*, Vol. 44, No. 1: 68–79
- Herold, M.; Liu, X. H.; Clarke, K. C. 2003: Spatial Metrics and Image Texture for Mapping Urban Land Use. In: *Photogrammetric Engineering & Remote Sensing*, Vol. 69, No. 9: 991–1001
- Herold, M.; Scepan, J.; Clarke, K. C. 2002: The use of remote sensing and landscape metrics to describe structures and changes in urban land uses. In: *Environment and Planning A*, Vol. 34, No. 8: 1443–1458
- Hirschmüller, H. 2008: Stereo processing by semiglobal matching and mutual information. In: *IEEE transactions on pattern analysis and machine intelligence*, Vol. 30, No. 2: 328–341
- Hirschmüller, H. 2011: Semi-Global Matching – Motivation, Developments and Applications. In: Fritsch, D. (Ed.): *53rd Photogrammetry Week*. Heidelberg, Germany: Herbert Wichmann Verlag, 173–184
- Jensen, J. R. 2005: *Introductory digital image processing: A remote sensing perspective*. Prentice Hall series in geographic information science. 3rd ed. Upper Saddle River, N.J.: Prentice Hall
- Jensen, J. R. 2007: *Remote sensing of the environment: An earth resource perspective*. Prentice Hall series in geographic information science. 2nd ed. Upper Saddle River, NJ: Pearson Prentice Hall
- Keene, D. 2000: London: metropolis and capital, A.D. 600-1530. In: Sohn, A.; Weber, H. (Eds.): *Hauptstädte und Global Cities an der Schwelle zum 21. Jahrhundert*. Herausforderungen, Bd. Bd. 9. Bochum: Dr. D. Winkler, 29–56
- Khoshelham, K.; Nardinocchi, C.; Frontoni, E.; Mancini, A.; Zingaretti, P. 2010: Performance evaluation of automated approaches to building detection in multi-source aerial data. In: *ISPRS Journal of Photogrammetry and Remote Sensing*, Vol. 65, No. 1: 123–133
- Kittmito, K.; Colin, C. V.; Venters, C.; Cooper, M. D.; Muller, J. P.; Morley, J. G.; Walker, A. H.; Rana, S. 2000: LANDMAP: Serving Satellite imagery to the UK academic. Retrieved from [http://learningzone.rspoc.org.uk/images/stories/support/publication/papers/landmap\\_serving.pdf](http://learningzone.rspoc.org.uk/images/stories/support/publication/papers/landmap_serving.pdf) (retrieved on 6/16/2015)
- Klotz, M. 2012: *Delimiting the Central Business District: A physical analysis using Remote Sensing*. published Masterthesis. London
- Krieger, G.; Moreira, A.; Fiedler, H.; Hajnsek, I.; Werner, M.; Younis, M.; Zink, M. 2007: TanDEM-X: A Satellite Formation for High-Resolution SAR Interferometry. In: *IEEE Transactions on Geoscience and Remote Sensing*, Vol. 45, No. 11: 3317–3341

## BIBLIOGRAPHY

---

- Kuffer, M.; Barros, J. 2011: Urban Morphology of Unplanned Settlements: The Use of Spatial Metrics in VHR Remotely Sensed Images. In: *Procedia Environmental Sciences*, Vol. 7, No. 2: 152–157
- Landis, J. R.; Koch, G. G. 1977: The Measurement of Observer Agreement for Categorical Data. In: *Biometrics*, Vol. 33, No. 1: 159
- Liaw, A.; Wiener, M. 2002: Classification and regression by randomForest. In: *R News: The Newsletter of the R Project*, Vol. 3, No. 2: 18–22
- Liaw, A.; Wiener, M. 2015: Package "randomForest".
- Lillesand, T. M.; Kiefer, R. W.; Chipman, J. W. 2004: Remote sensing and image interpretation. 5th ed. New York: Wiley
- Luck, M.; Wu, J. 2002: A gradient analysis of urban landscape pattern: a case study from the Phoenix metropolitan region, Arizona, USA. In: *Landscape Ecology*, Vol. 17, No. 4: 327–339
- Mahmoud, A.; Elbially, S.; Pradhan, B.; Buchroithner, M. 2011: Field-based landcover classification using TerraSAR-X texture analysis. In: *Advances in Space Research*, Vol. 48, No. 5: 799–805
- Mhangara, P.; Odindi, J. 2013: Potential of texture-based classification in urban landscapes using multispectral aerial photos. In: *South African Journal of Science*, Vol. 109, No. 3/4: 1–8
- Moreira, A.; Krieger, G.; Hajnsek, I.; Hounam, D.; Werner, M.; Riegger, S.; Settelmeier, E. 2004: TanDEM-X: a terraSAR-X add-on satellite for single-pass SAR interferometry. In: *IEEE International IEEE International IEEE International Geoscience and Remote Sensing Symposium, 2004. IGARSS '04. Proceedings. 2004*, 1000–1003
- Niebergall, S.; Loew, A.; Mauser, W. 2008: Integrative Assessment of Informal Settlements Using VHR Remote Sensing Data—The Delhi Case Study. In: *IEEE Journal of Selected Topics in Applied Earth Observations and Remote Sensing*, Vol. 1, No. 3: 193–205
- OECD 2012: Compact city policies: A comparative assessment. OECD green growth studies. Paris: OECD
- OSM - OpenStreetMap 2012: OSM - Shapefile data of building footprints. Downloaded via QuantumGIS for the Testsite of Paris
- Osmond, P. 2011: Application of the urban structural unit method to inform post-carbon planning and design. In: *Urban Morphology and the Post-Carbon City*
- Pacifici, F.; Chini, M.; Emery, W. J. 2009: A neural network approach using multi-scale textural metrics from very high-resolution panchromatic imagery for urban land-use classification. In: *Remote Sensing of Environment*, Vol. 113, No. 6: 1276–1292
- Pal, M. 2005: Random forest classifier for remote sensing classification. In: *International Journal of Remote Sensing*, Vol. 26, No. 1: 217–222

- Patino, J. E.; Duque, J. C. 2013: A review of regional science applications of satellite remote sensing in urban settings. In: *Computers, Environment and Urban Systems*, Vol. 37, No. 1: 1–17
- Pauleit, S.; Duhme, F. 2000: Assessing the environmental performance of land cover types for urban planning. In: *Landscape and Urban Planning*, Vol. 52, No. 1: 1–20
- Pesaresi, M.; Guo, H.; Blaes, X.; Ehrlich, D.; Ferri, S.; Gueguen, L.; Halkia, M.; Kauffmann, M.; Kemper, T.; Linlin, L.; Marin-Herrera, M. A.; Ouzounis, G. K.; Scavazzon, M.; Soille, P.; Syrris, V.; Zanchetta, L. 2013: A Global Human Settlement Layer From Optical HR/VHR RS Data: Concept and First Results. In: *IEEE Journal of Selected Topics in Applied Earth Observations and Remote Sensing*, Vol. 6, No. 5: 2102–2131
- Pham, H. M.; Yamaguchi, Y.; Bui, T. Q. 2011: A case study on the relation between city planning and urban growth using remote sensing and spatial metrics. In: *Landscape and Urban Planning*, Vol. 100, No. 3: 223–230
- Prastacos, P.; Chrysoulakis, N.; Kochilakis, G. 2011: Urban Atlas, land use modelling and spatial metric techniques. In: *European Regional Science Association (Ed.): 51st European Congress of the Regional Science Association International*, 1–14
- Prastacos, P.; Chrysoulakis, N.; Kochilakis, G. 2012: Spatial Metrics for Greek cities using land cover information from the Urban Atlas. In: *Gensel, J.; Josselin, D.; Vandenbroucke, D. (Eds.): Multidisciplinary Research on Geographical Information in Europe and Beyond: Proceedings of the 15th AGILE International Conference on Geographic Information Science*, 261–266
- R Core Team 2014: *R: A Language and Environment for Statistical Computing*. Vienna, Austria: R Foundation for Statistical Computing
- Richards, J. A.; Jia, Xiuping 2006: *Remote sensing digital image analysis: An introduction*. 4th ed. Berlin: Springer
- Rodriguez-Galiano, V. F.; Chica-Olmo, M.; Abarca-Hernandez, F.; Atkinson, P. M.; Jegathan, C. 2012a: Random Forest classification of Mediterranean land cover using multi-seasonal imagery and multi-seasonal texture. In: *Remote Sensing of Environment*, Vol. 121, No. 1: 93–107
- Rodriguez-Galiano, V. F.; Ghimire, B.; Rogan, J.; Chica-Olmo, M.; Rigol-Sanchez, J. P. 2012b: An assessment of the effectiveness of a random forest classifier for land-cover classification. In: *ISPRS Journal of Photogrammetry and Remote Sensing*, Vol. 67, No. 1: 93–104
- Sapena, M.; Ruiz, L. A. 2015: Analysis of urban development by means of multi-temporal fragmentation metrics from LULC data. In: *ISPRS - International Archives of the Photogrammetry, Remote Sensing and Spatial Information Sciences*, Vol. XL-7/W3, No. 5: 1411–1418
- Schneider, A.; Friedl, M. A.; Potere, D. 2009: A new map of global urban extent from MODIS satellite data. In: *Environmental Research Letters*, Vol. 4, No. 4: 044003

## BIBLIOGRAPHY

---

- Seifert, F. M. 2009: Improving Urban Monitoring toward a European Urban Atlas. In: Gamba, P.; Herold, M. (Eds.): Global mapping of human settlement: Experiences, datasets, and prospects. Taylor & Francis series in remote sensing applications. Boca Raton: CRC Press, 231–248
- Seto, K. C.; Fragkias, M.; Güneralp, B.; Reilly, M. K. 2011: A meta-analysis of global urban land expansion. In: PloS one, Vol. 6, No. 8: e23777
- Simmie, J.; Sennet, J. 2001: London: International Trading Metropolis. In: Simmie, J. (Ed.): Innovative cities. London, New York: Spon Press, 191–228
- Sirmacek, B.; Taubenböck, H.; Reinartz, P.; Ehlers, M. 2012: Performance Evaluation for 3-D City Model Generation of Six Different DSMs From Air- and Spaceborne Sensors. In: IEEE Journal of Selected Topics in Applied Earth Observations and Remote Sensing, Vol. 5, No. 1: 59–70
- Sohn, A. 2000: Hauptstadtwerdung in Frankreich: Die mittelalterliche Genese von Paris (6.-15. Jahrhundert). In: Sohn, A.; Weber, H. (Eds.): Hauptstädte und Global Cities an der Schwelle zum 21. Jahrhundert. Herausforderungen, Bd. Bd. 9. Bochum: Dr. D. Winkler, 81–101
- Stathakis, D.; Tsilimigkas, G. 2013: Applying Urban Compactness Metrics on Pan-European Datasets. In: ISPRS - International Archives of the Photogrammetry, Remote Sensing and Spatial Information Sciences, Vol. XL-4/W1, No. 2: 127–132
- Sukopp, H.; Wittig, R. 1998: Stadtökologie. Stuttgart: Gustav Fischer Verlag
- Taubenböck, H.; Esch, T.; Felbier, A.; Wiesner, M.; Roth, A.; Dech, S. 2012: Monitoring urbanization in mega cities from space. In: Remote Sensing of Environment, Vol. 117, No. 2: 162–176
- Taubenböck, H.; Heldens, W.; Wurm, M. 2010: Physische Indikatoren für die Stadtplanung. In: Taubenböck, H. (Ed.): Fernerkundung im urbanen Raum: Erdbeobachtung auf dem Weg zur Planungspraxis. Darmstadt: WBG, 86–93
- Taubenböck, H.; Klotz, M.; Wurm, M.; Schmieder, J.; Wagner, B.; Wooster, M.; Esch, T.; Dech, S. 2013: Delineation of Central Business Districts in mega city regions using remotely sensed data. In: Remote Sensing of Environment, Vol. 136, No. 4: 386–401
- Taubenböck, H.; Kraff, N. J. 2014: The physical face of slums: a structural comparison of slums in Mumbai, India, based on remotely sensed data. In: Journal of Housing and the Built Environment, Vol. 29, No. 1: 15–38
- Taubenböck, H.; Kraff, N. J. 2015: Das globale Gesicht urbaner Armut? Siedlungsstrukturen in Slums. In: Taubenböck, H.; Wurm, M.; Esch, T.; Dech, S. (Eds.): Globale Urbanisierung. Berlin, Heidelberg: Springer Berlin Heidelberg, 107–119
- Taubenböck, H.; Wiesner, M.; Felbier, A.; Marconcini, M.; Esch, T.; Dech, S. 2014: New dimensions of urban landscapes: The spatio-temporal evolution from a polynuclei area to a

- mega-region based on remote sensing data. In: *Applied Geography*, Vol. 47, No. 2: 137–153
- Thünen, J. H. 2011: *Der isolierte Staat*. Paderborn: Salzwater Verlag
- Trimble GmbH 2014a: *eCognition Developer 9.0 - Reference Book*. München: Trimble Germany GmbH
- Trimble GmbH 2014b: *eCognition Developer Version 9.0*. München: Trimble Germany GmbH
- UKMap building inventory © The Geoinformation Group 2012: Building footprints and heights. Retrieved from <http://www.landmap.ac.uk/index.php/Datasets/> (retrieved on 4/11/2012)
- United Nations 2012: *World Urbanization Prospects: The 2011 Revision*. New York
- United Nations 2013: *World Population Prospects: The 2012 Revision: Key Findings and Advance Tables*. Working Paper No. ESA/P/WP.227
- United Nations 2014: *World urbanization prospects: The 2014 revision*. New York
- Uttenthaler, A.; Barner, F.; Hass, T.; Makiola, J.; dAngelo, P.; Reinartz, P.; Carl, S.; Steiner, M. 2013: *Euro-Maps 3D - a Transnational, High-Resolution Digital Surface Model for Europe*. In: ESA (Ed.): *Special Publication SP-722*
- Voltersen, M.; Berger, C.; Hese, S.; Schmullius, C. 2014: Object-based land cover mapping and comprehensive feature calculation for an automated derivation of urban structure types at block level. In: *Remote Sensing of Environment*, Vol. 154, No. 2: 192–201
- Waske, B.; Fauvel, M.; Benediktsson, J. A.; Chanussot, J. 2009: Machine learning techniques in remote sensing analysis. In: Camps-Valls, G.; Bruzzone, L. (Eds.): *Kernel methods for remote sensing data analysis*. Hoboken, NJ: Wiley, 3–24
- Weng, Q.; Quattrochi, D. A. 2007: *Urban remote sensing*. Boca Raton: CRC Press
- Wirsching, A. 2000: Paris in der Neuzeit (1500-2000). In: Sohn, A.; Weber, H. (Eds.): *Hauptstädte und Global Cities an der Schwelle zum 21. Jahrhundert. Herausforderungen*, Bd. Bd. 9. Bochum: Dr. D. Winkler, 103–128
- Wurm, M. 2013: *Verknüpfung von Fernerkundungsdaten und Survey-Daten (SOEO und BASE-II) in städtischen Räumen für sozialwissenschaftliche Analysen*. Dissertation. Graz
- Wurm, M.; dAngelo, P.; Reinartz, P.; Taubenböck, H. 2014: Investigating the Applicability of Cartosat-1 DEMs and Topographic Maps to Localize Large-Area Urban Mass Concentrations. In: *IEEE Journal of Selected Topics in Applied Earth Observations and Remote Sensing*, Vol. 7, No. 10: 4138–4152
- Wurm, M.; Goebel, J.; Taubenböck, H.; Wagner, G. G. 2015a: Am Ende der Kernstadt – ein Versuch der Abgrenzung des Physischen durch das Subjektive. In: Taubenböck, H.; Wurm, M.; Esch, T.; Dech, S. (Eds.): *Globale Urbanisierung*. Berlin, Heidelberg: Springer Berlin Heidelberg, 179–189

## BIBLIOGRAPHY

---

- Wurm, M.; Taubenböck, H. 2010a: Fernerkundung als Grundlage zur Identifikation von Stadtstrukturtypen. In: Taubenböck, H. (Ed.): Fernerkundung im urbanen Raum: Erdbeobachtung auf dem Weg zur Planungspraxis. Darmstadt: WBG, 94–103
- Wurm, M.; Taubenböck, H. 2010b: Das 3-D-Stadtmodell als planungsrelevante Grundlageninformation. In: Taubenböck, H. (Ed.): Fernerkundung im urbanen Raum: Erdbeobachtung auf dem Weg zur Planungspraxis. Darmstadt: WBG, 66–75
- Wurm, M.; Taubenböck, H.; Dech, S.; Michel, U.; Civco, D. L. 2010: Quantification of urban structure on building block utilizing multisensoral remote sensing data. In: Remote Sensing. SPIE Proceedings: SPIE, 1–12
- Wurm, M.; Taubenböck, H.; Goebel, J.; Wagner, G. G. 2015b: At the edge of the city center: Discrimination of the physical city center by subjective perception and satellite data. In: Proceedings of the Joint Urban Remote Sensing Event. Proceedings of the Joint Urban Remote Sensing Event. Lausanne, Switzerland
- Wurm, M.; Taubenböck, H.; Roth, A.; Dech, S. 2009: Urban structuring using multisensoral remote sensing data: by the example of German cities Cologne and Dresden. In: Urban Remote Sensing Joint Event, 1–8

APPENDIX

**Appendix 1:** Urban Atlas dataset of London.....ii

**Appendix 2:** Urban Atlas dataset of Paris .....iii

**Appendix 3:** Cartosat-1 nDSM of London .....iv

**Appendix 4:** Cartosat-1 nDSM of Paris.....v

**Appendix 5:** “Global Urban Footprint” extract of London .....vi

**Appendix 6:** Confusion matrices of a) D3H3 classification, b) D3H2 classification, c) D2H3 classification, d) D3 classification and e) D2 classification of London on Urban Atlas level ..... vii

**Appendix 7:** Confusion matrices of a) D2H2 classification, b) H3 classification and c) H2 classification of Paris (London trained) on Urban Atlas level .....xi

**Appendix 8:** D2H2 classification of Paris on Urban Atlas level: a) reference data and b) classification result..... xiii

**Appendix 9:** H2 classification of Paris on Urban Atlas level: a) reference data and b) classification result..... xiv

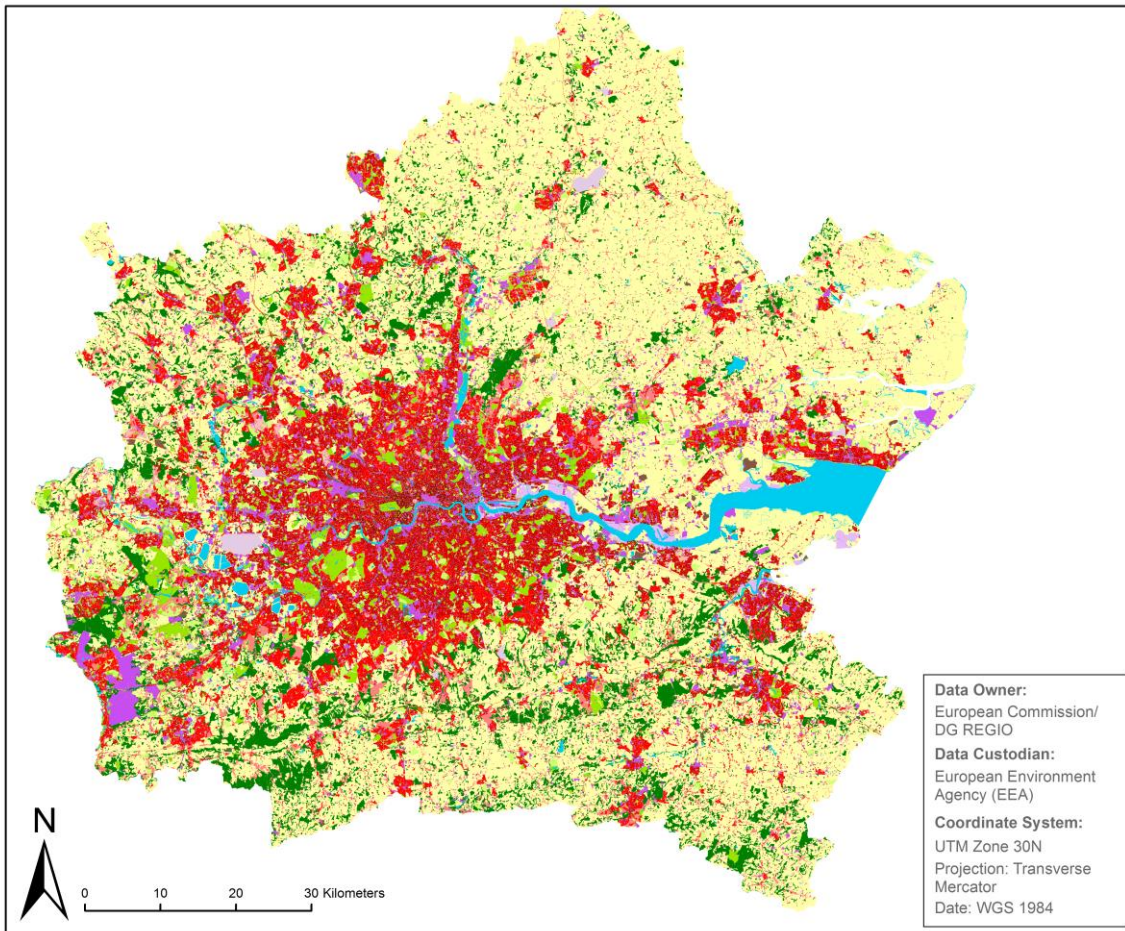
**Appendix 10:** Confusion matrices of a) D2H2 classification, b) H3 classification and c) H2 classification of London on square object level ..... xv

**Appendix 11:** D2H2 classification of London on square object level: a) reference data and b) classification result..... xvii

**Appendix 12:** H2 classification of London on square object level: a) reference data and b) classification result..... xviii

## APPENDIX

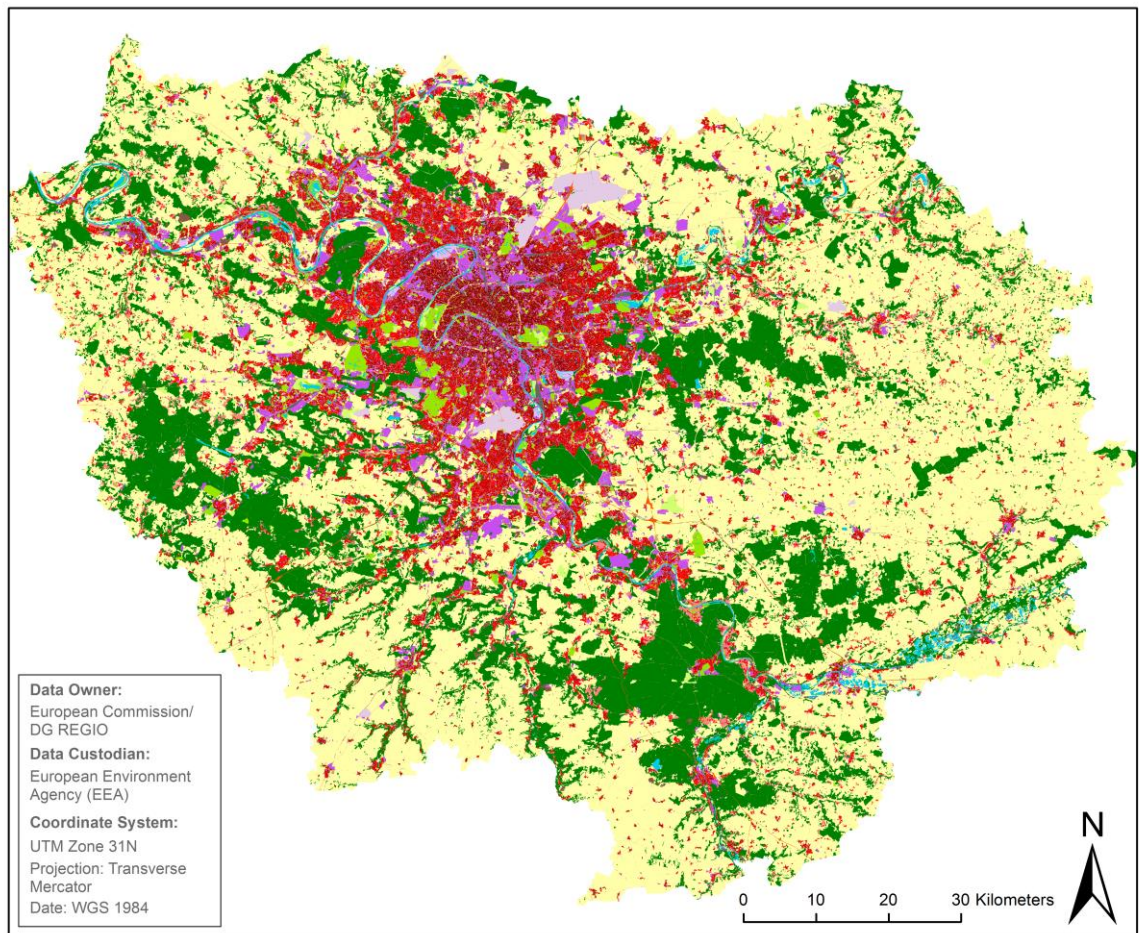
### Appendix 1: Urban Atlas dataset of London



#### Legend

<ul style="list-style-type: none"> <li><span style="display: inline-block; width: 15px; height: 15px; background-color: #800000; margin-right: 5px;"></span> 11100: Continuous Urban fabric (S.L. &gt; 80%)</li> <li><span style="display: inline-block; width: 15px; height: 15px; background-color: #FF0000; margin-right: 5px;"></span> 11210: Discontinuous Dense Urban Fabric (S.L.: 50% - 80%)</li> <li><span style="display: inline-block; width: 15px; height: 15px; background-color: #FF0000; margin-right: 5px;"></span> 11220: Discontinuous Medium Density Urban Fabric (S.L.: 30% - 50%)</li> <li><span style="display: inline-block; width: 15px; height: 15px; background-color: #FF6347; margin-right: 5px;"></span> 11230: Discontinuous Low Density Urban Fabric (S.L.: 10% - 30%)</li> <li><span style="display: inline-block; width: 15px; height: 15px; background-color: #FFB6C1; margin-right: 5px;"></span> 11240: Discontinuous very low density urban fabric (S.L. &lt; 10%)</li> <li><span style="display: inline-block; width: 15px; height: 15px; background-color: #A52A2A; margin-right: 5px;"></span> 11300: Isolated Structures</li> <li><span style="display: inline-block; width: 15px; height: 15px; background-color: #800080; margin-right: 5px;"></span> 12100: Industrial, commercial, public, military and private units</li> <li><span style="display: inline-block; width: 15px; height: 15px; background-color: #FF8C00; margin-right: 5px;"></span> 12210: Fast transit roads and associated land</li> <li><span style="display: inline-block; width: 15px; height: 15px; background-color: #FFDAB9; margin-right: 5px;"></span> 12220: Other roads and associated land</li> <li><span style="display: inline-block; width: 15px; height: 15px; background-color: #696969; margin-right: 5px;"></span> 12230: Railways and associated land</li> <li><span style="display: inline-block; width: 15px; height: 15px; background-color: #DDA0DD; margin-right: 5px;"></span> 12300: Port areas</li> </ul>	<ul style="list-style-type: none"> <li><span style="display: inline-block; width: 15px; height: 15px; background-color: #D8BFD8; margin-right: 5px;"></span> 12400: Airports</li> <li><span style="display: inline-block; width: 15px; height: 15px; background-color: #8B4513; margin-right: 5px;"></span> 13100: Mineral extraction and dump sites</li> <li><span style="display: inline-block; width: 15px; height: 15px; background-color: #D2B48C; margin-right: 5px;"></span> 13300: Construction sites</li> <li><span style="display: inline-block; width: 15px; height: 15px; background-color: #654321; margin-right: 5px;"></span> 13400: Land without current use</li> <li><span style="display: inline-block; width: 15px; height: 15px; background-color: #32CD32; margin-right: 5px;"></span> 14100: Green urban areas</li> <li><span style="display: inline-block; width: 15px; height: 15px; background-color: #90EE90; margin-right: 5px;"></span> 14200: Sports and leisure facilities</li> <li><span style="display: inline-block; width: 15px; height: 15px; background-color: #FFFF00; margin-right: 5px;"></span> 20000: Agricultural Areas</li> <li><span style="display: inline-block; width: 15px; height: 15px; background-color: #006400; margin-right: 5px;"></span> 30000: Forests and semi-natural areas</li> <li><span style="display: inline-block; width: 15px; height: 15px; background-color: #9370DB; margin-right: 5px;"></span> 40000: Wetlands</li> <li><span style="display: inline-block; width: 15px; height: 15px; background-color: #00CED1; margin-right: 5px;"></span> 50000: Water</li> </ul>
--	--

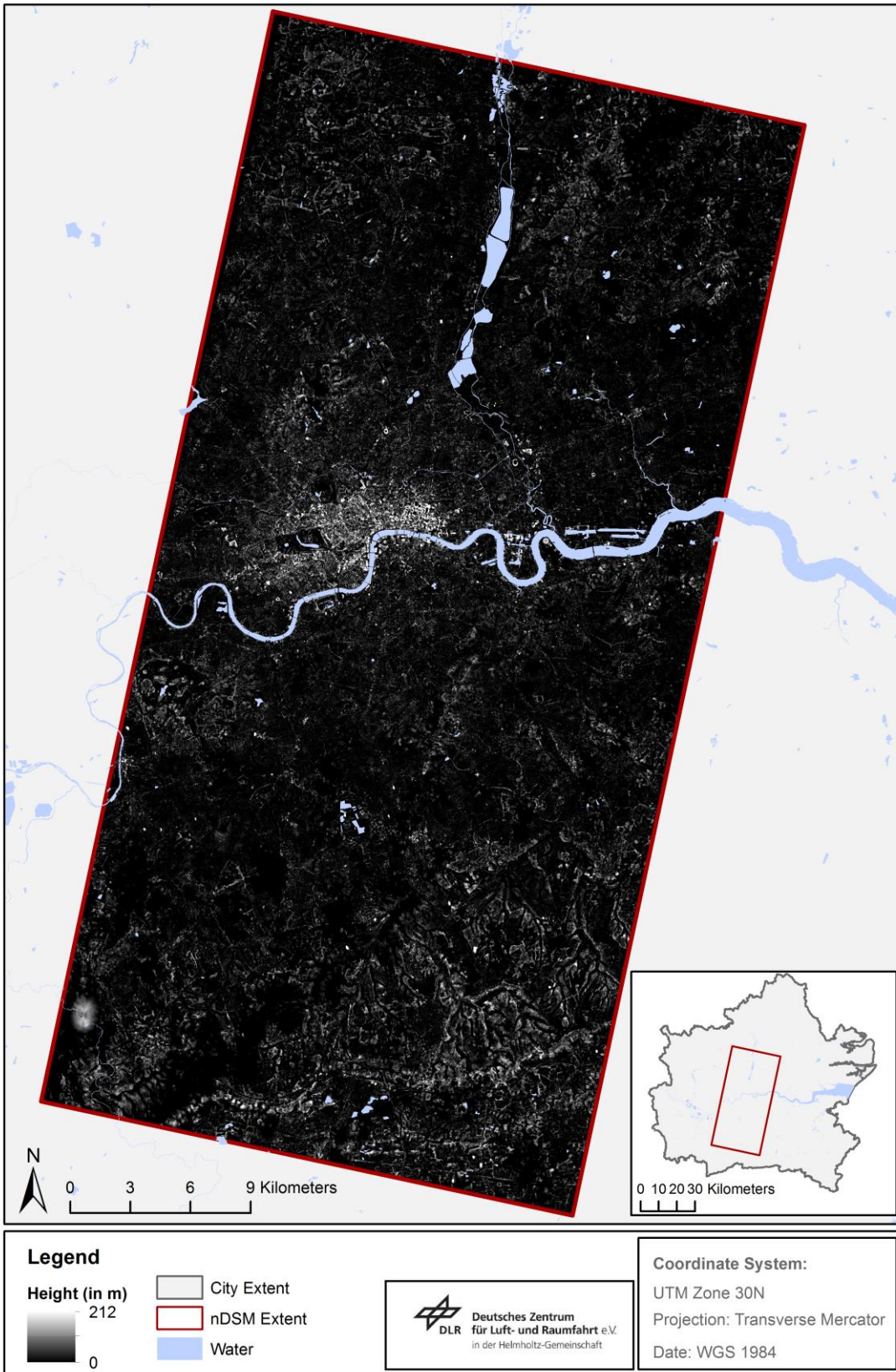
Appendix 2: Urban Atlas dataset of Paris



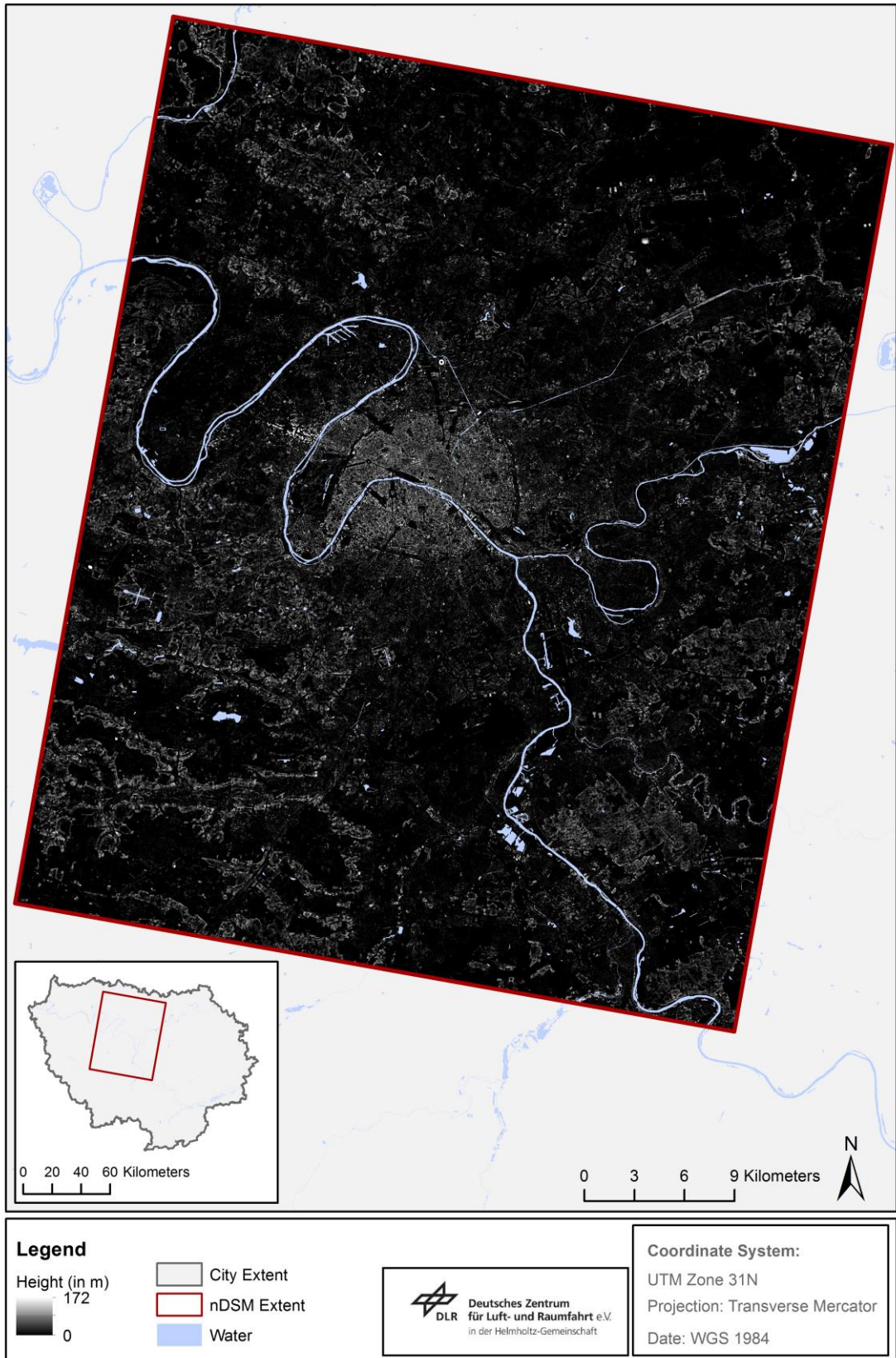
**Legend**

 11100: Continuous Urban fabric (S.L. > 80%)	 12400: Airports
 11210: Discontinuous Dense Urban Fabric (S.L.: 50% - 80%)	 13100: Mineral extraction and dump sites
 11220: Discontinuous Medium Density Urban Fabric (S.L.: 30% - 50%)	 13300: Construction sites
 11230: Discontinuous Low Density Urban Fabric (S.L.: 10% - 30%)	 13400: Land without current use
 11240: Discontinuous very low density urban fabric (S.L. < 10%)	 14100: Green urban areas
 11300: Isolated Structures	 14200: Sports and leisure facilities
 12100: Industrial, commercial, public, military and private units	 20000: Agricultural Areas
 12210: Fast transit roads and associated land	 30000: Forests and semi-natural areas
 12220: Other roads and associated land	 40000: Wetlands
 12230: Railways and associated land	 50000: Water
 12300: Port areas	

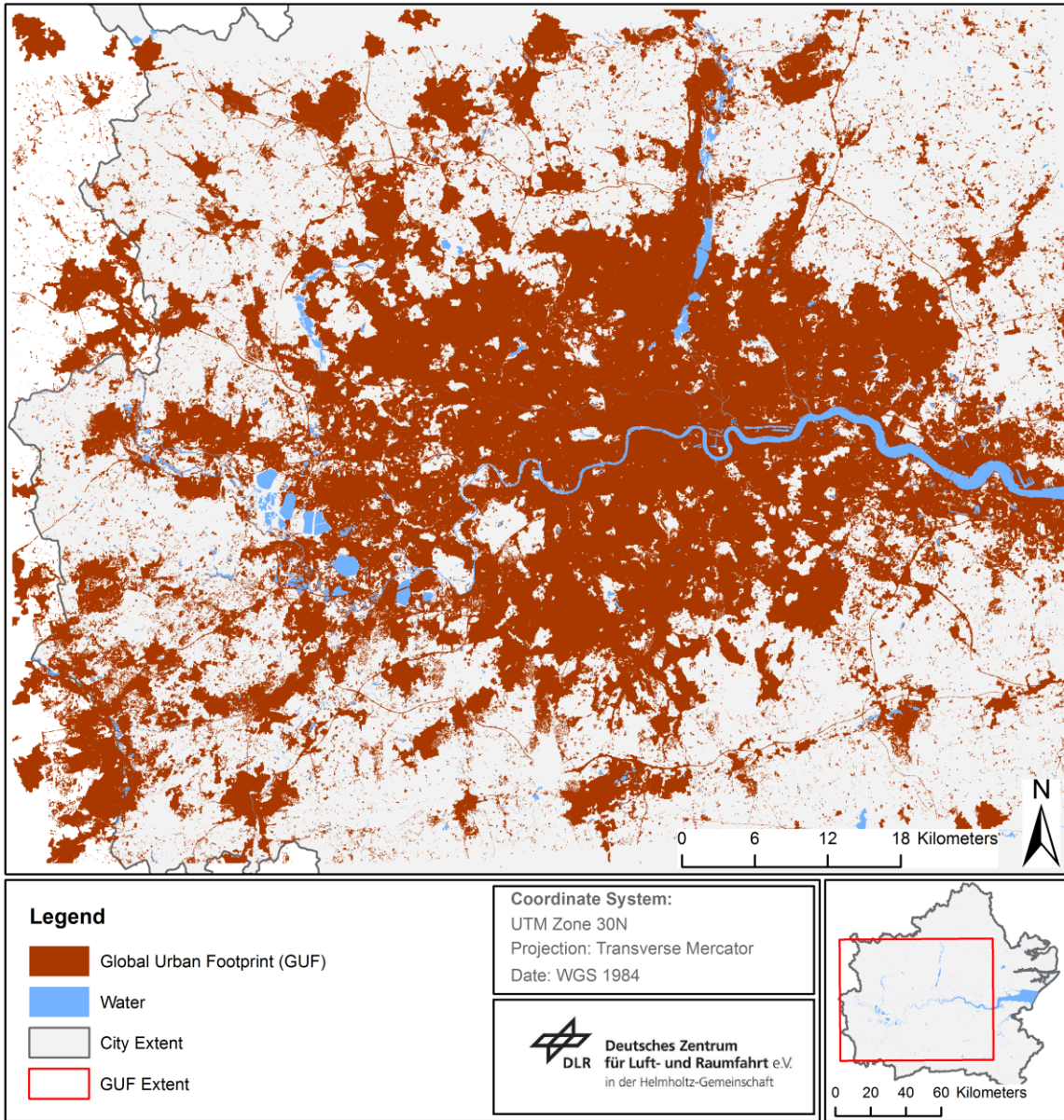
Appendix 3: Cartosat-1 nDSM of London



Appendix 4: Cartosat-1 nDSM of Paris



Appendix 5: "Global Urban Footprint" extract of London



**APPENDIX**

**Appendix 6:** Confusion matrices of a) D3H3 classification, b) D3H2 classification, c) D2H3 classification, d) D3 classification and e) D2 classification of London on Urban Atlas level

**Reference Data**

<b>Prediction</b>	<b>a) D3H3</b>	<i>11</i>	<i>12</i>	<i>13</i>	<i>21</i>	<i>22</i>	<i>23</i>	<i>31</i>	<i>32</i>	<i>33</i>	<b>Row Total</b>
	<i>11</i>	6,972	850	42	3,191	1,002	29	611	310	38	13,045
	<i>12</i>	243	540	72	124	591	72	36	237	45	1,960
	<i>13</i>	8	20	32	4	30	29	1	15	17	156
	<i>21</i>	2,069	343	9	2,583	518	1	921	202	3	6,649
	<i>22</i>	573	931	115	481	1,596	121	195	807	91	4,910
	<i>23</i>	5	55	75	1	71	142	0	71	163	583
	<i>31</i>	61	11	1	93	15	1	52	13	2	249
	<i>32</i>	58	168	62	56	299	91	41	373	137	1,285
	<i>33</i>	20	77	187	3	91	440	1	144	1,910	2,873
<b>Col- umn Total</b>	10,009	2,995	595	6,536	4,213	926	1,858	2,172	2,406	31,710	
<b>Omis- sion Error</b>	0.31	0.82	0.95	0.60	0.62	0.85	0.97	0.83	0.21		
<b>Pro- ducer's Accu- racy</b>	0.69	0.18	0.05	0.40	0.38	0.15	0.03	0.17	0.79		
<b>Com- mis- sion Error</b>	0.47	0.72	0.69	0.61	0.67	0.76	0.79	0.71	0.34		
<b>User's Accu- racy</b>	0.53	0.28	0.21	0.39	0.33	0.24	0.21	0.29	0.66		

**APPENDIX**

---

**Reference Data**

<b>Prediction</b>	<b>b) D3H2</b>	<i>11</i>	<i>12</i>	<i>21</i>	<i>22</i>	<i>31</i>	<i>32</i>	<b>Row Total</b>
	<i>11</i>	8,080	325	4,095	395	829	156	13,880
	<i>12</i>	118	186	74	261	45	184	868
	<i>21</i>	3,160	226	4,221	316	1,621	204	9,748
	<i>22</i>	234	483	212	725	69	529	2,252
	<i>31</i>	262	23	459	41	313	33	1,131
	<i>32</i>	124	378	81	795	67	2,385	3,830
	<b>Col- umn Total</b>	11,978	1,621	9,142	2,533	2,944	3,491	31,709
<b>Omis- sion Error</b>	0.33	0.89	0.54	0.71	0.89	0.32		
<b>Pro- ducer' s Ac- curacy</b>	0.67	0.11	0.46	0.29	0.11	0.68		
<b>Com- mis- sion Error</b>	0.42	0.79	0.57	0.68	0.72	0.38		
<b>User's Accu- racy</b>	0.58	0.21	0.43	0.32	0.28	0.62		

**APPENDIX**

---

**Reference Data**

<b>Prediction</b>	<b>c) D2H3</b>	<i>11</i>	<i>12</i>	<i>13</i>	<i>21</i>	<i>22</i>	<i>23</i>	<b>Row Total</b>
	<i>11</i>	10,498	1,535	37	3,326	1,058	36	16,490
	<i>12</i>	770	1,553	154	251	1,020	123	3,871
	<i>13</i>	5	26	58	0	27	65	181
	<i>21</i>	1,262	221	7	1,374	247	4	3,115
	<i>22</i>	504	1,331	197	380	1,853	301	4,566
	<i>23</i>	29	171	449	3	338	2,496	3,486
	<b>Col- umn Total</b>	13,068	4,837	902	5,334	4,543	3,025	31,709
	<b>Omis- sion Error</b>	0.20	0.68	0.94	0.74	0.59	0.17	
	<b>Pro- ducer' s Ac- curacy</b>	0.80	0.32	0.06	0.26	0.41	0.83	
<b>Com- mis- sion Error</b>	0.36	0.60	0.68	0.56	0.59	0.28		
<b>User's Accu- racy</b>	0.64	0.40	0.32	0.44	0.41	0.72		

**APPENDIX**

---

**Reference Data**

<b>Prediction</b>	<b>d) D3</b>	<i>1</i>	<i>2</i>	<i>3</i>	<b>Row Total</b>
	<i>1</i>	8,980	5,183	1,278	15,441
	<i>2</i>	3,992	5,353	2,485	11,830
	<i>3</i>	627	1,139	2,672	4,438
	<b>Column Total</b>	13,599	11,675	6,435	31,709
	<b>Omission Error</b>	0.34	0.54	0.58	
	<b>Producer's Accuracy</b>	0.66	0.46	0.42	
	<b>Commission Error</b>	0.42	0.55	0.40	
	<b>User's Accuracy</b>	0.58	0.45	0.60	

**Reference Data**

<b>Prediction</b>	<b>e) D2</b>	<i>1</i>	<i>2</i>	<b>Row Total</b>
	<i>1</i>	15,153	6,251	21,404
	<i>2</i>	3,653	6,651	10,304
	<b>Column Total</b>	18,806	12,902	31,708
	<b>Omission Error</b>	0.19	0.48	
	<b>Producer's Accuracy</b>	0.81	0.52	
	<b>Commission Error</b>	0.29	0.35	
	<b>User's Accuracy</b>	0.71	0.65	

**APPENDIX**

**Appendix 7:** Confusion matrices of a) D2H2 classification, b) H3 classification and c) H2 classification of Paris (London trained) on Urban Atlas level

**Reference Data**

<b>Prediction</b>	<b>a) D2H2</b>	<i>11</i>	<i>12</i>	<i>21</i>	<i>22</i>	<b>Row Total</b>
	<i>11</i>	22,661	2,308	3,649	874	29,492
	<i>12</i>	660	1,714	323	1,424	4,121
	<i>12</i>	5,350	691	2,370	514	8,925
	<i>22</i>	754	3,378	531	9,750	14,413
	<b>Column Total</b>	29,425	8,091	6,873	12,562	56,951
	<b>Omission Error</b>	0.23	0.79	0.66	0.22	
	<b>Producer's Accuracy</b>	0.77	0.21	0.34	0.78	
	<b>Commission Error</b>	0.22	0.58	0.73	0.32	
	<b>User's Accuracy</b>	0.78	0.42	0.27	0.68	

**Reference Data**

<b>Prediction</b>	<b>b) H3</b>	<i>1</i>	<i>2</i>	<i>3</i>	<b>Row Total</b>
	<i>1</i>	23,796	6,133	423	30,352
	<i>2</i>	2,213	10,179	2,661	15,053
	<i>3</i>	121	1,560	9,865	11,546
	<b>Column Total</b>	26,130	17,872	12,949	56,951
	<b>Omission Error</b>	0.09	0.43	0.24	
	<b>Producer's Accuracy</b>	0.91	0.57	0.76	
	<b>Commission Error</b>	0.22	0.32	0.15	
<b>User's Accuracy</b>	0.78	0.68	0.85		

---

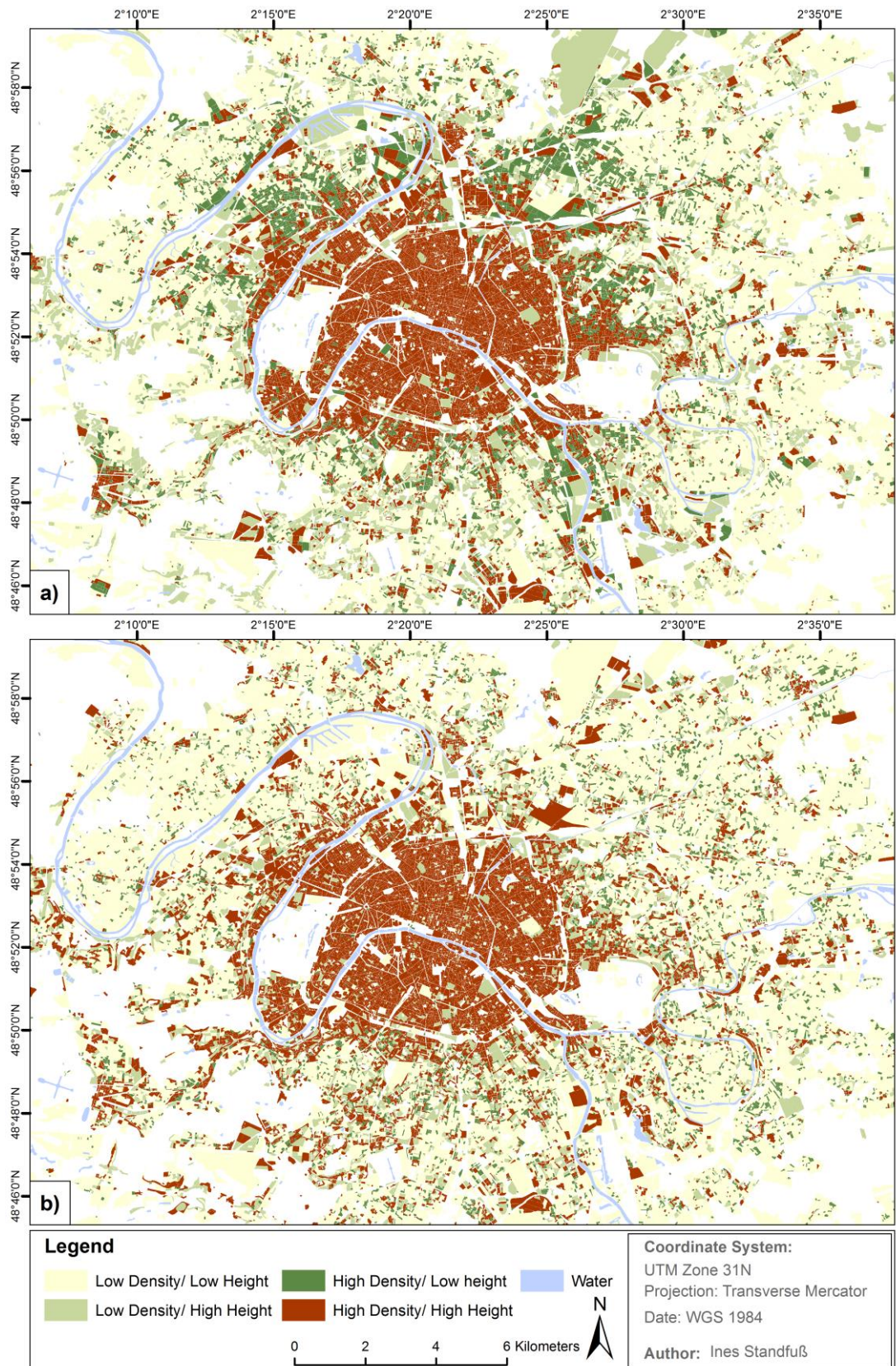
---

**APPENDIX**

**Reference Data**

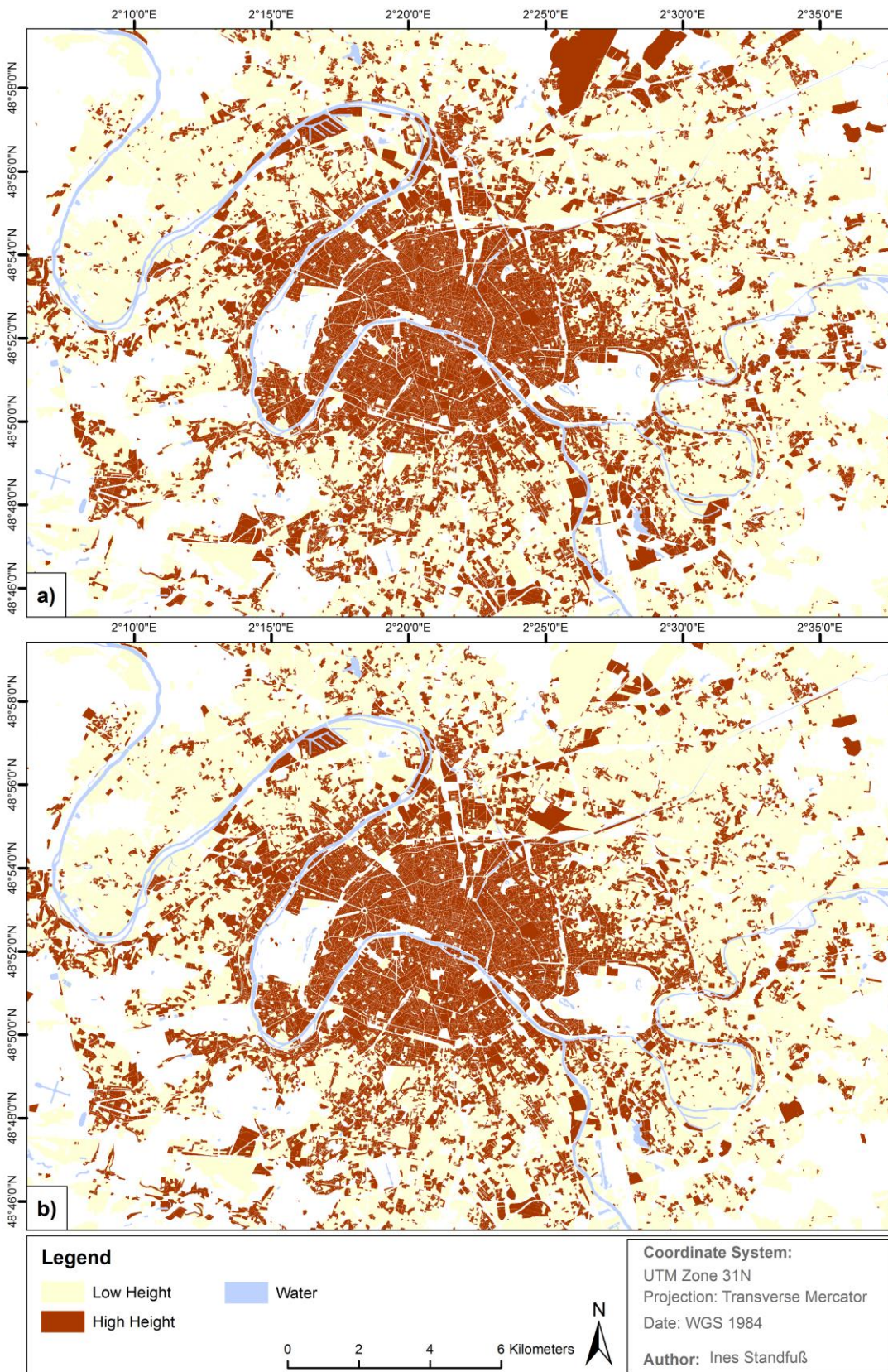
<b>Prediction</b>	<b>c) H2</b>	<i>1</i>	<i>2</i>	<b>Row Total</b>
	<i>1</i>	33,809	4,136	37,945
	<i>2</i>	2,489	16,517	19,006
	<b>Column Total</b>	36,298	20,653	56,951
	<b>Omission Error</b>	0.07	0.20	
	<b>Producer's Accuracy</b>	0.93	0.80	
	<b>Commission Error</b>	0.11	0.14	
	<b>User's Accuracy</b>	0.89	0.86	

Appendix 8: D2H2 classification of Paris on Urban Atlas level: a) reference data and b) classification result



# APPENDIX

Appendix 9: H2 classification of Paris on Urban Atlas level: a) reference data and b) classification result



**APPENDIX**

**Appendix 10:** Confusion matrices of a) D2H2 classification, b) H3 classification and c) H2 classification of London on square object level

**Reference Data**

<b>Prediction</b>	<b>a) D2H2</b>	<i>11</i>	<i>12</i>	<i>21</i>	<i>22</i>	<b>Row Total</b>
	<i>11</i>	15,107	1,226	1,563	223	18,119
	<i>12</i>	399	1,037	46	429	1,911
	<i>21</i>	47	2	21	4	74
	<i>22</i>	82	217	2	581	882
	<b>Column Total</b>	15,635	2,482	1,632	1,237	20,986
	<b>Omission Error</b>	0.03	0.58	0.99	0.53	
	<b>Producer's Accuracy</b>	0.97	0.42	0.01	0.47	
	<b>Commission Error</b>	0.17	0.46	0.72	0.34	
	<b>User's Accuracy</b>	0.83	0.54	0.28	0.66	

**Reference Data**

<b>Prediction</b>	<b>b) H3</b>	<i>1</i>	<i>2</i>	<i>3</i>	<b>Row Total</b>
	<i>1</i>	12,119	2,293	169	14,581
	<i>2</i>	1,293	3,472	433	5,198
	<i>3</i>	57	209	940	1,206
	<b>Column Total</b>	13,469	5,974	1,542	20,985
	<b>Omission Error</b>	0.10	0.42	0.39	
	<b>Producer's Accuracy</b>	0.90	0.58	0.61	
	<b>Commission Error</b>	0.17	0.33	0.22	
<b>User's Accuracy</b>	0.83	0.67	0.78		

---

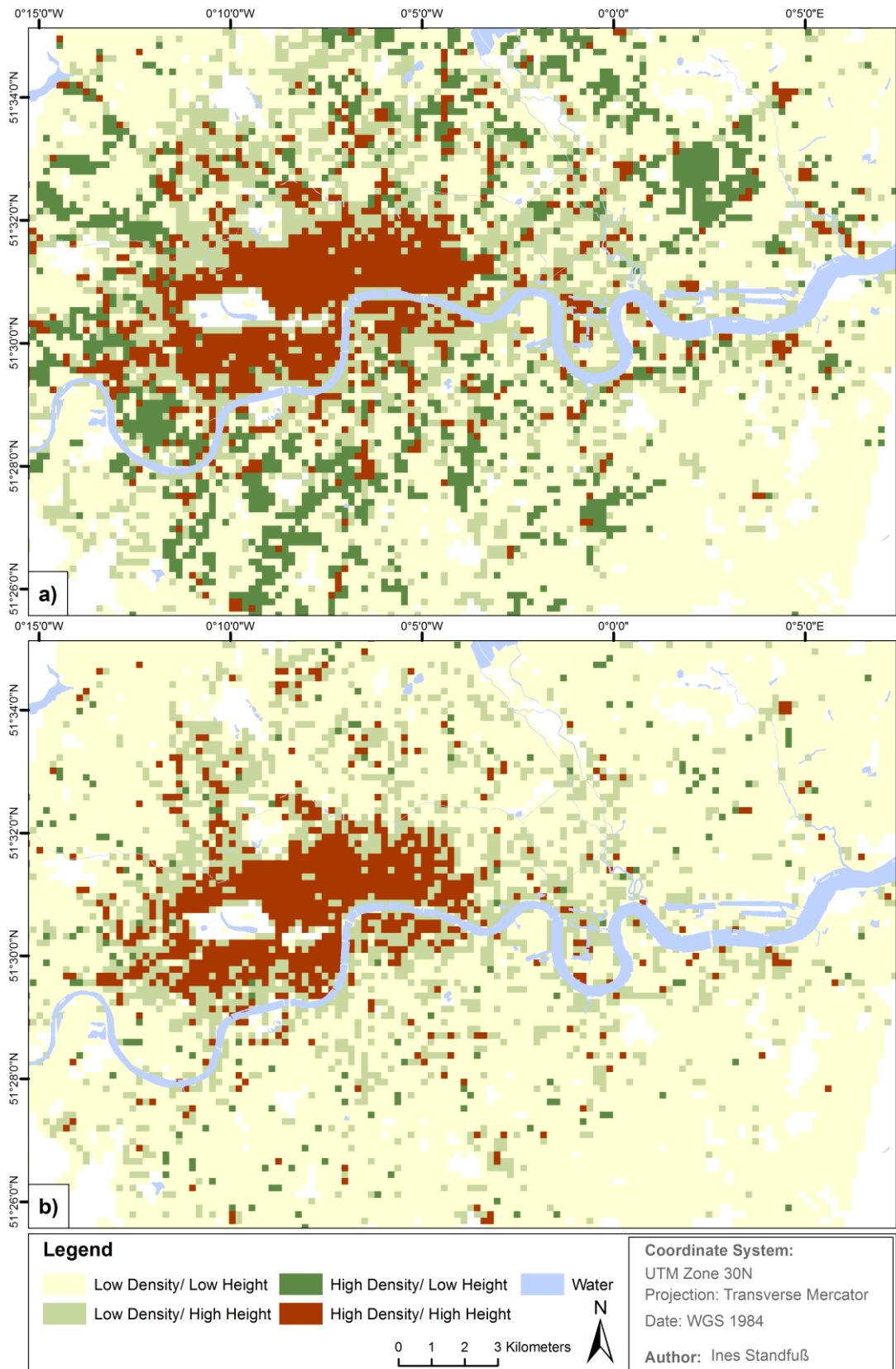
---

**APPENDIX**

**Reference Data**

<b>Prediction</b>	<b>c) H2</b>	<i>1</i>	<i>2</i>	<b>Row Total</b>
	<i>1</i>	16,688	1,399	18,087
	<i>2</i>	579	2,320	2,899
	<b>Column Total</b>	17,267	3,719	20,986
	<b>Omission Error</b>	0.03	0.38	
	<b>Producer's Accuracy</b>	0.97	0.62	
	<b>Commission Error</b>	0.08	0.20	
	<b>User's Accuracy</b>	0.92	0.80	

Appendix 11: D2H2 classification of London on square object level: a) reference data and b) classification result



Appendix 12: H2 classification of London on square object level: a) reference data and b) classification result

